United States
Department of
Agriculture

Forest Service

Forest
Products
Laboratory

General
Technical
Report
FPL–GTR–196

Proceedings, Sixth International Symposium: Moisture and Creep Effects on Paper, Board and Containers

Abstract

The USDA Forest Products Laboratory sponsored the 6th International Symposium: Moisture and Creep Effects on Paper, Board and Containers at the Monona Terrace Convention Center, Madison, WI, USA on 14-15 July 2009. Attendees heard 20 technical presentations; presenters were from seven different countries and three continents. Session topics included Corrugated Performance, Moisture Flow, Component Behavior, Industry Efforts, Other Materials, Moisture and Creep Response.

Keywords: cellulose, paper, paperboard, corrugated containers, moisture, humidity, creep, relaxation, mechano-sorption, proceedings

February 2011

Considine, John M.; Ralph, Sally A. 2011. Proceedings, sixth international symposium: moisture and creep effects on paper, board, and containers. General Technical Report FPL-GTR-196. Madison, WI: U.S. Department of Agriculture, Forest Service, Forest Products Laboratory. 166 p.

A limited number of free copies of this publication are available to the public from the Forest Products Laboratory, One Gifford Pinchot Drive, Madison, WI 53726–2398. This publication is also available online at www.fpl.fs.fed.us. Laboratory publications are sent to hundreds of libraries in the United States and elsewhere.

The Forest Products Laboratory is maintained in cooperation with the University of Wisconsin.

The use of trade or firm names in this publication is for reader information and does not imply endorsement by the United States Department of Agriculture (USDA) of any product or service.

The USDA prohibits discrimination in all its programs and activities on the basis of race, color, national origin, age, disability, and where applicable, sex, marital status, familial status, parental status, religion, sexual orientation, genetic information, political beliefs, reprisal, or because all or a part of an individual's income is derived from any public assistance program. (Not all prohibited bases apply to all programs.) Persons with disabilities who require alternative means for communication of program information (Braille, large print, audiotape, etc.) should contact USDA's TARGET Center at (202) 720–2600 (voice and TDD). To file a complaint of discrimination, write to USDA, Director, Office of Civil Rights, 1400 Independence Avenue, S.W., Washington, D.C. 20250–9410, or call (800) 795–3272 (voice) or (202) 720–6382 (TDD). USDA is an equal opportunity provider and employer.

Proceedings, Sixth International Symposium: Moisture and Creep Effects on Paper, Board and Containers

Madison, Wisconsin, USA
14–15 July 2009

Organized by the U.S. Forest Service,
Forest Products Laboratory (FPL)

Editors: John M. Considine, Sally A. Ralph

Sponsors: TAPPI, International Paper Physics Committee

Proceedings, Sixth International Symposium: Moisture and Creep Effects on Paper, Board and Containers

Madison, Wisconsin, USA
14–15 July 2009

Organized by the U.S. Forest Service, Forest Products Laboratory (FPL)

Editors: John M. Considine, Sally A. Ralph
U.S. Forest Service, Forest Products Laboratory, Madison, Wisconsin

Sponsors: TAPPI, International Paper Physics Committee

Preface

The 6th International Symposium: Moisture and Creep Effects on Paper, Board and Containers was held at the Monona Terrace Convention Center, Madison, Wisconsin, USA, on 14–15 July 2009.

Locations and dates of previous symposia in this series were as follows:

- **1st Symposium, September 1992, Madison, Wisconsin, USA.** Coordinated by Ted Laufenberg, FPL, and Dr. Craig Leake, National Starch & Chemical Company, Bridgewater, New Jersey, USA
- **2nd Symposium, December 1994, Stockholm Sweden.** Coordinated by Dr. Christer Fellers, STFI (now INNVENTIA, Stockholm, Sweden) and Ted Laufenberg, FPL
- **3rd Symposium, February 1997, Rotorua, New Zealand.** Coordinated by Dr. Ian Chalmers, PAPRO (now SCION, Rotorua, New Zealand)
- **4th Symposium, March 1999, Grenoble, France.** Coordinated by Dr. Jean-Marie Serra-Tosio, EFPG, and Dr. Isabelle Vullierme, EFPG
- **5th Symposium, April 2001 Victoria Australia.** Coordinated by Dr. Ian Parker, Monash University, Victoria, Australia

These symposia are held on an irregular basis. At the Paper Physics Committee meeting held at the International Paper Physics Conference in Gold Coast, Australia, 2007, members voted to invite FPL to host the next Moisture Symposium.

Demographics on this Symposium

- Presentations: 1 keynote, 20 technical
- 50 authors/co-authors
- Presenters from 7 countries and 3 continents
- 19 at-large attendees came from the USA, Canada, and New Zealand

Readers will notice a variety of format and style in these proceedings. The authors were given great flexibility for their material content; formats include full length papers, extended abstracts, and short abstracts, and are included as received from the authors.

The question and answer time after each presentation was lively; coffee breaks and social gatherings allowed for active interaction and development of potential scientific collaboration.

An informal vote taken at the final session suggested Rome as an excellent choice for the next Moisture Symposium with an undecided date.

Acknowledgments

This book was made possible through extensive assistance from the FPL Office of Communications, especially Susan Paulson, Tivoli Gough, James Anderson, and Madelon Wise.

Furthermore, financial and material support by TAPPI, University of Wisconsin – College of Agriculture and Life Sciences (CALS) Conference Planning Services and FPL. In particular the support of Rich Lapin, TAPPI, Raj Lal, FPL Office of Communications, and Heather Cooper, CALS, was timely and effective.

Introduction

The interaction of moisture and cellulose is beneficial and problematic. It is beneficial for manufacturing, processing, and converting needs, where water is used for fiber transport and softening. It is problematic because it can reduce performance. This symposium, like others in this series, was devoted to understanding, characterizing, and reducing the detrimental effects of this interaction.

Synthetic petrochemical plastics have made serious inroads within the packaging sector; however, recyclability of cellulosic materials is a significant advantage. Hybrid plastic/cellulose composites, which try to enhance each constituent material's benefits and reduce their liabilities, create even more demand for investigations of moisture/cellulose interactions.

Papermaking additives are used to enhance physical, mechanical, and optical properties. Sophisticated syntheses, layer-by-layer technology, and nanoparticles comprise but a few of the many methods to improve paper properties. Retention of the additives and maintaining the achieved behavior are often affected by moisture transport.

Even the paper machine is not exempt from examination for techniques and methods to enhance properties. Local fiber orientation, residual drying stresses, and formation can be affected during paper production and can influence moisture behavior.

After paper is made, it is converted or processed to produce an end product. Interaction of multiple paper (or non-cellulose) components requires advanced modeling techniques because analytical solutions exist for only the most basic configurations. These models often need to account for post-converting damage.

These symposia provide a venue for government, academic, and industrial researchers to share results and exchange ideas on the important topic of the interaction of moisture and cellulose. Industrial competition is strong, so the introduction of value-added products and consumer education can provide real advantages for economic viability. Immediate feedback encourages the researcher to clarify ideas and identify shortcomings. New research directions, acknowledgement of well-solved problems, and regular involvement of graduate researchers suggest that this series is meeting the needs of the community it is seeking to serve.

Scientific Committee

Conference Chairman

JunYong Zhu
U.S. Forest Service, Forest Products Laboratory, USA

Conference Secretary

John Considine
U.S. Forest Service, Forest Products Laboratory, USA

International Scientific Committee

Marco Evangelos Biancolini
University of Rome, Italy

Jean-Francis Bloch
CFPG, France

Ian Chalmers
Scion, New Zealand

Doug Coffin
Miami University, USA

Christer Fellers
INNVENTIA, Sweden

Benjamin Frank
Packaging Corporation of America, USA

Terry Gehardt
Sonoco Products Company, USA

Yanfeng Guo
Xi'an University of Technology, China

Contents

Some Thoughts on Fundamental Aspects of Mechanosorption
Coffin, D. **5**

Session 1: Corrugated Performance (Benjamin Frank, Chair) 11

Failure of corrugated board panels at different loading rates and during creep
Alfthan, J. 12

Crush damage of corrugated board and its effects on cyclic humidity creep performance of boxes
Chalmers, I. 19

Effects of medium strength properties and component rotation on corrugated endurance
Popil, R.. 24

Session 2: Moisture Flow (JY Zhu, Chair) 27

Steady-state moisture diffusion through corrugated fiberboard
Glass, S.V. 28

The effect of hysteresis on moisture sorption of paperboard
Lavrykov, S. 29

Analysis of the hygroexpansion of paperboard and small flute corrugated board by digital correlation of images obtained by X-ray microtomography
Viguié, J. 30

Session 3: Component Behavior (Doug Coffin, Chair) 31

Formation and edgewise compressive creep properties
Fellers, C. 32

Effect of moisture on defect interaction in paper and paperboard
Considine, J. 33

Experimental characterisation of paper for corrugated board
Biancolini, M.E. 35

Session 4: Industry Efforts (Ian Chalmers, Chair) 39

End-user focused creep
Wikström, A. 40

Effects of strain rate on the stress relaxation of wet paper
Kekko, P. 49

Repulpable water vapor barrier coatings made easy
Hostetler, R 59

Session 5: Other Materials (David Vahey, Chair) 67

Strength properties of low moisture content yellow-poplar and Southern Pine
Kretschmann, D.E. 68

Hygroexpansion of plant-based fiber mats for “green” composites
Dumont, P.J.J. 69

Modelled and measured bending stiffness of polyethylene coated multi-layer paperboard at two moisture contents
Paunonen, S. 70

Session 6: Modeling and Creep Response (Sergiy Lavrykov, Chair) 81

Corrugated board box design using full detailed FEM modelling
Biancolini, M.E. 82

Mechanical model on creep properties of double-wall corrugated paperboard
Guo, Y. 84

Compression fatigue creep of paperboard
Scott, C.T. 92

Session 7: Moisture and Time Response (M.E. Biancolini, Chair) 93

Use of ultrasonic velocity measurement to investigate moisture-induced stress relaxation in paper
Vahey, D. 94

Wood fibres do indeed show mechano-sorptive creep
Salmén, L. 97

Hygroexpansivity of thermally aged papers
Turner, K. 98

Participants 99

Index of Authors 103

Appendix—5th International Symposium, courtesy of Dr. Ian Chalmers 105

Some Thoughts on Fundamental Aspects of Mechanosorption

Douglas W. Coffin, Professor
Department of Chemical and Paper Engineering
Miami University, Oxford OH 45056
coffindw@muohio.edu

Introduction

Mechanosorption refers to the response of a material or structure to superimposed loading from mechanical loads and moisture changes. For many materials, linear superposition does not apply for such a combined loading, and the observed response can be quite different from an expectation framed around consideration of only averages. The major focus of mechanosorptive research in the paper industry is directed towards the practical problem of the lifetime of stacked corrugated boxes. A box on the bottom of a stack is subjected to a constant compressive load from the weight of boxes and contents stacked above it. In addition, these stacked boxes are often stored in warehouses where the environment is not controlled. The relative humidity of the surrounding air is cyclic in nature. The amount of moisture in the air will change with the temperature, weather, and seasons. These transient changes in the surrounding environment will cause the moisture content of the box to fluctuate, which induces expansions and shrinkages. The dead load causes the box to creep. The combined effects result in a creep rate that is accelerated compared to the creep rate under constant high moisture. Testing has shown that the lifetime is shortest for a box subjected to both dead load and cyclic moisture.

Understanding this behavior and determining how to overcome it was the trigger for the first of these symposiums. Since 1992, much progress has been made on understanding mechanosorption. We have studied the effects from scale-levels of boxes down to fibers. We have modeled the phenomenon and we have developed treatments that can reduce the effects. Now we are at a place where one begins to question just what role mechanosorptive effects actually play in failures in the field. For example, mechanosorption is probably a major factor of boxes used in shipping fruit and vegetables. For other cases, perhaps variability, defects, and poor construction may be more important than the actual increased creep rates.

The following provides a summary of some of my thoughts on mechanosorption, accelerated creep, and box performance. In addition, a simple analysis is presented to illustrate how mechanosorptive effects can arise.

The Issue

The subtitle to the talk I gave at this symposium was “Why 1+1 = 3 makes sense.” What I meant by this is that for mechanosorption we combine two well-studied behaviors and produce something that, superficially, is unexpected. The first “1” is the mechanical response. If we apply a load under constant environmental conditions we can study, describe, and predict the creep response. The second “1” is the addition of moisture. If we study the effects of the environment on an unloaded paper, we can describe and predict the response. We take these two factors and add them together (1 + 1) and we get a response (= 3) that we did not predict. That is, we expected one plus one to equal two, but we got three instead. What this really means is that we have not considered the problem correctly and our extrapolation of the combination of two separate effects cannot be made by superimposing the bulk responses. That means we need to step back and reconsider the subject of mechanosorption differently. We could start by considering the life of a box.

Consider what a box experiences during its lifetime. The corrugated box is born from a process that damages it such that the paper may lose half its initial strength. During converting, the board could be crushed, causing more damage. Even when the box is formed and loaded with contents, it may not be perfectly square. We take this damaged box and expose it to a variety of environmental conditions that alter its temperature and moisture content. During transportation, the box will likely be knocked around, causing irreparable damage. A box may have to carry the weight of other boxes with their contents, which causes its sides to bulge and ultimately to its failure. It is not the life that one would aspire to, but the box has no choice.

Boxes do not respond well to cycles of moisture content especially when they are under a state of stress. It is this combined effect of moisture and load that is the focus for mechanosorption. Various mechanosorptive effects have been observed for paper. If the load is constant, and the moisture cycled, we describe the observed phenomena as accelerated creep. If we look

at changes in creep compliance as a function of time lapsed after a moisture excursion, the phenomena resembles physical aging. If we measure the dynamic mechanical properties during a moisture change, we record transients in those properties. All three observations are linked and manifestations of the same underlying phenomena.

How to deal with Mechanosorption

The mechanosorptive effects are real and must be dealt with. Even the United States Government provides guidance. The U.S. National Archives and Records Administration states that "if wet, boxes must be replaced …" A box maker cannot simply replace all problem boxes and they must develop preventive measures to combat box design. The box maker must provide the customer with a box that will protect the contents for a required length of time.

The box must be cost effective, developed and produced efficiently, and perform adequately. Essentially one wants a box that is fast, good, and cheap. The design rule of three says you can only have two of the needed attributes. One can produce a good box fast but it will not be cheap. Conversely, to develop a cheap good box will take a long time. The box makers have found solutions that work and the customer has to decide where they want to be on the issue of performance versus cost.

Applied scientists have also developed solutions to combat mechanosorption be introducing chemicals or composite materials. Again, these sacrifice cost for performance. Scientists have also developed testing equipment and protocol to evaluate the severity of mechanosorption and thus allow manufacturers to evaluate their materials and potential solutions.

The fundamental researcher focuses on understanding the phenomena, testing hypotheses, interpreting observations, and providing understanding. The role of fundamental research is one step removed from the practical solutions box makers face every day, but the results of such research may help guide the industry to providing a good cheap box fast.

A Simple Analysis to Illustrate the Origin of Mechanosorptive Effects

Since I consider myself to be more fundamental than practical I will describe my view of the origin of mechanosorptive effects. This analysis is based solely on the utilization of classical Newtonian mechanics and Fickan diffusion. The point is to establish how nothing new or special needs to be adopted to describe and understand mechanosorptive behavior. I have not seen the particular analysis given below in the literature, so I will provide details. It does not address how specific materials affect mechanosorption. Nor does it provide any insight into the role of fiber, paper, or board structure. The only requirement is that some type of heterogeneity exists on some scale-level. Information of a more practical nature is found in the rest of the proceedings of this symposium.

Consider a material that is linear elastic, hygroexpansive, and Fickian. Assume that only the elastic modulus is a function of moisture. Consider only a two-dimensional case where the material is under uni-axial tension (x-direction) and moisture is only a function of the perpendicular direction, z. For such a material, the constitutive equation relating stress, σ, to strain, ε, can be written as

$$\sigma = E[\varepsilon - \beta(m - m_0)] \tag{1}$$

where E is elastic modulus, β is the coefficient of hygroexpansion, m is the moisture content, and m_0 is the initial moisture content. The equation governing the diffusion of moisture is

$$D\frac{d^2m}{dz^2} = \frac{dm}{dt} \tag{2}$$

where D is the diffusivity of the material.

Consider the case of constant strain resulting in a constant axial force, N (assume unit width in y-direction). The axial force can be related to the stress by integrating over the thickness, h, as

$$N = \int_0^h \sigma dz = \int_0^h E[\varepsilon - \beta(m - m_0)]dz \tag{3}$$

Equation (3) can be re-written using the average values, $(\bar{\ })$, as

$$N = \bar{E}h\varepsilon - \beta\bar{E}h(\bar{m} - m_0) - \int_0^h E[\beta(m - \bar{m})]dz \tag{4}$$

Note in Equation (4) the term, $\bar{E}h\bar{m}$, is just added and subtracted. Equation (4) is solved for the strain and written as

$$\varepsilon = \frac{N}{\bar{E}h} + \beta(\bar{m} - m_0) + \beta\bar{m}\left[\int_0^1 \frac{E}{\bar{E}}\frac{m}{\bar{m}}\, d\xi - 1\right] \tag{5}$$

Equation (5) can be viewed as the summation two parts; the expected bulk or average response

$$\varepsilon_b = \frac{N}{\bar{E}h} + \beta(\bar{m} - m_0) \tag{6}$$

And a transient response due to the coupling of the moisture and mechanical response,

$$\varepsilon_{ms} = \beta\bar{m}\left[\int_0^1 \frac{E}{\bar{E}}\frac{m}{\bar{m}}\, d\xi - 1\right] \tag{7}$$

Equation (6) is the response based on using the average properties at any given time. Equation (7) is a mechanosorptive effect. If equation (7) is nonzero, the response of the material will be different than that predicted from the average properties. Consider the simple case of steady-state moisture transport through the material. Furthermore, assume that the elastic modulus linearly depends on moisture content. For this case we have

$$m(z) = m_1 + (m_2 - m_1)\frac{z}{h} \tag{8}$$

and

$$E(m) = E_1 + (E_2 - E_1)\frac{(m - m_1)}{(m_2 - m_1)} \tag{9}$$

where the subscript value 1 represents the value at $z = 0$ and the subscript 2 represents the value at $z = h$. Substituting Equations (8) and (9) into Equation (10) gives

$$\varepsilon_{ms} = \beta\frac{(E_2 - E_1)}{6(E_2 + E_1)}(m_2 - m_1) \tag{10}$$

The mechanosorptive effect is only present if both the modulus and the moisture vary through the thickness. Also, the extra strain is negative if the modulus decreases with increases in moisture. In a real material, there would be no sustained mechanosorptive effect under stead-state moisture transport because relaxation would even out the distribution of stresses, which is equivalent for this simple case to having equal modulus in Equation (10).

The instructive component of the analysis given above is that when there is a spatial distribution of stresses and moisture, the response of the material will differ from the expected result based on bulk averaged properties.

Consider next, the transient case where the moisture changes from the initial moisture content, m_i, to the final moisture, m_f, content. The moisture content can be expressed as

$$m(z,t) = m_f + \frac{4}{\pi}(m_i - m_f)\sum_{n=1}^{\infty}\frac{\sin((2n-1)\pi z/h)}{(2n-1)}e^{-\left(\frac{(2n-1)\pi}{L}\right)^2 D} \tag{11}$$

The average moisture content at any given time is

$$\overline{m}(t) = m_f + \frac{8}{\pi^2}\left(m_i - m_f\right)\sum_{n=1}^{\infty}\frac{1}{(2n-1)^2}e^{-\left(\frac{(2n-1)\pi}{h}\right)^2 D} \tag{12}$$

Assuming the modulus as a function of moisture is given as $\overline{E}(t) = E_0 + k\overline{m}(t)$, the mechanosorptive strain is given as

$$\varepsilon_{ms}(t) = \frac{\beta k}{\overline{E}}\left(\overline{m} - m_f\right)^2\left[\frac{\pi^2}{8}\frac{\sum_{n=1}^{\infty}\frac{1}{(2n-1)^2}e^{-2\left(\frac{(2n-1)\pi}{h}\right)^2 D}}{\left(\sum_{n=1}^{\infty}\frac{1}{(2n-1)^2}e^{-\left(\frac{(2n-1)\pi}{h}\right)^2 D}\right)^2} - 1\right] \tag{13}$$

Figure 1 illustrates the effect that Equation (13) has on the strain.

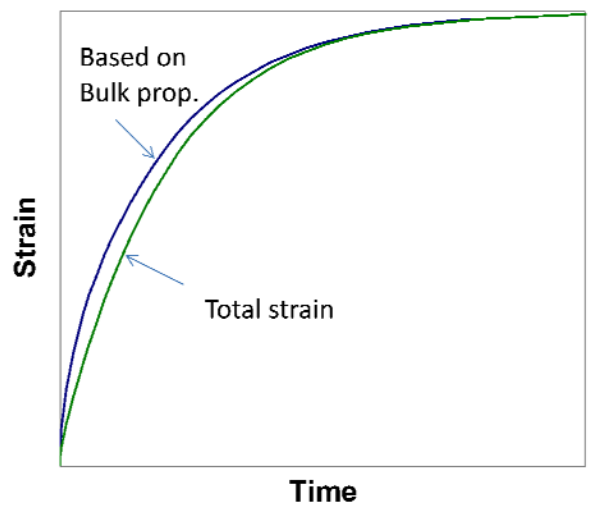

Figure 1. Strain based on bulk properties compared to total strain including mechanosorptive strain for a case of transient moisture increase.

The effect shown in Figure 1 is small, but it is important in that it is a predicted behavior even for the simple case of a linear elastic material coupled with simple diffusion. For the case shown here the response is transient and at equilibrium there are no lasting effects. In the case of real materials, and the necessary complications of energy dissipation would cause sustained effects.

The important conclusions from this analysis are the following:

- One cannot predict the transient deformation based on bulk properties alone.
- The transient response is caused by a coupling of the spatial distribution of stresses arising from the effects of moisture on swelling and magnitude of intrinsic material properties.
- Interpreting experimental data that only measures the bulk response is difficult when trying to understand the causes of mechanosorptive effects.

At this point, creep has not even been included. If one were to add a creep compliance to the strain, Jσ, Equation (5) would become.

$$\varepsilon = \frac{\overline{\sigma}}{\overline{E}} + \beta\left(\overline{m} - m_0\right) + \overline{\sigma}\int_0^t J(\overline{\sigma},\overline{m},\tau)d\tau + \beta\overline{m}\left[\int_0^1 \frac{E}{\overline{E}}\frac{m}{\overline{m}}d\xi - 1\right] + \int_0^1\int_0^t\left[\sigma J(\sigma,m,\tau) - \overline{\sigma}J(\overline{\sigma},\overline{m},\tau)\right]d\tau \tag{14}$$

Where the last term is the mechanosorptive creep and the creep compliance is written as a possible function of load, moisture.

The mechanosorptive creep component

$$\varepsilon_{ms\,creep} = \int_0^1\int_0^t\left[\sigma J(\sigma,m,\tau) - \overline{\sigma}J(\overline{\sigma},\overline{m},\tau)\right]d\tau \tag{15}$$

will change the creep rate during moisture changes and the total creep strain will accumulate if the compliance is a nonlinear function of stress level.

Equation (15) tells us there is nothing special that needs to be added to the constitutive equation to account for mechanosorptive behavior. So if the heterogeneity of the system is modeled on the appropriate scale and stress-distributions are accounted for, the mechanosorptive effects will be a natural outcome of the analysis. If an analysis only looks at the bulk response without consideration for the distribution of stresses, then Equation (15) would need to be incorporated as some function we could call a mechanosorptive strain. This does not mean some new phenomenological description needs to be invented to go along with the additional strain term; only that it is added because of a lack of consideration for the distribution of stresses within the material.

Summary

The mechanosorptive effects are fascinating. Some of the observed responses reported in the literature show the extreme effect that coupling moisture changes and mechanical loading can have on the response of paper and board. These effects are not something that can be simply turned off. Analysis of the mechanisms of mechanosorptive effects suggests that certain strategies could reduce the detrimental effects. For instance, reducing hygroexpansion, reducing heterogeneity, and reducing moisture variations could help. Product performance could be improved simply by reducing creep compliance and improving product uniformity.

If one accepts the implications of the analysis given above, then one can design future research based on this view to help industry better achieve all three goals of good, cheap, and quick. If one disagrees with the analysis or believes other factors dominate the magnitude of mechanosorptive effects, then they too can formulate their hypothesis and design their tests and discount the effects predicted above as negligible. Either way, there is still work to be done in this area. I look forward to seeing what is to come in the future.

This page intentionally left blank.

Session 1
Corrugated Performance

Benjamin Frank, Chair

Packaging Corporation of America

Corrugated board represents the great majority of materials used for packaging, protection and transportation. Failure of corrugated board ranges from excessive deformation and box bulging to damage of contents. Understanding and characterizing moisture effects on corrugated board have the potential to save significant property loss and maintain the market segment in the paper industry. Innovative geometry, design, and production that use paperboard orthotropy to its advantage may prospectively increase market share.

Failure of corrugated board panels at different loading rates and during creep

Johan Alfthan and Tomas Hansson
Innventia AB, Box 5604, SE-114 86 Stockholm Sweden

Abstract
Static tests at different loading rates and creep tests at different loads were carried out on corrugated board panels. The panels were loaded in compression in the flute direction (cross-machine direction). Two different panel geometries were tested at different relative humidity levels. It was found that a panel of a given geometry failed at a constant deformation independent of the type of test and the humidity level, and that alterations of the panel dimensions affected the deformation at failure. The failure mode in all experiments was buckling. The results indicated that the compression failure deformation of corrugated board panels (and hence containers) is controlled by structural properties like panel dimensions, thickness of the board etc, rather than by the material properties of the board constituents.

Introduction

Is it possible to find a failure criterion for corrugated board panels and containers loaded in compression that is independent of different loading rates, independent of whether failure takes place immediately or after some creep has taken place, and perhaps also independent of humidity? Published data seem to suggest so, and motivated this work on the failure of corrugated board panels.

Dagel and Brynhildsen (1959) perform compression tests on corrugated board containers at different loading rates and find that the force at failure increases with loading rate, but the deformation at failure remains constant. Koning and Stern (1977), Leake (1988), Leake and Wojcik (1989) and Bronkhurst (1997) investigate the creep of corrugated board containers and find a relation between secondary creep rate and time to failure of the form

$$t = A\left(\dot{\varepsilon}^{\mathrm{c}}\right)^{-b}, \tag{1}$$

where t is the time to failure, $\dot{\varepsilon}^{\mathrm{c}}$ is the secondary creep rate and A and b are fitting parameters. In all cases, the parameter b is close to 1. That means that the time multiplied by the creep rate, i.e. the creep strain, is almost constant. This indicates that the deformation at failure for a given type of container is almost constant. The effect of humidity is somewhat unclear. Koning and Stern (1977) find that the humidity level does not have any influence on the relation between secondary creep rate and time to failure. According to Leake (1988), varying humidity gives a much higher value of the parameter A in Eq. (1), perhaps indicating a change of the failure mechanism.

In the present work, panels of corrugated board rather than containers were studied, since experiments on the former are more easily controlled. The panels were mounted in a rig and loaded in compression in the flute direction (cross-machine direction, CD). Static tests at different loading rates and creep tests at different loads were carried out. Tests were done at different constant humidity levels, but the effect of varying humidity was not investigated.

Materials and methods

Rectangular corrugated board panels were tested in a hydraulic testing machine using a special rig designed for compressive loading (Nordstrand, 2004). The corrugated board used in the experiments was a symmetric single wall B flute board. In the rig, the panels were mounted so that rotations but no deflections were allowed along the four edges. The load was applied in the direction parallel to the flutes. During testing, forces and deformations were measured continuously. Two types of experiments were carried out: Static tests, where the deformation increased in a ramp until failure, and creep tests, where a constant force was applied and the time-dependent deformation was measured until failure. The static tests were performed for different deformation rates, from 1 mm/min up to 100 mm/mm, and the creep tests were performed for different load levels. Two different humidity levels were used for each kind of test, 50% and 80% RH for the static tests and 50% and 70% RH for the creep tests. Two different geometries were tested, 260 mm × 385 mm and 400 mm × 385 mm, where the first number refers to the length in the flute direction (CD). In the creep experiments, only the smaller panel type, 260 mm × 385 mm, was tested.

Finite element simulations of the corrugated board panel tests were performed. Shell elements were used to model the liners and the corrugated fluting. In the finite element model, the liner and fluting were described by anisotropic elastic-plastic material models. An ideally plastic Hill model was used to model plasticity. The compressive strength of the materials was used as yield stress. Symmetry was exploited, so that only a quarter of the panel was modelled. The analysis was performed in two steps. First a linear buckling analysis was performed. An imperfection of the same shape as the first buckling mode from the first analysis was then added to the model of the panel and a second, non-linear analysis was performed. In the second analysis, the whole panel test was simulated, including the post-buckling behaviour. The forces and displacements were obtained from the analysis.

The most important material parameters used in the finite element calculations were provided by the corrugated board manufacturer, while the remaining required material parameters were estimated. The used material parameters are summarised in Table 1.

Table 1 Material parameters used in the finite element calculations.

Property	Liner	Fluting	Comment
Thickness	0.17 mm	0.16 mm	Measured
Elastic modulus MD	6.35 GPa	6.08 GPa	Measured
Elastic modulus CD	2.81 GPa	2.23 GPa	Measured
Elastic modulus ZD	63.5 MPa	60.8 MPa	Estimated (MD modulus divided by 100)
Poisson ratio MD-CD	0.34	0.34	Estimated
Poisson ratio MD-ZD	0.01	0.01	Estimated
Poisson ratio CD-ZD	0.01	0.01	Estimated
Shear modulus MD-CD	1.54 GPa	1.32 GPa	Calculated from 45° tensile test
Shear modulus MD-ZD	115 MPa	111 MPa	Estimated (MD modulus divided by 55)
Shear modulus CD-ZD	80.3 MPa	63.7 MPa	Estimated (CD modulus divided by 35)
Compressive stress at failure MD	25 MPa	25 MPa	Estimated (tensile stress at failure divided by 2)
Compressive stress at failure CD	15 MPa	8 MPa	Estimated (tensile stress at failure divided by 2)

Results

Figure 1 shows a typical load-deformation curve from the static tests. Initial buckling of the panel occurred at a load around 0.35 kN, which resulted in the decrease of stiffness exhibited in the load-deformation curve. After the buckling had been initiated, the panel continued to carry an increasing load until the final failure occurred at the peak load of the curve.

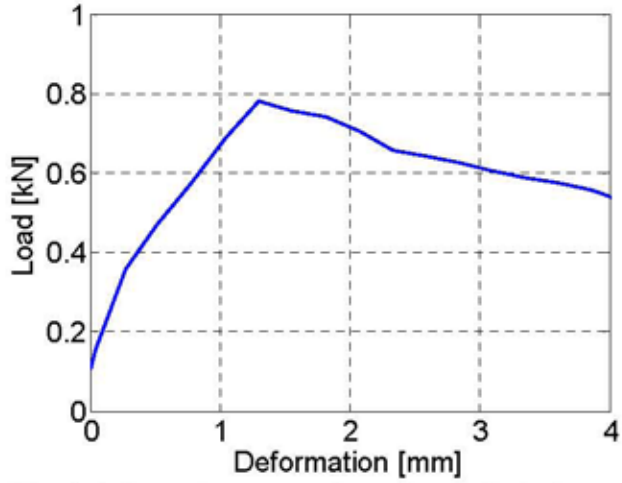

Figure 1 A typical load-deformation curve from the static test on a 260 mm × 385 mm panel at 100 mm/min and 50% RH. The panel fails at the peak load.

Figure 2 shows a typical time-deformation curve from the creep tests. The curve shows a fast increase of deformation at initial loading, followed by a slow increase of deformation for several hours. When the creep deformation reached a critical value the panel failed in buckling. At this point, the deformation increased in an unstable manner.

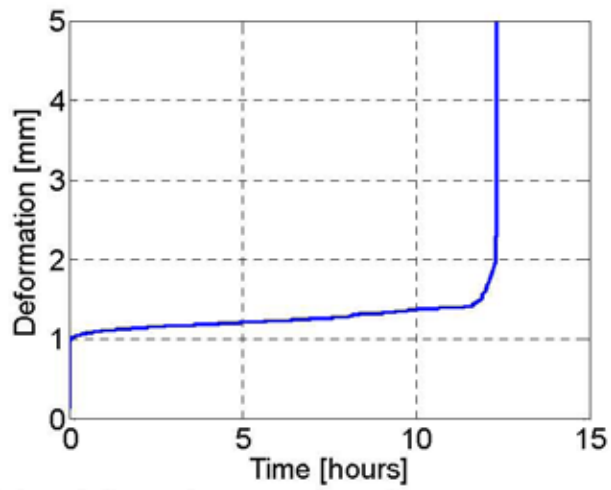

Figure 2 A typical time-deformation curve from the creep test on a 260 mm × 385 mm panel at 0.53 kN and 50% RH. The panel fails at the sharp increase in the slope of the curve.

In both the static tests and the creep tests the deformation at failure was the similar for a given panel geometry independently of the relative humidity, strain rate or load level, see Figures 3-4.

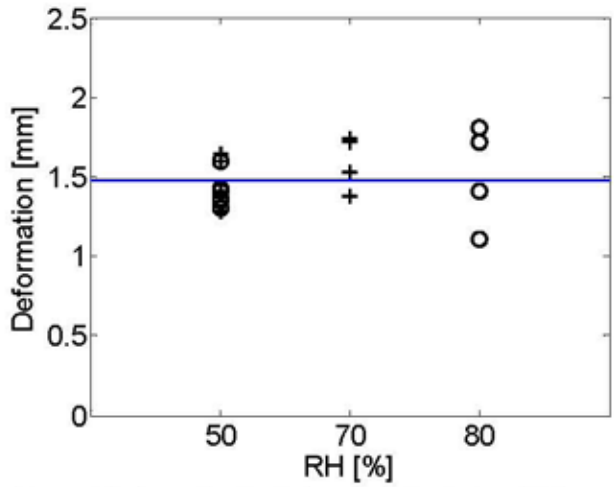

Figure 3 Deformation at failure for both kinds of tests for 260 mm × 385 mm panels at different humidity levels. The static tests, where deformation increased in a ramp until failure, are marked O and the creep tests are marked +. The line is the mean deformation at failure.

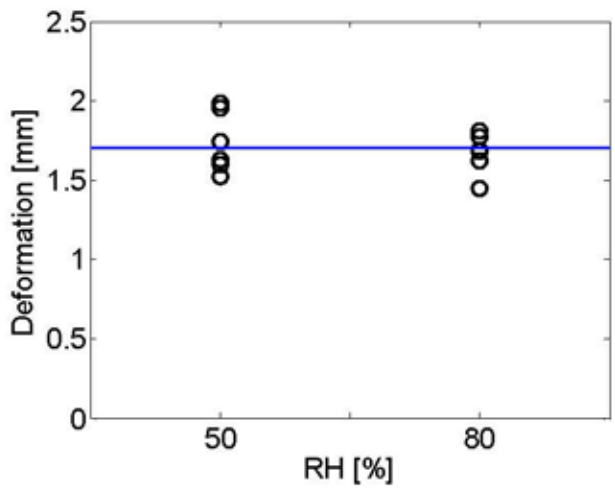

Figure 4 Deformation at failure for static tests, where deformation increased in a ramp until failure, for 400 mm × 385 mm panels at different humidity levels. The line is the mean deformation at failure.

In the finite element calculations the effect of different loading rates and different humidity conditions was estimated by changing the stiffness of the constituent materials of the corrugated board. To estimate the effect of changing the loading rate from 100 mm/min to 1 mm/min, the stiffness was decreased 10% and to estimate the effect of an increase in humidity from 50% to 80% RH the stiffness was decreased 30%. The results are shown in Figure 5. The peak load drops as a result of the decreased stiffness but the corresponding failure deformation is almost the same.

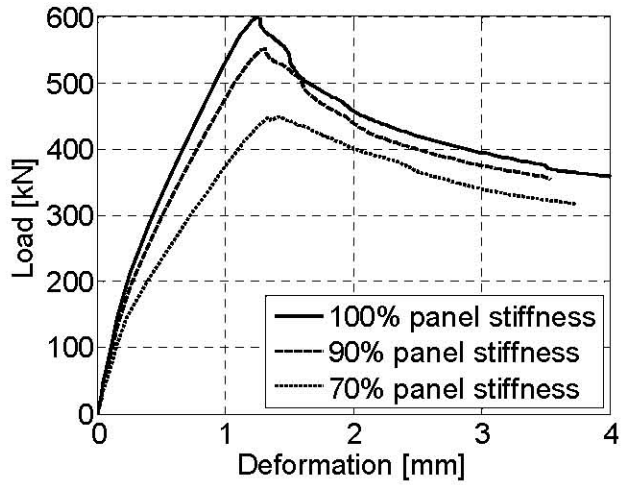

Figure 5 Effect of changed material stiffness in the finite element calculations.

Discussion

In all tests carried out, the deformation at failure was approximately the same for a given panel geometry, as seen in Figures 3-4. The failure mode was buckling, which seemed to occur at the same deformation irrespectively of how the deformation was reached, thus being only a function of the panel geometry. Finite element simulations of the panel tests confirmed these results. This observation can be attributed to that failure in buckling is controlled by structural properties rather than by the material properties of the constituents of the corrugated board.

The results of Dagel and Brynhildsen (1959) for static tests were confirmed, and in addition it was shown that the results hold for different humidity levels.

The results of Koning and Stern (1977), Leake (1988), Leake and Wojcik (1989) and Bronkhurst (1997) suggest that the creep failure of corrugated board containers for a given geometry occur at a critical strain or deformation that is independent of the load in the creep test. The deformation at failure also appears to be independent of the equilibrium moisture content of the materials. However, another deformation at failure is obtained for cyclic humidity (Leake, 1988). In this work the independence of constant humidity level was confirmed, and it was shown that the deformation at failure was approximately the same for creep tests as for static tests. The effect of cyclic humidity was not investigated. There might be a difference in the failure mode between creep at constant and creep at cyclic humidity, e.g. that a different buckling mode is triggered during the humidity cycling.

Conclusions

- Failure in static tests at different loading rates and creep tests at different loads under different constant humidity levels occurred at a constant deformation level.
- The failure deformation depended on the panel geometry.
- The failure mode was buckling.
- Finite element analysis of the corrugated board panels confirmed that buckling collapse occurs at constant deformation for a given panel geometry.

References

Bronkhurst, C. A. 1997. ”Towards a more mechanistic understanding of corrugated container creep deformation behaviour”. Journal of Pulp and Paper Science, Vol. 23, No. 4, pp. J174-J181.

Dagel, Y. and H. O. Brynhildsen. 1959. ”Tidens inverkan på papplådors belastningsförmåga” (in Swedish). Svensk Papperstidning, Vol. 62, No. 3, pp. 77-82.

Koning, J. W. and R. K. Stern. 1977. “Long-term creep in corrugated fibreboard containers”. Tappi, Vol. 60, No. 12, pp. 128-131.

Leake, C. H. 1988. “Measuring corrugated box performance”. Tappi Journal, Vol. 71, No. 10, pp. 71-75.

Leake, C. H. and R. Wojcik. 1989. “Influence of the combining adhesive on box performance”. Tappi Journal, Vol. 72, No. 8, pp. 61-65.

Nordstrand, T. 2004. “Analysis and testing of corrugated board panels into the post-buckling regime”. Composite Structures, Vol. 63, No. 2, pp. 189-199.

Crush damage of corrugated board and its effects on cyclic humidity creep performance of boxes

IAN R. CHALMERS
Senior Scientist, Scion, Private Bag 3020, Rotorua, New Zealand

Keywords: corrugated board, crush damage, box performance, shear stiffness, torsional stiffness, fluting medium, quality control

ABSTRACT
Most studies on corrugated box performance in the simulated service environment with 50-90% RH cyclic humidity are conducted either on undamaged boxes or boxes that are damaged to an unknown extent.

This study demonstrates that boxes made from corrugated board, which has been crushed to different levels, will perform quite differently in lifetime tests compared to undamaged board. Currently, nearly every box supplied from a corrugating plant has its flutes crush-damaged to some extent or other.

For this study, boxes were made from blanks crushed to varying degrees and the effect of this crush on machine direction (MD) torsional stiffness was measured using a torsional stiffness tester. Individual boxes were then subjected to a range of compressive creep loads in a cyclic humidity environment. As expected, the boxes that received greater crush damage performed significantly worse than less crushed or undamaged board. It was found on one set of samples, that board crushed to give a drop in MD torsional stiffness of about 47% resulted in a reduction in cyclic humidity lifetime of the boxes by 80% of the undamaged value. The crush damage and expected final performance of a box was accurately quantified by MD torsional stiffness while measures like ECT and box crush test (BCT) were poorly correlated. Board thickness measurements also significantly underestimated the amount of flat crush the boards had received.

INTRODUCTION
For storage and carriage situations utilising corrugated board where the contents require protection from compressive forces, heavy weight corrugating components are required. From experience, corrugated box manufacturers very often over-specify their raw materials to achieve adequate performance of their boxes in service. Many manufacturers do not realise that substandard performance in the field is often caused by poor manufacturing techniques that damage the boxes before they leave the corrugating plant. This reduced performance is caused by damage to the corrugated medium itself either by poor formation on the corrugator or by crushing in subsequent printing and converting operations. In many situations, the heavy duty components could be reduced in weight if the board was not damaged during conversion.

It has been shown many times (1) that failure of corrugated boxes in a stack occurs by compressive creep failure and in uncontrolled atmospheric storage conditions this creep is exacerbated by changing humidity conditions.

The strength of corrugated boxes is determined by most producers by measuring top-to-bottom compression strength (BCT) of the box in a large compression tester. To allow for creep influences in the real world, the BCT failure result is divided by a safety factor which is dependant on the method of stacking, the length of time the stack is required and the environmental conditions the box is subjected to. The safety factors vary from 3 to 8 for most box contents but can be up to 20 for high value contents. There are recommendations for safety factors in the literature (2) but they are largely determined in industry using experience with the boxes supplied in service.

This paper investigates the relationship between corrugated board crush damage and compressive creep performance in the service environment as described by a cyclic humidity regime from 50% RH to 90% RH over a twelve hour period.

EXPERIMENTAL

BOX PREPARATION
Corrugated box blank samples were supplied courtesy of Visy Board Carole Park (Queensland), full trials of four similar boxes were received. The components of one of the boards were a 205g/m² kraft single facer, a 170g/m² RF medium and a 205g/m² kraft double backer. The "C" flute combined board grammage was 695g/m² and obtained from the knife on the corrugator before any feed rollers likely to damage the board. The board blanks were supplied with different levels of crush being undamaged and damaged by compression between rollers at three different levels to provide four levels of crush. The box blanks were cut on a sample table using an X-Y plotter type knife and supplied flat on a pallet. The box size was 260 x 340 x 295 mm high. The boxes were erected using hotmelt adhesive on the join and a slightly oversize apple tray put into the box to make sure the panels all failed outwards.

STANDARD BOARD AND BOX TESTING
Standard corrugated board tests were performed using universal tensile tester type instruments, at the standard conditions of 23°C and 50%RH.

BCT testing was performed on the boxes by Visy at Carole Park (Queensland Australia) with the rest of the laboratory testing of standard corrugated board

properties and cyclic humidity compression creep tests being performed on the board and boxes at Scion.

BOX COMPRESSION CREEP TESTING

Scion's box compression cyclic humidity facility consists of a cool-room converted into a cyclic humidity chamber that cycles between 50% and 90% RH at temperatures typically around 12°C- but cycling as the RH control cycles. The box compression creep testers (Figure 1) utilise loadcell platforms for load measurement, linear potentiometers (Waycon LZW1-S-50) for strain measurement and air rams for load application. Room control, load application and data collection is via an Andover system which samples the loadcells, strain gauges and environmental conditions continuously and downloads the data every two minutes. Eight units are available.

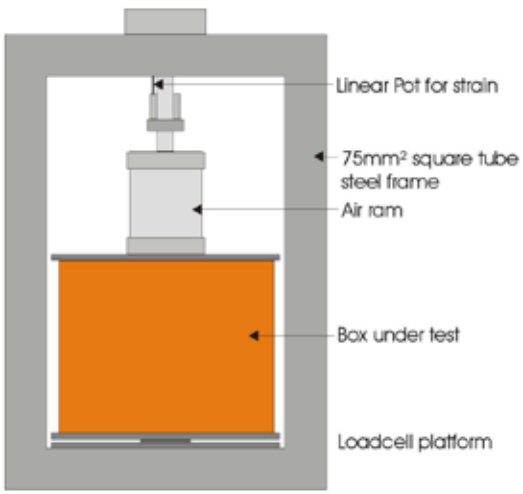

Figure 1: Box compression creep tester.

During testing, a constant load (under PID control from the loadcell) is applied to the box while the relative humidity environment is cycled from 50% RH to 90% RH with four hours at 90% RH and eight hours at 50% RH. It was found to take longer to dry the boxes down to 50% RH than to take them up to 90% RH. Twelve hour cycles are the shortest practically possible.

Figure 2 shows a typical box after failure. All boxes failed in this mode,which was aided by the oversize apple trays.

Figure 4 shows a plot of a completed test run with box loads, strains, RH and temperature data.

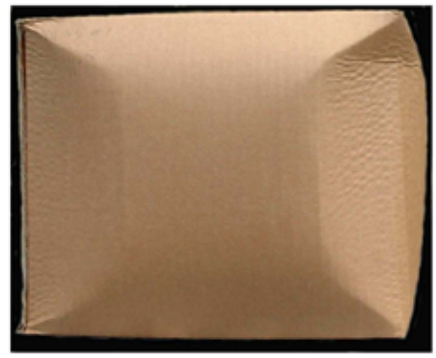

Figure 2: Failed box after compressive creep testing.

MD TORSIONAL STIFFNESS TESTING

To accurately gauge the quality of the corrugated board in the boxes, MD shear tests were performed using a torsional stiffness technique (Chalmers DST) (3). Samples for torsional stiffness testing were cut from the centre of the bottom flaps of each box. At this position where the box is sitting squarely on the bottom plate of the tester, there is no effect on the box compression test. The corrugated board sample taken is about 147mm long by exactly 25mm wide in the MD. This is placed in the tester then one end is displaced by a few degrees to initiate a natural oscillation. The angular frequency squared (ω^2), which is directly proportional to the torsional stiffness (3) is calculated. This oscillation is repeated four times and the average of the last two values taken as the result.

The commercial Chalmers DST is shown in Figure 3. For easier use in an industrial situation the ω^2 value is divided by 100 to bring the figure within the range of 3 significant digits with one decimal place and this unit is called the "board performance indicator" unit or bpi.

Figure 3: C1 Chalmers DST.

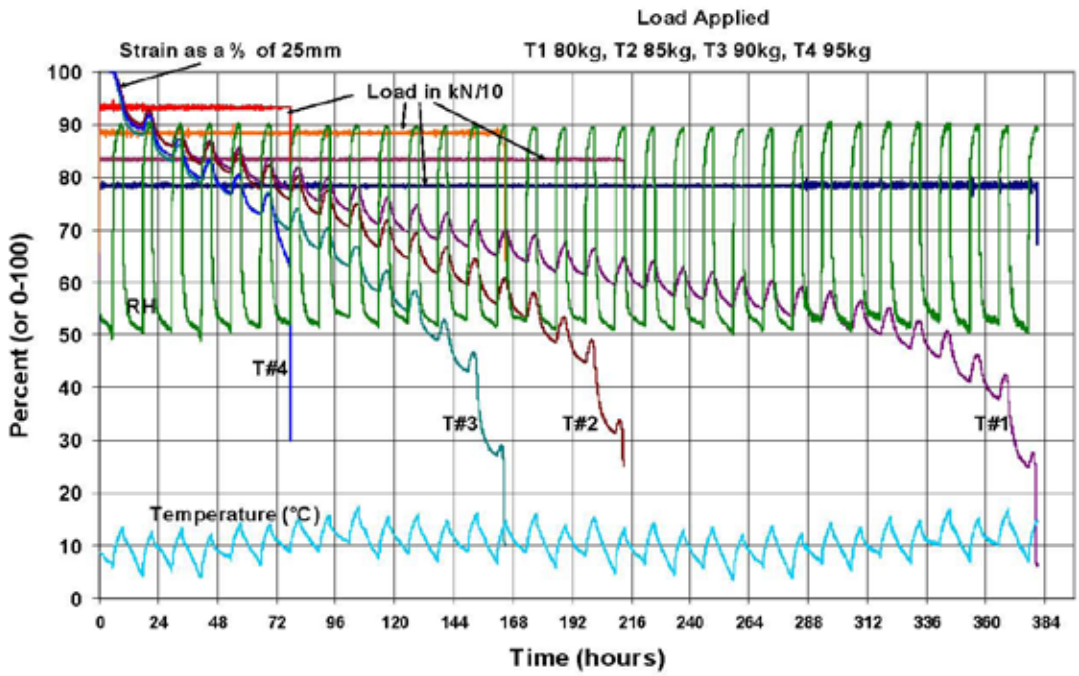

Figure 4: A plot of a completed test run with 4 boxes at different loads.

In Figure 4 the y-axis is a 0 to 100 scale and is used as a percentage for relative humidity (RH) and the compression strain. The compression strain gauge has 25mm travel and the strain is reported here as a percentage of that. The load is plotted as kN divided by 10, so for example 80 = 800kN. Temperature is read directly as °C. On the x-axis it can be seen that one cycle occurs every twelve hours. Unfortunately, due to the way the RH control system operates, it was not possible to hold the temperature constant so it follows the RH cycle and varies depending on the outside temperature.

RESULTS

THE EFFECT OF BOARD CRUSHING ON BOX PERFORMANCE.

Using the box compression creep testers (Figure 1, many tests were made on boxes made from corrugated board of two different compositions and with different degrees of crush damage. Figure 5 shows typical results for box lifetime as measured by the number of completed RH cycles versus compressive load. The power curve fit to the data is typically very good and power curves were used for all data evaluation.

Figure 6 shows typical box lifetime results for three trial boards with different levels of crush, expressed through the bpi, as measured on the DST. Figure 6 also shows normal curves for the BCT results on the same boxes.

The average DST results were 24 bpi, 21 bpi and 14 bpi; the bpi decreasing with increasing crush.

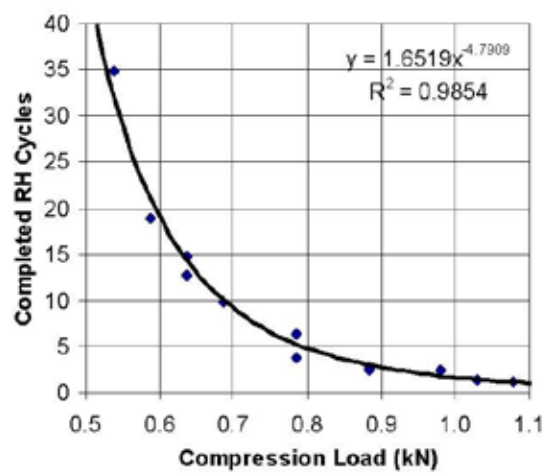

Figure 5: Lifetime curve for a 205/170/205 C flute box with no component board crush damage.

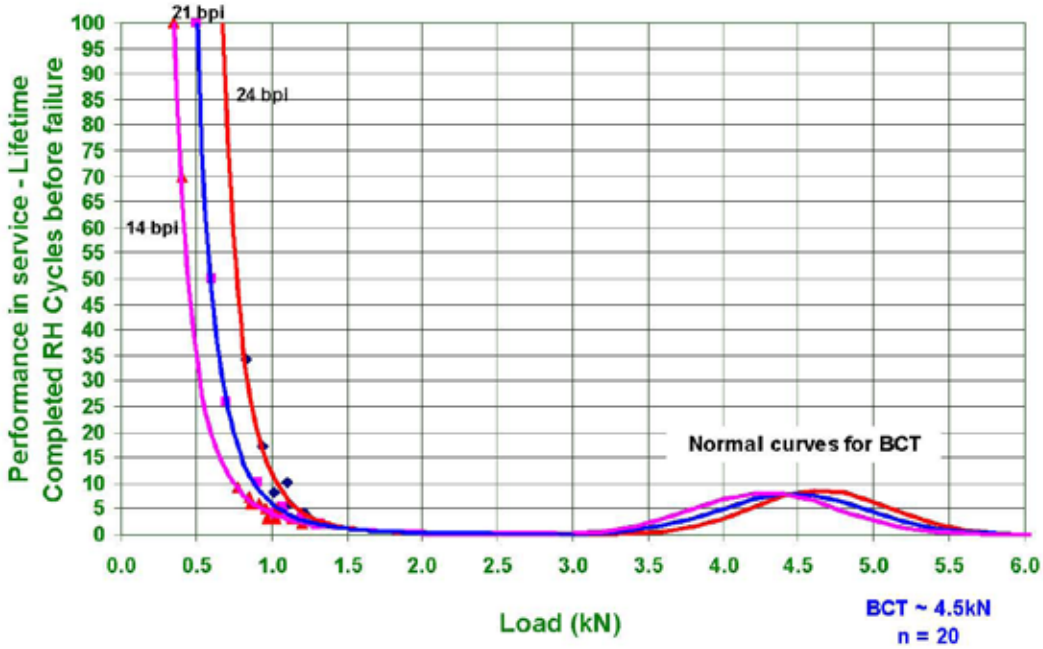

Figure 6: Two completely different data sets plotted on the same X axis being:- Cyclic humidity box performance vs BPI for 3 series of boxes with different crush levels (loads 0 to 2kN) plus BCT normal curves for the same boxes (loads above 3 kN).

STANDARD CRUSH DAMAGE TESTING

Historically, thickness measurements have been used to gauge the quality or effect of damage on corrugated board. However this method presents difficulties with spring back of the damaged medium and a less-than-clear relationship between thickness and damage. There is also statistical noise inherent in the test (4) and, of course, thickness is not a strength measurement. Figure 7 gives typical results for Standard corrugated board tests plus DST results on board crushed to 4 different levels.

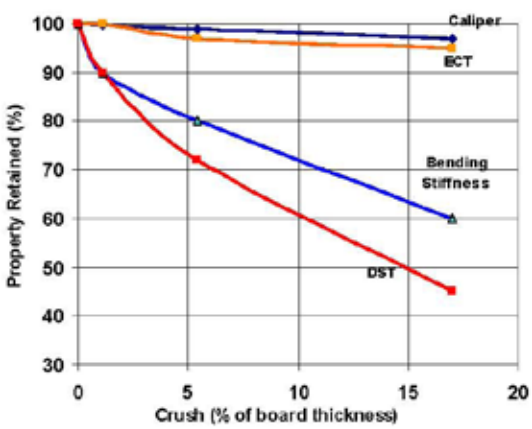

Figure 7: Standard board and DST testing on crushed board

Markström (5) also found similar results for corrugated board to those shown in Figure 7.

MD shear stiffness as determined by the torsional stiffness technique has been used at Scion (3) since 2004 to evaluate the effects of different levels of corrugated board damage that has occurred during board conversion. Many different studies at Scion since 2004 have shown that compared to standard board tests, MD torsional stiffness is a very sensitive and efficient way to measure board quality.

Table 1: Board parameters versus board crush

Percent Crush (%)	Caliper (mm)	ECT (kN/m)	BCT (kN)	DST (bpi)	Load for 30 cycles (kN)	Safety factor (ratio)
0	4.1	8.8	4.65	24	0.84	5.5
2	4.1	8.8	4.46	21	0.67	6.7
10	3.9	8.4	4.27	14	0.52	8.2

Table 1 shows the means for the standard board test and box performance data shown in Figure 6. It can be seen that Caliper, ECT and BCT are not as sensitive as DST or cyclic humidity creep to board crush.

In Table 1, if the box had to withstand 30 RH cycles to be satisfactory then column 6 gives the load that could be applied to just obtain this goal. Column 7 is the Safety factor obtained by dividing the column 6 figure into the associated BCT. Undamaged board has a much lower safety factor than 10% crushed board. In the service environment, the number of cycles required for satisfactory box performance will depend entirely on the job and service conditions.

These results are typical of several different studies and in an other similar exercise on another board, at the highest level of applied crush the DST value (bpi) dropped to 38% of the original value whilst the ECT dropped to 89% and the BCT to 88%. Once again showing the relative lack of sensitivity of these measures to crush damage.

DISCUSSION

Observing the effect of different levels of crush on corrugated board thickness, ECT, bending stiffness and MD torsional stiffness has shown MD torsional stiffness to be a very sensitive indicator of board damage.

BCT results also do not show the effects of board crush damage to be anywhere near as great as that indicated by MD torsional stiffness. The cyclic humidity box compression creep tests however showed significant differences in box performance of boards with different levels of crush as predicted by the MD torsional stiffness results for the board.

In the service environment, corrugated boxes do not fail under a quickly applied load as performed in a BCT test. It is known that there is very little creep component in a BCT test. This is also true for the ECT test and this is why the BCT results are more similar to an ECT result than that from MD torsional stiffness measurements.
In general, a loaded box will fail over time at a much lower load than indicated by a BCT test. This failure is exacerbated under cyclic humidity conditions (1). The internal shear strength of the corrugated board is much more likely to play a part in the creep failure over time and this is the most likely reason why shear stiffness is a better indicator of box performance in the service environment as modelled in cyclic humidity testing than either BCT or ECT.

REFERENCES

1. The international symposium series on moisture and creep effects on paper, board and containers. *Organised by Tappi, Appita, US Forest Products Laboratory, STFI, EFPG, Papro et al 1992 – 1999.*

2. Wright P.G, McKinlay P.R and Shaw E.Y.N *Corrugated Fibreboard Boxes, Their design, use, Quality Control and testing.* Edition 3 APM Packaging 1988.

3. Chalmers I.R. – A new method for determining the shear stiffness of corrugated board. *Appita Journal 59(5) Sep 2006 P357-36.*

4. Frank B. – Caliper or weighted caliper for evaluating boxes? *Corrugating International (Tappi) Oct 2004 P3-8.*

5. Markström H. – Testing Methods and Instruments for Corrugated Board. *Published by Lorentzen & Wettre 1988 Kista Sweden.*

Effects of medium strength properties and component rotation on corrugated endurance

Roman E. Popil, Barry Hojjatie*, Michael K. Schaepe†

Institute for Paper Science and Technology
Georgia Institute of Technology
Atlanta, Georgia 30332
USA

Abstract

This experimental study seeks to determine the impact of corrugated fluted medium physical properties, box component orientation, and hygroexpansivity on the cyclic humidity creep response. Several series of custom-made corrugated boards and test boxes were produced using the IPST pilot single-facer and manual double-backing. All sample series were subjected to static loads at about 20% of their failure load and placed in cyclic humidity environments ranging from 50 to 80% RH.

One set consisted of A-flute boards devised to examine the effects of out-of-plane shear, ECT, BCT, SCT, and fluting basis weight on lifetime. The basis weight of the fluted medium varied from 68 to 205 g/m^2 while the basis weight of the linerboard facing remained fixed at 205 g/m^2. This selection of materials varied the out-of-plane shear stiffness by a factor of three. Additionally, investigations included the role of horizontal flap edges in RSC container creep, rotation of component orientation, and the effect of barrier coating on C-flute HSC containers. Both ECT and BCT creep response to failure were measured for the A-flute variable medium basis weight series.

Variability of creep rate and lifetime for A-flute RSC containers was about 50% and for the equivalent boards of this series, it was approximately 25% about mean values. This variability in the data obfuscates firm quantification of relationships between lifetime and the selected physical properties including shear. However, in general, boards and boxes made with heavier basis weight medium substantially outperformed boards/boxes made with lighter weight medium when all are

* Valdosta State University, Valdosta Georgia, USA.
† Cargill, Cedar Iowa, USA.

loaded to the same safety factor. The secondary creep slope was inversely proportional to lifetime for all data sets. Measurement of ECT creep rate with its reduced variability compared to BCT creep appears to be a reasonable means to assess relative box performance.

Component orientation effects on creep used C-flute container samples prepared with rotation of linerboard, medium or both by 90 degrees to equalize hygroexpansivity. For the board that were produced with MD of all components in the direction of loading (linear corrugating), the lifetime of the RSC containers increased by a factor of two. We attribute this to reduced hygroexpansivity and higher strengths in the MD. Reduced hygroexpansive oscillations in creep response were also observed with application of experimental pigmented barrier coatings to the double-facing in another series of corrugated test boxes. In this case, the reduced vapor permeability resulted in boxes lasting several months compared to less than two weeks for untreated boxes.

The results of this study show that increased lifetime of the containerboard is obtained by increased homogenization of the component properties. Increased medium basis weight relative to the linerboard weight, component rotation (lateral or linear corrugating), application of vapor barrier coating, all increased lifetime significantly. These observations tend to support the concept of moisture sorption induced stress gradients in the board as being the dominant mechanism driving accelerated creep.

This page intentionally left blank.

Session 2
Moisture Flow

JY Zhu, Chair

U.S. Forest Service, Forest Products Laboratory

Paperboard is a porous material and so moisture migration affects its material properties but also the amount of protection it can offer in packaging applications. Moisture hysteresis, as measured in diffusion experiments, and hygroexpansion are quantifiable measures of moisture sensitivity that are affected by processing, chemical additives, and other means. Environmental moisture changes should be considered in the material selection procedure.

Steady-state moisture diffusion through corrugated fiberboard

Samuel V. Glass

U.S. Forest Service, Forest Products Laboratory, Madison, Wisconsin

Abstract

Moisture transfer through corrugated fiberboard is measured under steady-state conditions. Several types of corrugated fiberboard are investigated, differing in flute size, number of flutes, and component basis weights. The experimental apparatus consists of two chambers, each of which has control of temperature and relative humidity. A specimen is sealed between the chambers, a gradient in humidity is established, and the rate of mass transfer is measured on both sides of the specimen. Experiments are carried out at 25°C over a range of relative humidity levels. The measured water vapor fluxes through the various types of corrugated fiberboard are used to construct a model for the effective diffusivity of the components as a function of relative humidity.

The effect of hysteresis on moisture sorption of paperboard

Sergiy Lavrykov and B.V. Ramarao

Empire State Paper Research Institute
Department of Paper and BioProcess Engineering
State University of New York ESF
Syracuse, NY 13210

Paperboard is subjected to high magnitude stresses and large deformations in many converting operations. The use of finite element analysis can enhance understanding and provide a convenient optimization tool. Creep of linerboard under changing relative humidity reduced the performance of corrugated boxes and can lead to premature box failure. If accelerated creep can be further understood and robust models for its prediction can be developed, it is possible to engineer the products for better performance. Our objective is to analyze the impact of humidity cycling, sorption hysteresis and the resultant transient moisture distributions in linerboard on accelerated creep performance.

A model for accelerated creep of linerboard was developed based on (a) a transient moisture diffusion model accounting for multiple diffusion paths within the pore spaces and the fiber matrix and localized sorption dynamics, (b) a robust local sorption equilibrium including sorption hysteresis (c) temperature transients due to adsorption heat effects within the paperboard and (d) a suitable material model for the linerboard incorporating elasto-plastic response under different moisture and temperature conditions. We conducted a parametric study to identify the impact of sorption hysteresis on moisture induced creep. Experimental results on sorption hysteresis and transient moisture uptake are presented.

Analysis of the hygroexpansion of paperboard and small flute corrugated board by digital correlation of images obtained by x-ray microtomography

J. Viguié[1], P.J.J. Dumont[1], I. Desloges[1], S. Rolland du Roscoat[2], P. Vacher[3], E. Mauret[1], J.-F. Bloch[1]

1. Laboratoire de Génie des Procédés Papetiers (LGP2), CNRS / Institut polytechnique de Grenoble (Grenoble INP) - BP 65 - 38402 SAINT MARTIN D'HERES CEDEX 9 e-mail : pierre.dumont@efpg.inpg.fr

2. Laboratoire Sols-Solides-Structures-Risques (3S-R), CNRS / Universités de Grenoble (UJF & Grenoble INP) - BP 53 - 38041 SAINT MARTIN D'HERES CEDEX 9

3. Laboratoire SYMME, Polytech Savoie, Université de Savoie Domaine Universitaire BP 80439 – 74944 ANNECY-LE-VIEUX

Paperboard and small flute corrugated board are increasingly used as stiff packaging materials in food, cosmetic, and pharmaceutical industries. They form stratified materials where specific pulps are used for each layer. The integrity of board packaging can be affected by moisture changes that can be induced by a variation of the relative humidity of the ambient air. An increase of relative humidity from 20 to 80% may be related to a hygroexpansion of a board sheet varying in a range of about 0.2 to 2% in its plane and about 8 to 12 % in its thickness direction. In parallel, a decrease of mechanical parameters such as the Young's moduli from 30 to 50% may be noticed. The degree of beating, the kinds of pulps and the drying conditions are significant parameters affecting the hygroexpansion behavior. Nonetheless, scarce information is available on the micromechanisms of hygroscopic strains of paperboard and small flute corrugated board. This is the purpose of this experimental study.

Tests were performed on two 450 g/m² paperboards composed by 11 layers made up of virgin pulps for the first one and recycled pulps for the second one. A 450 g/m² corrugated board with G flutes was also studied. The evolution of the moisture content with respect to the relative humidity of the ambient air was measured using a specially designed apparatus at constant ambient temperature for various relative humidity cycles. The hygroexpansion of these materials was evaluated by two methods for the same changes in relative humidity. At the macroscopic scale, the dimensional in-plane variations of rectangular samples (dimensions of 150×15 mm²) were measured by a dedicated apparatus. Samples were cut along the machine and cross directions of the boards, as well as in off-axis directions. At the microscopic scale, the fields of displacement and strain of the fibrous networks were measured by using a Digital Image Correlation (DIC) method. For that purpose, images of cross-sections of volumes obtained by X-ray microtomography at ESRF (European Synchrotron Radiation Facility) were analyzed, as well as some images obtained using an Environmental Scanning Electron Microscope SEM (ESEM).

Experimental results permit to calculate the average in-plane and out-of-plane hygroexpansivities of the tested boards for variation ranges of the moisture content. Hygroexpansivities are found to be highly anisotropic. Moreover out-of-plane hygroexpansivities are preponderant compared to in-plane ones. The DIC method permits to reveal that the hygroexpansion is highly heterogeneous. For instance, in the case of a paperboard made up of virgin pulps, out-of-plane hygroscopic strains mainly occur in the core layers of samples. This might be related to the nature of the layers. Core layers are indeed essentially made of pulps obtained by a mechanical process whereas external layers are composed of chemical pulps.

Session 3
Component Behavior

Doug Coffin, Chair

Miami University, Oxford, Ohio

An accurate constitutive model for corrugated components is a fundamental element of packaging design. Several models exist and have their proponents; recently, those models easily incorporated in numerical analysis software, such as finite element programs, have gained increased acceptance. The ability to identify the effect of formation or periodic defects on constitutive behavior may allow more precise safety factors in packaging design formulations.

Formation and edgewise compressive creep properties

Christer Fellers, Anne-Mari Ohlsson, Anders Mähler, and Lucina Lason
STFI-Packforsk, Sweden

The mechanical properties of paper depend on unevenness of the paper on different structural levels. It is not yet known which structural level has the greatest influence on these properties but it is well known that the formation, chemical additives, and forming concentration plays a great role for the mechanical properties of paper. Few studies have reported actual magnitudes of the effects and it is of fundamental interest to increase the knowledge in this area.

The experimental paper machine FEX at STFI-Packforsk was used for the trials. Different formation levels were achieved by varying the forming concentration and by adding chemicals that increased or decreased the formation.

The focus of the investigation was on creep properties of which there are very little results available in the literature but also tensile and edgewise compressive properties were investigated.

The creep properties were measured in various constant or changing climates between 50 and 90% RH and were expressed in terms of isochronous and isocyclic creep curves and corresponding creep stiffness index values, respectively. An isochronous or isocyclic stress-strain curve may be viewed as a stress-strain curve at a specific time, i.e., 3 days or different number of cycles, i.e., 3 cycles (Panek, Fellers, Haraldsson 2004). From the initial slope of the curve, the isochronous or isocyclic creep stiffness may be extracted.

The following figure shows one significant finding.

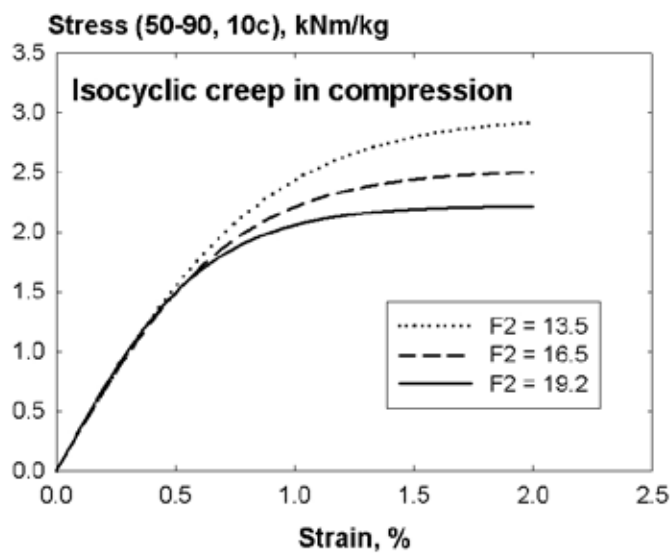

Isocyclic compressive creep curves for papers with different formation.

When the formation number increased (worse formation), no change in stress at a given strain was noted at small strains (constant isocyclic creep stiffness index).

Only at higher strains, a decrease in stress due to a worse formation was noted.

Reference

Panek, J., Fellers, C., Haraldsson, T. (2004) Principles of evaluation for the creep of paperboard in constant and cyclic humidity. Nordic Pulp and Paper Research Journal 19(2): 155–163.

Effect of moisture on defect interaction in paper and paperboard

J. Considine[1], J. Decker[2], D. Vahey[1], K. Turner[2], R. Rowlands[2]

1. U.S. Forest Service, Forest Products Laboratory, Madison, Wisconsin
2. University of Wisconsin, Madison, Wisconsin, USA

Poor formation in paper, as denoted by large local variation of mass, tends to reduce maximum tensile strength, but this reduction has not been quantified. The effect of grammage variation and moisture on tensile strength was studied by introducing carefully placed holes in tensile specimens made of five different paper materials and testing at static 50% and 90% RH. The point-stress criterion (PSC) [1] was used to estimate inherent defect size and predict maximum potential tensile strength for each RH level.

The goal of this research was to estimate inherent defect size and predict maximum possible tensile strength, i.e., tensile strength of a defect-free material made from the same furnish, with the PSC (point-stress criterion) and to examine the effect of relative humidity on these parameters. Successful completion of this work will provide the paper industry will necessary tools to perform cost-benefit analysis on papermachine modifications to improve formation and strength.

Five commercial paper materials were examined in this work. Their physical and mechanical properties are given in Table 1. Sheet thickness was measured with a Mitutoyo® (Kawasaki, Japan) 543-396B Digital Indicator equipped with a 4-mm-diameter ball tip. Elastic moduli and Poisson's ratio were obtained ultrasonically with a Nomura Shoji Corporation (Tokyo, Japan) Sonic Sheet Tester (SST). The SST is equipped with one sensor pair, which operates at 25 kHz; measurements were taken at 5° intervals by rotating the sample on a turntable.

Materials A and L are commercial unbleached kraft, single-ply linerboards. Material C is a commercial copy paper, containing about 8% ash. Material E is a commercial envelope paper. Material F is a commercial filter paper, manufactured by Whatman® International (Maidstone, Kent, UK) and identified as Chromotography Paper, Model 3MM CHR. The latter was chosen as it is 100% cellulose.

Table 1. 50% RH properties of materials

	A	C	E	F	L
Grammage (g/m^2)	268	76	92	187	209
Thickness (mm)	0.38	0.11	0.13	0.31	0.30
Density (kg/m^3)	717	721	734	603	688
E_{11} (GPa)	7.80	7.82	7.38	4.52	7.75
E_{22} (GPa)	3.71	2.56	3.40	2.12	3.73
G_{12} (GPa)	2.10	1.63	1.85	1.27	2.15
ν_{12}	0.20	0.17	0.23	0.18	0.23
E_{11}/E_{22}	2.10	3.05	2.20	2.13	2.08

Tensile tests were performed employing an Instron® (Norwood, Massachusetts) Model 5865 test machine equipped with line-clamp pneumatic grips. Specimens were 25 mm wide with a gage length of 125 mm. The test sequence started with a pre-load to 1 N at 12 N/min followed by displacement at a constant speed of 1.5 mm/min that continued to specimen failure. Load and grip displacement data were collected at 10 Hz. Tests were performed in one of two controlled environments, either 50% RH, 23°C or 90% RH, 23°C. To prevent possible long-axis buckling, all specimens were restrained transversely with glass plates. The two 100-mm-long glass plates that were used as restraints were separated by a gap of twice the specimen thickness and placed at the vertical center of the tensile specimen.

Tests were performed in the MD (machine direction) and CD (cross-machine direction) for each material. Six specimen geometries were tested: (1) standard tensile test, (2) 0.5 mm radius hole, (3) 1.25 mm radius hole, (4) 1.88 mm radius hole, (5) 2.5 mm radius hole and (6) 5.0 mm radius hole. Holes were centrally located in the specimens with an alignment fixture and made with an inside-taper hole punch.

The Whitney and Nuismer [1] failure criterion predicts that a sheet containing a central circular hole of radius *R* fails when the longitudinal stress, σ_y at a characteristic distance, d_0, from the hole edge achieves the unnotched tensile strength of the material in the y-direction, σ_U (i.e., failure occurs when $\sigma_y(R+d_0,0)=\sigma_U$). This theory is called the point-stress criterion (PSC) and intuitively suggests that failure occurs when the longitudinal stress throughout the distance adjacent to the edge of the hole, d_0, exceeds the unnotched tensile strength, σ_U.

The PSC can be formally written as

$$\sigma_U = \frac{\sigma_H^\infty}{2}\left\{2+\left(\frac{R}{R+d_0}\right)^2+3\left(\frac{R}{R+d_0}\right)^4-(K_T^\infty-3)\left[5\left(\frac{R}{R+d_0}\right)^6-7\left(\frac{R}{R+d_0}\right)^8\right]\right\} \qquad \text{Eq. (1)}$$

Where σ_H^∞ is the tensile strength of the material containing the central circular hole

K_T^∞ tensile stress concentration factor for an infinite plate

For our case, we have made two modifications to Equation (1). First, using the same technique as Kortschot and Trakas [2], the stress concentration factor for an infinite plate, K_T^∞, is replaced in Equation (1) by that for our finite-width specimens, K_T, according to the following equation developed by Tan [3]:

$$\frac{K_T^\infty}{K_T} = \left[2-(2R/W)^2-(2R/W)^4\right]/2+(2R/W)^6\left(K_T^\infty-3\right)\left[1-(2R/W)^2\right]/2 \qquad \text{Eq. (2)}$$

Where: *W* is the specimen width, 25 mm.

Second, we assume σ_U is an unknown. This last modification seems reasonable in that all commercial material have inherent defects due to the manufacturing process

We will show how inherent defect size and maximum possible tensile strength vary with humidity and relate these parameters to formation measurements.

References

Whitney JM, Nuismer RJ. (1974) Stress fracture criteria for laminated composites containing stress-concentrations. Journal of Composite Materials,8: 253-265.

Kortschot MT, Trakas K. (1998) Predicting the strength of paper containing holes or cracks with the point stress criterion. Tappi Journal,81: 254-259.

Tan SC. (1988) Finite-width correction factors for anisotropic plate containing a central opening. Journal of Composite Materials,22: 1080-1097.

Experimental Characterisation of Paper for Corrugated Board

M.E. Biancolini, C. Brutti, S. Porziani

Department of Mechanical Engineering, Tor Vergata University, Rome
Contact: biancolini@ing.uniroma2.it

Corrugated board is widely used to ship and keep any kind of goods across the entire world. Due to ecological and economical reasons, the main goal in box design is to fit required box performances while minimizing paper material consumption.

An efficient utilisation of raw materials can be achieved if all design parameters affecting the performance of a container, as box dimensions number of layers and paper material, are carefully controlled. Predictive tools that rely on design formula or complex structural models require a complete characterisation of paper material constants.

Paper, due to its manufacturing process, can be treated as an orthotropic, fibrous material. As can be seen in Fig.1, it is possible to identify three main directions: Machine Direction MD, Cross Direction CD, and Thickness Direction TD (those direction can be also be applied in corrugated cardboard panels). Using this paper model and referring to the paper reference coordinate system, a complete characterisation of paper can be achieved considering five elastic constants and five strength constants. For an orthotropic 2D fibrous material, stress strain relation can be expressed as

$$\begin{pmatrix} \sigma_1 \\ \sigma_2 \\ \tau_{12} \end{pmatrix} = \begin{bmatrix} \frac{E_1}{1-\nu_{12}\nu_{21}} & \frac{\nu_{21}E_1}{1-\nu_{12}\nu_{21}} & 0 \\ \frac{\nu_{12}E_2}{1-\nu_{12}\nu_{21}} & \frac{E_2}{1-\nu_{12}\nu_{21}} & 0 \\ 0 & 0 & G_{12} \end{bmatrix} \begin{pmatrix} \varepsilon_1 \\ \varepsilon_2 \\ \gamma_{12} \end{pmatrix} \qquad \text{Eq. (1)}$$

Where index 1 refers to MD and index 2 refers to CD (stresses and strains in TD are neglected considering a 2D material). Matrix components in Eq. 1 can be identified performing simple tensile tests with a general purpose testing machine (Fig. 2) on differently oriented paper specimen (fig.4): for each material several specimens in three directions (0°-Machine direction, 90°-Cross direction, 45° direction) by means of a CNC cutter has been extracted. Elastic constants were computed as reported in Table 1. Five strength constants have been computed for each paper: tensile strength in CD and MD, compression strength in CD and MD, and shear strength (Table 2). Strength constants reported in Table 2 can be used to verify tensional state of paper subject to a specific load, by means of an appropriate failure criterion, such as Tsai-Wu or Tsai-Hill, which can take in account paper's different behaviour in both principal directions. A wide test campaign has been carried on, based on the actual papers used at Smurfit-Kappa Anzio Plant. The complete range of paper tested is reported in Table 3. Computed constants are reported in Table 4 and Table 5.

Table1. Elastic constants

E_1	Young Modulus from 0° specimen
E_2	Young Modulus from 90° specimen
G_{12}	Theoretical relation: $G_{12} = \left(\frac{2\nu_{12}}{E_1} - \frac{1}{E_1} - \frac{1}{E_2} + \frac{4}{E_{45°}} \right)^{-1}$
ν_{12}	Empirical relation: $\nu_{12} = 0.293\sqrt{E_2/E_1}$
ν_{21}	Theoretical relation: $\nu_{21} = \nu_{12} \cdot E_2/E_1$

Table 2. Strength constants

σ_{1t}	tensile strength in MD	Ultimate stress in 0° specimens
σ_{2t}	tensile strength in CD	Ultimate stress in 90° specimens
σ_{1c}	compression strength in MD	SCT tests
σ_{2c}	compression strength in CD	RCT tests
τ_{12}	shear strength	Empirical relation: $\tau_{12} = \sqrt{\sigma_{1c} \cdot \sigma_{2c}}$

Table 3. Paper commonly used for facings. Class names following GIFCO nomenclature.

Code	Grammage [g/m^2]	Class	Code	Grammage [g/m^2]	Class
KB3	140	White Kraft	F2	112	Fluting
KB5	175	White Kraft	F4	140	Fluting
K3	140	Kraftliner	S4	127	Semichemical
K5	170	Kraftliner	S6	150	Semichemical
LB3	135	White test 2	S9	175	Semichemical
LB5	185	White test 2	SS4	130	Semichemical
TB3	145	White test 3	SS6	160	Semichemical
T2	115	Testliner 4	SS9	180	Semichemical
T3	135	Testliner 4			
T5	185	Testliner 4			
L3	150	Testliner 3			
L5	185	Testliner 5			
L6	200	Testliner 6			
KL3	140	Testliner 1			
KL5	200	Testliner 1			
KL6	230	Testliner 1			

Table 4. Elastic constants for tested papers.

	Density [kg/m^3]	E_1 [Mpa]	E_2 [Mpa]	G_{12} [Mpa]	ν_{12}	ν_{21}
K 5	656.49	3678	1473	1361	0.185	0.074
K 3	638.53	4363	534	579	0.103	0.013
TB 3	684.65	2567	1129	746	0.194	0.086
LB 5	817.26	4024	2036	1172	0.208	0.105
LB 3	807.22	4619	1611	1166	0.173	0.060
KB 5	800.48	3280	1978	1138	0.228	0.137
KB 3	805.75	4874	2257	1711	0.199	0.092
KB 3	696.43	3262	1672	1031	0.210	0.107
T 5	548.48	2577	1354	758	0.212	0.112
T 3	614.04	3490	1273	980	0.177	0.065
T 2	610.11	3822	1256	971	0.168	0.055
L 6	649.71	2673	1759	984	0.238	0.156
L 5	643.27	2646	1589	914	0.227	0.136
L 3	648.71	3576	1607	1023	0.196	0.088
KL 6	655.14	2803	1723	964	0.230	0.141
KL 5	653.07	3167	1577	1129	0.207	0.103
KL 3	675.47	4134	1806	1122	0.194	0.085
SS 9	645.19	2968	1643	1054	0.218	0.121
SS 6	683.04	3752	1689	1027	0.197	0.088
SS 4	689.47	4179	2124	1288	0.209	0.106
S 9	645.45	3396	1764	1014	0.211	0.110
S 6	665.24	3980	1876	931	0.201	0.095
S 4	648.48	4245	1965	1241	0.199	0.092
F 4	569.92	3858	801	618	0.134	0.028
F 2	593.75	3600	960	733	0.151	0.040

Table 5. Strength constants for tested papers.

	σ_{1t} [Mpa]	σ_{2t} [Mpa]	σ_{1c} [Mpa]	σ_{2c} [Mpa]	τ_{12} [Mpa]
K 5	56.16	15.38	9.45	6.80	8.02
K 3	72.80	17.65	9.08	5.18	6.86
TB 3	18.41	6.50	5.95	4.53	5.20
LB 5	39.37	10.80	8.96	7.00	7.92
LB 3	37.65	9.54	7.64	5.78	6.64
KB 5	48.62	12.39	11.04	8.96	9.95
KB 3	66.58	19.40	10.12	8.32	9.17
KB 3	46.54	12.16	9.81	6.88	8.21
T 5	18.95	7.55	6.66	4.92	5.72
T 3	25.31	6.89	6.27	4.44	5.27
T 2	25.29	7.29	5.49	3.64	4.47
L 6	32.62	10.92	9.24	6.94	8.01
L 5	26.55	8.96	8.37	6.77	7.53
L 3	30.01	9.51	7.93	5.98	6.89
KL 6	48.79	12.37	11.08	8.06	9.45
KL 5	48.12	11.39	11.14	8.45	9.70
KL 3	40.58	11.97	9.75	6.98	8.25
SS 9	35.39	10.61	8.65	6.88	7.71
SS 6	33.67	11.31	7.95	6.17	7.00
SS 4	42.77	13.16	8.36	6.26	7.24
S 9	33.23	11.36	8.21	6.76	7.45
S 6	38.09	11.89	7.28	6.17	6.70
S 4	38.07	12.07	6.87	5.38	6.08
F 4	32.44	4.35	6.29	3.66	4.80
F 2	22.27	5.78	4.89	3.06	3.87

Figure 2. Testing Machine

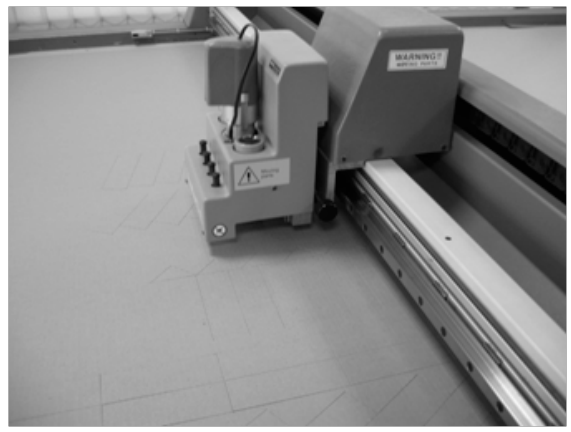

Figure 3. Specimen preparation at Smurfit-Kappa Anzio Plant

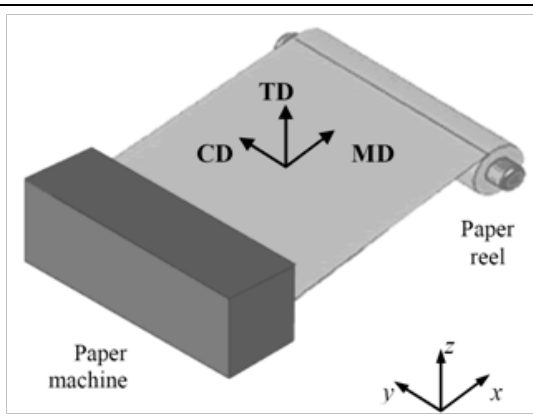

Figure 1. Paper reference coordinate system

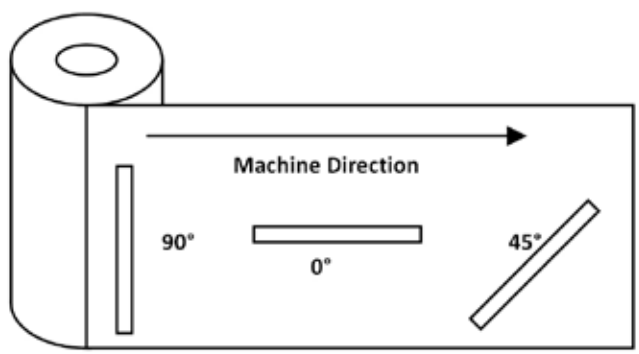

Figure 4. Specimen orientations.

References

[McKee1963] - McKee, C.; Gander, J. W. & R., W. J. “Compression strength formula for corrugated boxes” - Paperboard Packaging, 1963, 55, 149-159

[Baum1981] - Baum, G.; Brennan, D. & Habeger, C. “Orthotropic elastic constants of paper” - TAPPI Journal, 1981, 64, 97-101

[Bronkhorst2003] - Bronkhorst, C. “Modelling paper as a two-dimensional elastic-plastic stochastic network” - International Journal of Solids and Structures, 2003, 40, 5441-5454

[Campbell1961] - Campbell, J. “The in-plane elastic constants of paper” - Australian Journal of Applied Sciences, 1961, 12, 356-357

This page intentionally left blank.

Session 4
Industry Efforts

Ian Chalmers, Chair

Scion, Rotorua, New Zealand

Ultimately, the paper and paperboard manufacturing industries need to educate their customers on the effects of moisture-induced behavior of cellulose-based materials. Several manufacturers have modernized mills to create unique linerboards or mediums that behave impressively in variable moisture environments. Such product differentiation improves profit margins and retains customers. By providing knowledge of paper behavior during converting or printing, customers recognize methods to reduce losses in their processes. Novel materials, e.g., paperboard with vapor barriers, offer alternatives to products that are ultimately landfilled.

End-user focused creep

Angelica Wikström

Billerud AB, Grums, Sweden

Abstract

Billerud is a packaging paper company. The company's business concept is to offer demanding customers packaging material and solutions that promote and protect their products - packaging that is attractive, strong and made of renewable material.

This work is focused on corrugated materials. The performance of a corrugated box used for e.g. fruit and vegetables or over seas transport is highly dependent on the ability of the included paper components to withstand compressive forces for long times during transport and storage in high humidity.

Billerud has studied long time performance for paper and boxes for more than a decade and is now aiming to develop a transparent and comprehensible standard for compressive creep of fluting paper. Our method, CCT_{10} is defined as the constant CCT-load a test strip can withstand for ten days in constant high humidity before collapse. Concluded is that virgin fibres are decisive for the ability to withstand creep.

Also presented is a project where the supply chain from grower to retailer for oranges, exported from Spain to Sweden was surveyed. The creep properties for boxes and stacked boxes were tested and based on the results, a construction with better performance and 15 % less weight than the average solution on the market was introduced. The new construction resulted in a total reduction of transport induced waste at the same time as 200 kg less paper had to be transported in each truck.

Introduction

Billerud is a packaging paper company. The company's business concept is to offer demanding customers packaging material and solutions that promote and protect their products - packaging that is attractive, strong and made of renewable material.

Corrugated boxes are frequently subjected to long time compressive forces during shipment and storage. In a review by Coffin, Kivlin is cited already in 1935 describing the problem of containers failing after a time under steady application of a load relatively low compared to the maximum test load which was subjected without failure [1]. Often, the contents such as fruit and vegetables require high relative humidity. Therefore, it is important to evaluate the long time performance of the components of the board and paper components in humid climate.

Creep is defined as the slow continuous deformation of a material subjected to constant load during a long time period. Billerud has been working with creep evaluation for more than a decade. An earlier approach called the "lead bucket method" was based on the ring crush test (RCT). The test piece was placed in a RCT holder and mounted under a bucket; which was filled with lead until desired load. Multiple buckets were placed in a climate chamber and the collapse of the test pieces were recorded by a video camera. A picture of the setup can be found in Figure 1 [2]. Billerud´s currently used method is instead based on the corrugated crush test (CCT).

Figure 1: The setup for the "lead bucket method", based on RCT for creep studies of fluting paper. To the right several rigs placed in a climate chamber.

CCT_{10}

The CCT_{10} value is defined as the corresponding CCT load the material can carry for 10 days (240 hours) in 20°C and 90 % rh. The method is based on standard CCT testing supplemented with a compressive tester able to hold constant load and record the deformation of the sample placed in a climate chamber.

Apparatus

Test apparatus used are cutting device, laboratory corrugator and holder defined in the SCAN 42 standard for CCT value and CCT index. Additionally, a compressive tester with parallel platens able to hold a constant load with an accuracy of ± 0.5 N, continuously recording the deformation of the sample and a climate chamber holding a constant climate of 20°C ± 1°C and 90 % ± 2 % relative humidity are needed. The compressive testers used in this study are Zwick/Roell Z010 (Ulm, Germany) and the climate system was provided by CTS (Alingsås, Sweden).

Test procedure

Test stripes were prepared in accordance with SCAN 42 standard. The samples were conditioned in 20°C, 90 % rh until moisture equilibrium was reached and then mounted in the holder and placed between the platens in the compression tester. The platens were set to move at a speed of 10 mm/min up to a preload of 10 N. Immediately after the preload was reached, the compression force was increased by 100 N/s until decided load was achieved The load was held constant until collapse of the sample could be detected.

For each quality tested at least eight stripes were tested. The first load was chosen to correspond to a value of about 40 % of the standard CCT result. The testing there after was following a scheme where the compression load was gradually reduced to find the load the test piece could carry for 10 days (240 h).

Figure 2: CCT-holder and compression tester.

Evaluation and obtained results

Figure 3 below shows a typical creep response of a test piece of semi-chemical fluting subjected to a load of about 30 % of the ordinary CCT value measured in standard climate (23°C, 50 % rh).

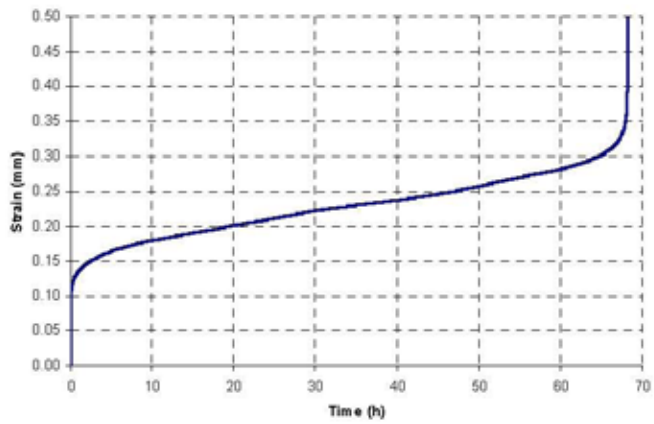

Figure 3: Typical creep response curve.

From the obtained creep curves, the time to collapse was plotted against the applied load. An exponential model was fitted to each set of data. Figure 4 below shows the fitted curves from creep measurements on three paper samples, one kraft flute, 175 g/m^2 containing an unknown fraction of recycled material and two of our 100 % virgin fibre semi chemical flute, 140 and 130 g/m^2. The fitted curves gave r^2-values for the exponential fittings ranging from 0.90 – 0.97. In table 1, the CCT-values measured in standard climate and the CCT_{10}-values calculated from the fittings are presented.

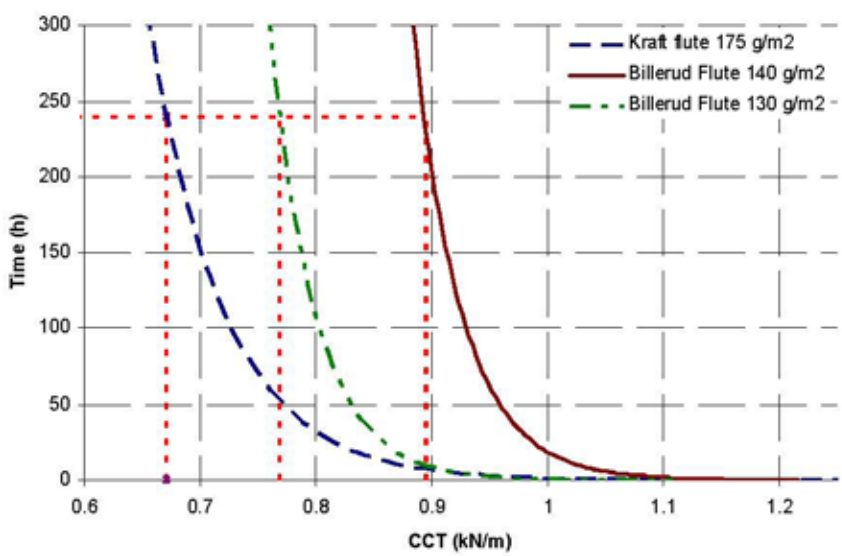

Figure 4: Fitted creep curves for one kraft flute and two Billerud Flute® papers with different grammages.

Table 1: Results from standard and creep testing

	Kraft flute 175 g/m²	*Billerud 140 g/m²*	*Billerud 130 g/m²*
Standard CCT	3.07 kN/m	3.11 kN/m	2.85 kN/m
CCT_{10}	0.67 kN/m	0.89 kN/m	0.77 kN/m
Remaining strength	22 %	27 %	29 %

The 140 g/m^2 Billerud Flute® and the 175 g/m^2 Kraft flute had approximately the same strength in standard testing and the lower grammage flute about 7 % lower. The creep evaluation however shows 33 and 15 % better long time performance for the Billerud grades. The results show the possibilities of reducing weight of the corrugated board and at the same time enhance the performance.

Discussion about the method

Our approach for developing a creep evaluation method for fluting paper is to make it as simple and comprehensible as possible using commercially available equipment. Using the time to collapse instead of more indirect methods is indeed very time consuming, but for us necessary. Few of our customers have the time or possibility to get a deeper understanding of the mechanisms of creep and methods for evaluating these properties. Therefore a straight forward method, based on properties already used by the converters is desirable. We need to speak the same language and show clearly what performance they can expect from the paper they buy.

As described we use constant and not cycling climate in our evaluation protocol. This has several reasons. One is transparency and comparability. Obtaining a stable adjusted climate is demanding and involving ramping and cycling further complicates the possibilities of comparisons between different labs. Another reason is that constant climate in fact better mimics the real conditions our paper faces. Leinberger [3] showed that the humidity variations of 40-50 % used in many creep evaluation methods are not occurring on sea transport. On land such variations can occasionally be seen in unrefrigerated storages and transports. However, as more then half of the semi chemical fluting Billerud produce is for the segment Fruit and Vegetables, the climate in refrigerated ambience is of greater interest. Our own measurements on refrigerated transports are further described below. A third reason for using constant climate is highlighted by Coffin [1]. When cycling the moisture, at least three components of strain is involved; the creep strain, the change in elastic strain and the hygroexpansion. Too many things are going on at the same time.

Value chain project – using creep evaluations to improve orange box performance

Problems with collapsed Spanish orange boxes were identified at the retailer Everfresh in Helsingborg. Collapsed pallets imply severe economical losses in terms of damaged fruit and extra manual work at the retailer (see figure 5). The total market for fruit and vegetables in Europe has a value of approximately 100 000 000 000 €. Losses are about 10 % or 10 000 000 000 €, and approximately 25 % is caused by unsatisfactory packaging. Besides economical consequences, the packaging related losses of 2.5 % of the total sales volume also have social and environmental consequences. The damages goods will not reach the consumer and has thus been produced, transported and consumed resources all in vain,

Figure 5. Collapsed pallet, causing loss of fruit quantities and requires manual work.

Methods

The value chain project started with analysing the supply chain from the converter to the retailer and the demands the packaging meets. Loggers from TinyTag were placed on pallets to continuously measure the temperature and humidity in the transports. A review of the box design was performed and both paper grades and minor structural details were changed. Also the converting of the corrugated board was supervised in order to reduce e.g. warp of the sheets.

After identifying the transportation and storage time of the boxes and the climate they were to be subjected to, a range of box compression tests (BCT) were performed on compressive testers from Zwick/Roell. Both the new boxes and the old reference boxes were subjected to standard BCT testing in standard climate and in humid climate defined as 23°C, 85 % rh. Also, testing on two boxes stacked on top of each other was performed, as were creep measurements until collapse of single boxes and boxes stacked together. The creep value was here defined as the load the boxes were expected to withstand for seven days (168 h).

Results

An example of a climate log is shown in figure 6. The average humidity on this five days transport in a hard top refrigerated truck was 93 % rh.

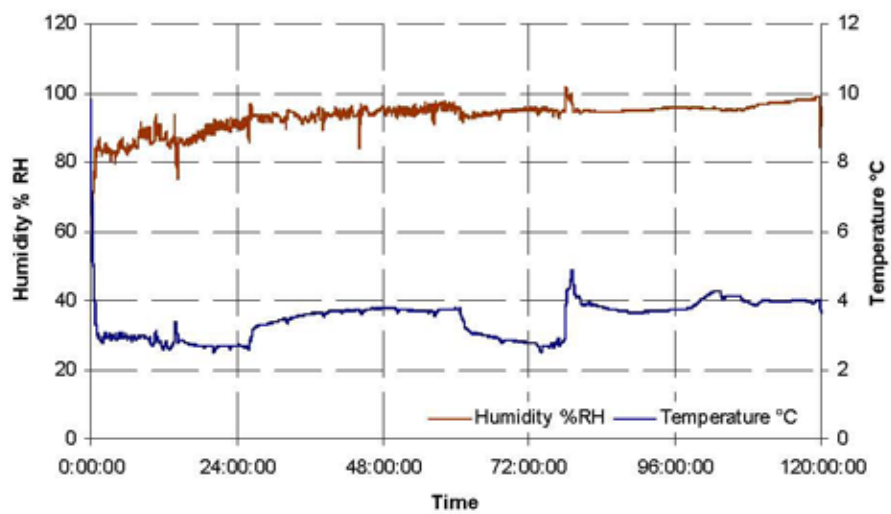

Figure 6: Logging the relative humidity and temperature in a refrigerated truck from Valencia, Spain to Helsingborg, Sweden.

In figure 7, the results from the different BCT tests are presented. The reference box showed higher strength in standard testing, but testing in humid conditions showed the opposite result, as did stacking experiments and creep measurements.

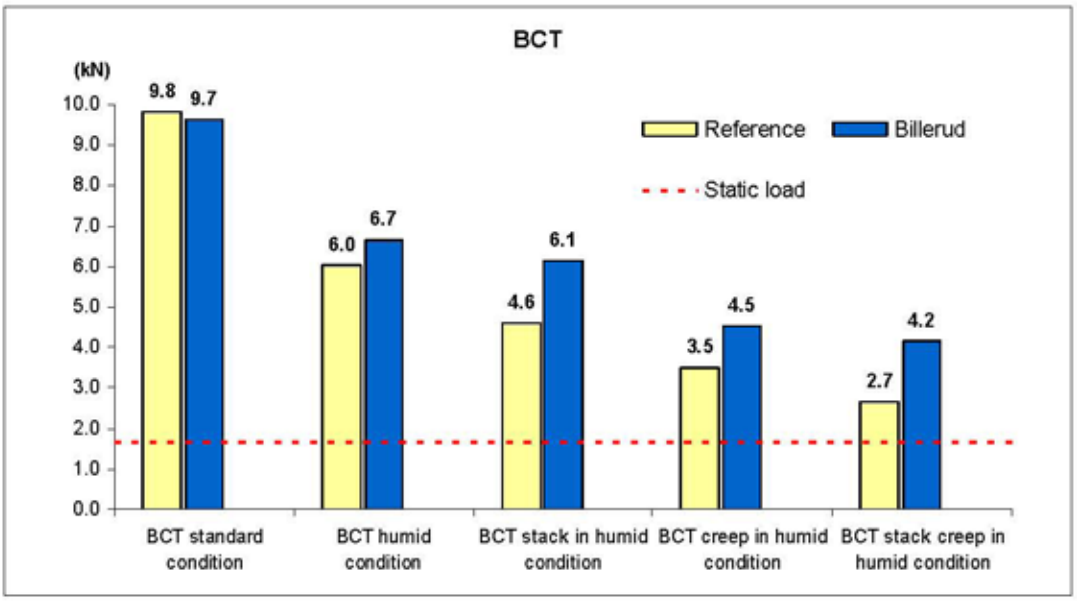

Figure 7: Showing the values of both standard BCT and creep values for previous used reference box and the box evolved in the project.

The red dashed line in the figure shows the static load the boxes at the bottom of the pallets are subjected to. Adding the dynamic forces the pallets face during the transport, the safety factor of six for the boxes is almost gone for the reference boxes, with collapses as a consequence.

Last year, 50 000 boxes with the new composition was transported from Valencia to Helsingborg. The weight reduction of the boxes in this project was 15 % as compared to the average box transporting Spanish oranges to Scandinavia. The results were a total elimination of transport damages – no claims were raised and a reduction of over 200 kg paper transported in each truck.

In times of limited resources, serious environmental problems and continuously growing populations all produced food should have the possibility to reach the consumer. To achieve this, we must use our knowledge to optimize the value chain and produce efficient packaging that fulfil their function.

References

[1] Coffin, D.W. ”The Creep Response of Paper” 13th Fundamental Research Symposium (September 2005)

[2] Westberg R. “A laboratory study concerning how different steps in the manufacturing process influence the strength- and creep properties of fluting” Masters Thesis, Karlstad University, June 2001

[3] Leinberger, D. “Temperature and Humidity in Ocean Containers” Ocean Container Temperature and Humidity Study (February 2007)

Correspondence:
Angelica Wikström, Lic. Eng.
Development Engineer
Billerud AB
Storjohanns väg 4
SE-664 28 GRUMS, Sweden
Tel. +46 730 25 10 33
E-mail: angelica.wikstrom@billerud.com

EFFECTS OF STRAIN RATE AND INITIAL STRAIN ON THE STRESS RELAXATION OF WET PAPER

[1]Pasi Kekko, [2]Jarmo Kouko, [2]Elias Retulainen, [3]Jussi Timonen

[1]Metso Paper, Inc., [2]VTT Technical Research Centre of Finland, [3]University of Jyväskylä

Abstract

Comprehensive experimental results are reported for the stress relaxation properties with varying strain rate and initial tension of wet newsprint, fine paper and LWC base paper. The samples analyzed were taken from wet webs on a pilot paper machine, or were hand sheets. High strain rates are needed so as to simulate web tension relaxation after draws in modern paper machines.

Wet and dry paper display similar stress relaxation behaviour. In wet paper relaxation can be described by a logarithmic time dependence, and the relaxation rate depends on the initial tension. The relaxation rate of wet hand sheets is different for chemical and mechanical pulps. As a function of initial tension, the relaxation curves for all chemical pulps fell on a single curve. The same was true for mechanical pulps, but the resulting relaxation curve was below the one for chemical pulps.

The initial tension was found to be proportional to the logarithm of strain rate independent of the span length, while the residual tension was found to decrease at high strain rates. It is thus evident that the mechanisms that govern tension build up are different from those in stress relaxation.

Introduction

It is well known that the rate of relaxation depends on the initial stress. However, relaxation rate also depends on the strain rate used for creating the initial stress. The objective of this study was to determine such strain-rate effects on the stress relaxation properties of never-dried wet paper for elongation speeds in the interval 0.001-1.0 m/s. Stress relaxation tests were done for different furnish compositions at several initial strains and strain rates.

Stress relaxation of paper is a very common phenomenon in papermaking and paper processing. Process speed may vary which affects the relaxation of paper web. The effect of initial strain rate on stress relaxation has been discussed only in a few articles [1-3, 6]. Viscoelastic material models may be used to handle the effect of strain rate, but typically the stress relaxation behaviour of wet paper as a function of preceding strain rate has not been systematically studied.

The relaxation of dry paper has been studied by several authors. Johansson and Kubat [2] modelled the relaxation process with a logarithmic time dependence. Okushima [6] found that after a relaxation of $6*10^5$ s the stress in dry paper did not depend on the strain rate (0.067 and 0.67 %/s). For dry paper Craven [5] found that relaxation rate depended only on the initial load.

Stress relaxation of wet paper has been studied much less than that of dry paper [3, 4, 7]. Kouko et al. found that increase of strain rate lead to higher initial tension in stress relaxation, and also to a higher relative stress relaxation after 0,475 s relaxation time. Higher stresses after a short relaxation period were typically detected after increasing the strain rate [3].

Jantunen [4] found that dependence of relative tensile stress relaxation (after a short time period of 300 or 600 ms) on dry solids content was quite weak in a dry solids content range of 35% to 75 %. Above the 75 % dry solids content, the relaxation rate declined. An increasing reinforcing pulp (BSK) content reduced the relative tensile stress relaxation when the dry solids content was less than 80 %, and the effect was already detected with a small amount of reinforcing pulp. Increase of initial strain, which automatically means increase of initial stress, increased the relative tensile stress relaxation over a wide range of moisture contents [4].

Draw (ε_{draw}) plays an important role in the paper and printing machines. It is the relative speed difference of adjacent supporting points in the web [10], e.g., of a roll (speed v_1) and the following roll (speed $v_2 > v_1$),

$$\varepsilon_{draw} \approx \frac{v_2 - v_1}{v_1} \quad . \qquad (1)$$

The open draw elongation speed v_{draw} is correspondingly

$$v_{draw} \approx v_2 - v_1 \qquad \text{[m/s]}. \quad (2)$$

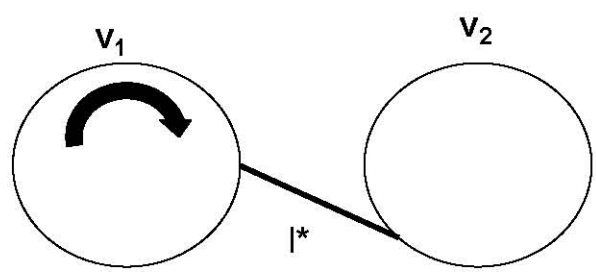

Figure 1. Open draw between two adjacent rolls, $v_2>v_1$. The length of the draw is l*.

Speed difference between the press section and the first dryer group typically causes the most important draw (2-4 %) imposed on wet paper. The level of this draw controls the stress and runnability of the web at the beginning of the dryer section [10].

The strain rate imposed on the web in a paper machine is determined by the elongation speed and the distance between the related rolls. For example, if the press section is running at 1200 m/min and the draw is 2-4 %, the corresponding elongation speed is 0.4-0.8 m/s. These are the kind of elongation speeds that one should be able to produce also in the laboratory in order to gain information relevant for the actual production processes.

A relative strain speed can be defined as

$$v_{relative} = \frac{v_{draw}}{l*} \quad . \qquad (3)$$

For a speed of 1200 m/min and a draw of 2 %, the relative strain speed is v(l*=1 m)=40 %/s, and v(I*=0.1 m)=400 %/s.

Possible causes for runnability disturbances in the dryer section are indicated in Fig. 2. If the paper web has a poor tension (dashed line), the web follows the dryer cylinder and runnability is poor. But if the tension is high enough, the web remains straight and follows the dryer fabric, and runnability is good.

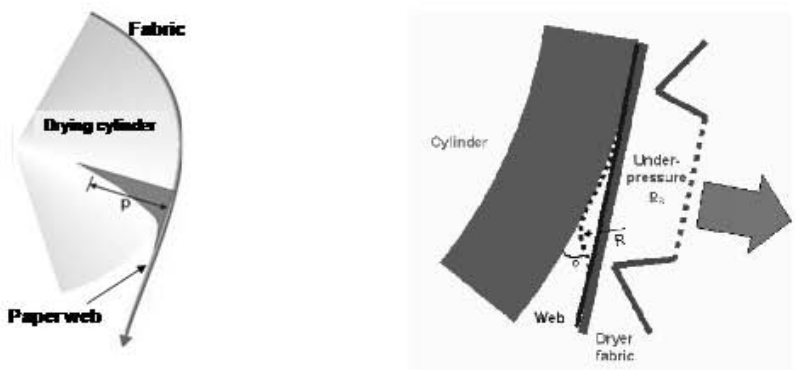

Figure 2. Web behaviour in the gap opening of a dryer cylinder.

Materials and methods

The samples studied were taken from wet webs produced on a pilot machine during LWC, newsprint and fine paper runs. The structure and furnish compositions of the webs were typical for these paper grades. Same furnishes were also studied in the form of laboratory sheets. Pilot machine paper was measured only in the machine direction (MD). Paper tension [N/m] was used instead of stress because the thickness of wet web was difficult to determine.

Tests for varying elongation speed were done with the C-Impact tester [8] except for the highest elongation-speed (1 m/s) in which case they were done with the Impact tester [7].

Results

From the stress relaxation curves the initial tension, *T(t=0 s)*, the highest tension before relaxation, and the residual tension, *T(t=0.475 s)*, the tension after 0.475 s relaxation, were determined.

The strain rate r can be determined from the elongation speed v such that

$$r = 100 \cdot \frac{v}{l} \text{ [\%/s]}, \qquad (4)$$

where l is the length of the sample (a strip). It is often advantageous to use a dimensionless strain rate r^* which can be defined as

$$r^* = \frac{r}{r_0}, \qquad (5)$$

in which the reference strain rate can be chosen, e.g., such that $r_0 = 1$ %/s.

It is evident from Fig. 3 that the initial tension *T(t=0 s)* in the relaxation tests is proportional to the logarithm of strain rate independent of the length of span, while the residual tension *T(t=0.475 s)* first stays more or less constant and then decreases at high strain rates.

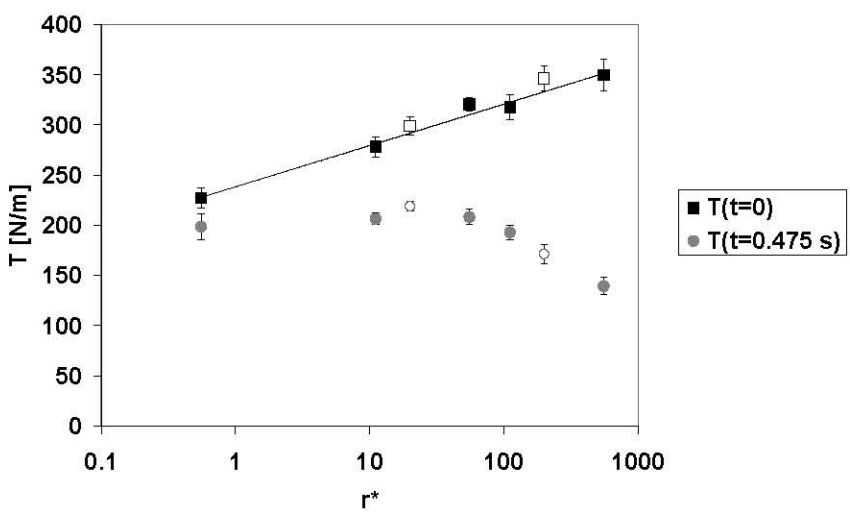

Figure 3. The initial *T(t=0 s)* and residual tension *T(t=0.475 s)* of newsprint measured at 42 % dry solids content as a function of strain rate r* for an applied strain of ε=1 %. The span lengths were 180 mm (filled squares) and 100 mm (open squares). The measurement was done in MD.

Figure 4 shows the measured residual tensions for wet fine paper, LWC and newsprint samples, and for dry newsprint and fine paper samples, at a constant applied strain of ε=1 %. After being rather constant at low strain rates, the residual tension decreases independent of paper grade and the dry solids content (d.s.c.) at large strain rates.

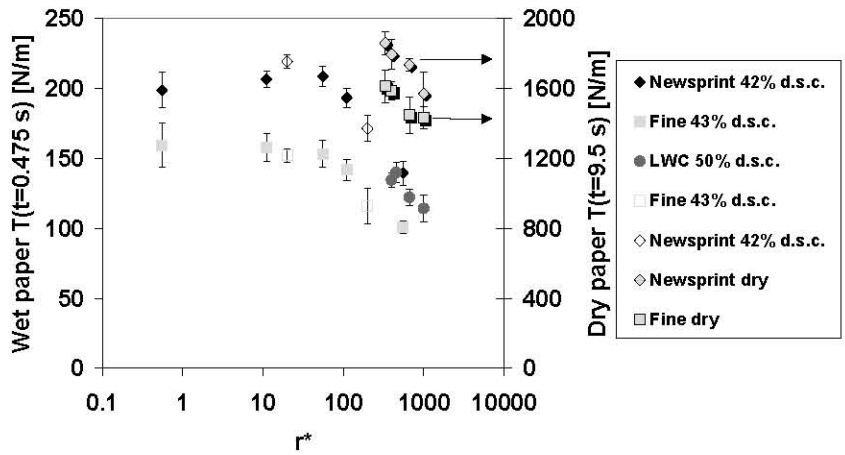

Figure 4. Residual tension of pilot machine produced newsprint, fine and LWC pilot paper as a function of strain rate for a constant strain of ε=1 %. For wet paper the residual tension is *T(t=0.475 s)* and for dry paper it is *T(t=9.5 s)*. The span lengths of wet paper were 180 mm (filled squares) and 100 mm (open squares), and for dry paper they were 100 mm – 350 mm. All measurements were done in MD. Elongation speed varied in the interval 0.001 m/s - 1 m/s.

In Fig. 5 we analyze the dependence of residual tension on the applied strain. It is evident from this figure that the behaviour of residual tension in wet newsprint does not depend on the applied strain apart from a small shift in the tension level (similar results were also found for ε=0.5 % and ε=1.5 %). Results for fine paper (dry solids content 43 %) at strains of ε=0.5 %, ε=1 %, ε=1.5 %, and ε=2 % displayed very similar behaviour.

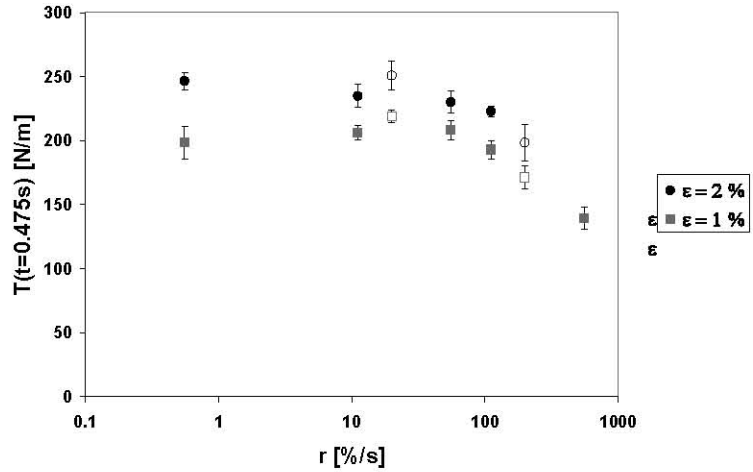

Figure 5. The residual tension *T(t=0.475 s)* of newsprint samples at 42 % dry solids content as a function of strain rate r for applied strains of ε=1 % and ε=2 %. The span lengths were 180 mm (filled squares) and 100 mm (open squares). All measurements were done in MD.

For hand sheets (Fig. 6) the residual tension was found to be linearly related to the initial tension for a ε=1 % applied strain, for a wide range of dry solids content (25-77 %). A similar relationship was found for dry hand sheets using the residual tension *T(t=9.5 s)*. In both cases the average relationship was not necessarily true for individual cases.

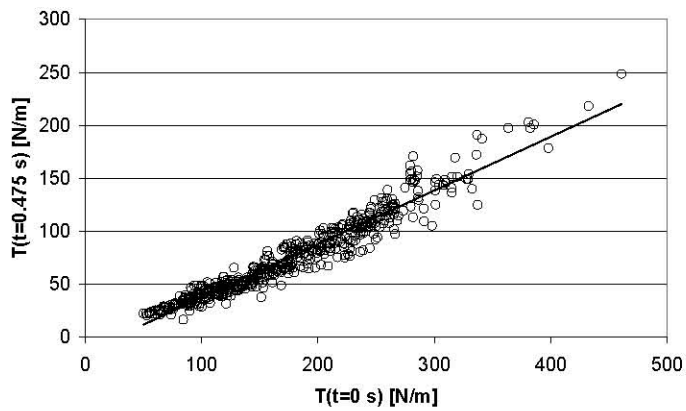

Figure 6. Correlation of initial, *T(t=0 s)*, and residual, *T(t=0.475 s)*, tension at a strain of ε=1 % for never dried hand sheets of 60 g/m^2 basis weight (varying ratio of mechanical and chemical pulp, N=537). The span length of the samples was 100 mm. Dryness varied in the interval 25 – 77 %, the filler contents in the interval 0 - 20 %, and the strain rate was 1000 %/s.

The relaxation rate of wet paper

Stress relaxation curves for wet and dry paper are shown in Fig. 7 in a semi-logarithmic scale. For a very short initial period of 20 - 30 ms the tension remains almost constant, after which stress relaxation begins. The initial delay before relaxation can most probably be attributed to signal propagation across the test strip and electronics delays in the measurement system. The asymptotic parts of the stress relaxation curves were then fitted by a logarithmic time dependence,

$$T(t) = T_c - R\log(t) \quad , \qquad (6)$$

where T_c is a constant and R the relaxation rate.

Fitting of wet-paper relaxation curves by Eq. (6) was done after a 20 ms initial period. For dry paper the initial period was about 100 ms.

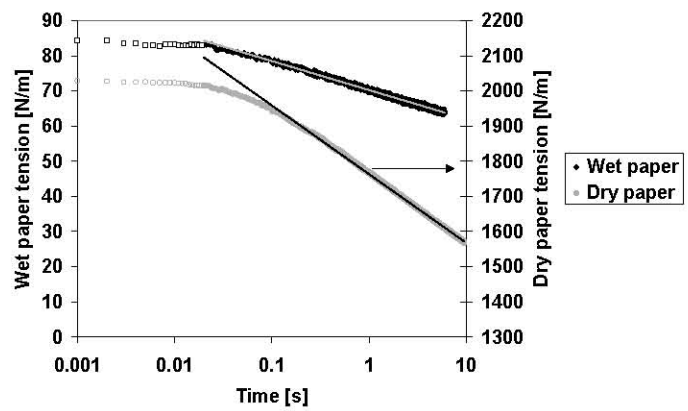

Figure 7. Stress relaxation curve for a fine paper handsheet of 45 % dry solids content with a ε=2 % applied strain, and for a dry pilot machine LWC base paper in MD with a ε=1.4 % strain. Fitting was done for the asymptotic part following an initial period of 20 ms (wet fine paper, gray line) or 100 ms (dry LWC base paper, black line).

In Fig. 8 we analyze the relationship between the initial tension *T(t=0 s)* and the relaxation rate *R*. The samples studied were fine-paper hand sheets and pilot-machine LWC base paper and fine paper. Fine-paper samples were cut in different angles with respect to MD (MD, MD+15°,MD+30°, MD+45°, MD+60°, MD+75°, MD+90°). It is evident from this figure that the relaxation rate *R* and initial tension *T(t=0 s)* have a linear correlation. This correlation seems to be independent of paper grade, orientation of the sample with respect to MD (preferred direction of fiber orientation), initial strain, strain rate and basis weight.

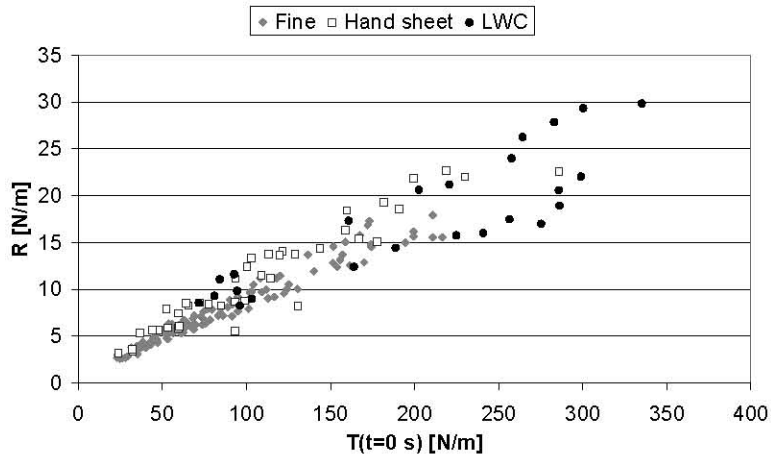

Figure 8. Relaxation rate *R* as a function of initial tension for 38 g/m^2 pilot-machine LWC base paper (dry solids content 45 % and 55 %), 70 g/m^2 pilot-machine fine paper (dry solids content 43 %), and fine-paper hand sheets (dry solids content 45 % and 50 %). Elongation speed changed in the interval 0.001 - 0.1 m/s and the strain in the interval 0.4 - 2.9 %.

In Fig. 9 we analyze the possible effect of furnish on the above correlation of relaxation rate and initial tension. The hand-sheet samples measured for an applied strain of ε=1 % were made of either eucalyptus, acacia, pine or birch chemical pulp, or TMP or PGW mechanical pulp. The results for chemical pulps seem to fall on the same curve, and the results for mechanical pulps on another curve slightly below that for the chemical pulps. Thus, samples made of chemical pulp display faster relaxation.

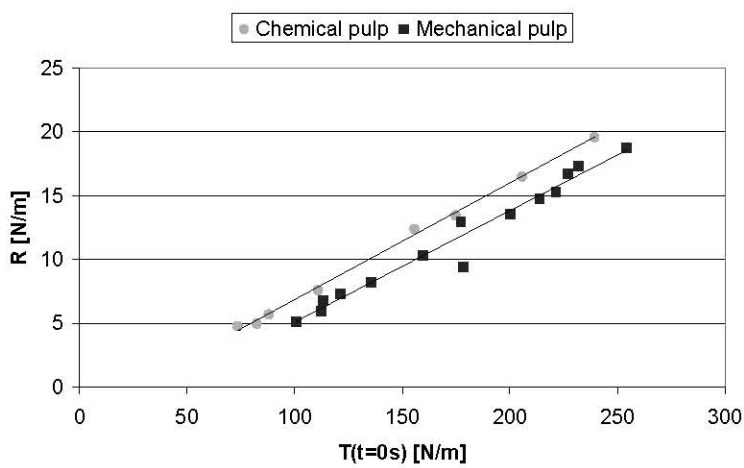

Figure 9. Relaxation rate as a function of initial tension for never-dried chemical-pulp hand sheets with a dry solids content of 42 - 58 % (birch, eucalyptus, acacia and pine), and for sheets made of mechanical pulp (TMP and PGW) with a dry solids content of 29 – 49 %. The applied strain was ε=1 % and the elongation speed 1 m/s.

Conclusions

Stress relaxation of never-dried samples was studied for different furnish compositions at several span lengths, elongation speeds and initial strains.

Stress relaxation of wet and dry paper display qualitatively similar behaviour, both are described by a logarithmic time dependence. Such dependence has previously been observed for dry paper [5]. In both cases the relaxation rate also depends on the initial tension alone [5, 9].

Relaxation rate was the same for all samples made of chemical pulp (birch, eucalyptus, acacia and pine), and it was higher than that for samples made of mechanical pulp (TMP and PGW).

The logarithm of strain rate was found to be proportional to the initial tension independent of the span length, while the residual tension was found to decrease at high strain rates. It thus seems evident that the mechanisms governing tension build up (straining) and relaxation are different.

The residual tension after straining at a high rate could not be predicted from slow-strain-rate results. Therefore, separate high-speed measurements are needed when, e.g., dynamic phenomena occurring in paper machines are studied. It can as well be concluded that web tension in a paper machine depends also on factors that affect the strain rate, such as the speed difference and the lengths of open draws.

Acknowledgements

Financial support by the Academy of Finland, Metso Paper and VTT is gratefully acknowledged.

References

1. Andersson, O., Sjöberg, L. 1953. Tensile Studies of Paper at Different Rates of Elongation. Svensk papperstidning, Vol. 56, No. 16, pp. 615-624.

2. Johansson, F. and Kubát, J. 1964. Measurements of Stress Relaxation in Paper. Svensk papperstidning, Vol. 67, No. 20, pp. 822-832.

3. Kouko, J., Salminen, K. and Kurki, M. 2007. Laboratory Scale Measurement Procedure for the Runnability of a Wet Web on a Paper Machine, Part 2. Paperi ja Puu, Vol. 89, No. 7-8, pp. 424-430.

4. Jantunen, J. 1985. Visco-elastic properties of wet webs under dynamic conditions, 8th Fundamental Research Symposium, Oxford, pp. 133-162.

5. Craven, B.D. 1962. Stress Relaxation And Work Hardening In Paper. Appita Vol. 16 No. 2, pp. 57-70.

6. Okushima, S. 1977. Rheological Deformation of Paper Sheet during Straining and Stress Relaxation. Mokuzai Gakkaishi, Vol. 23, No. 12, pp. 666-669.

7. Kurki, M. Kouko, J., Kekko, P. and Saari, T. 2004. Laboratory Scale Measurement Procedure of Paper Machine Wet Web Runnability: Part 1. Paperi ja Puu, Vol. 86, No. 4, pp. 256-262.

8. Kouko, J., Kekko, P. and Kurki, M. 2006. "Effect of strain rate on strength properties of paper" Proceedings of the 2006 Progress in Paper Physics -A Seminar, Miami University, Oxford OH, October 1-5. pp. 90-94.

9. Johansson, F., Kubát, J. and Pattyranie, C. 1967. Internal Stresses, Dimensional Stability and Deformation of Paper. Svensk papperstidning, Vol. 70, No. 10, pp. 333-338.

10. Kurki, M., Pakarinen, P., Juppi, K. and Martikainen, P. 2000. "Web handling". In Markku Karlsson (ed.), Papermaking part 2, drying, pp. 374-431.

Repulpable water vapor barrier coatings made easy

Ronald E Hostetler
U.S. Paper Consulting, Vancouver, WA, USA

The *process* for creating a recyclable water vapor barrier coating for packaging papers, paperboard and/or corrugated containers will be covered in this paper. Sustainability, the ability to recycle into like kind, is the key driver to reduce solid-waste going to land-fill and to lower carbon-footprint when difficult to recycle packaging materials are incinerated. Latex, pigment and additives *selection* along with the *proper equipment* for manufacture and to determine the change in barrier properties with change in formulation will be described. Barrier coating designs using water resistance latices, large platy pigments and low additives levels provide a winning combination for *water vapor barrier coatings* under the challenge of *tropical conditions*.

The Drive to Sustainable Packaging Products

Expanded polystyrene (EPS) containers became the standard for the transport of grapes from field to retail stores. Solid waste disposal costs grew rapidly on these and on the waxed corrugated containers also used for produce. These, in turn, have partially been replaced by polymeric coatings on corrugated containers. The Sustainable Packing Coalition cites a study[1] where disposal costs for EPS reached $95/ton while recyclers of polymeric coated corrugated containers were paying $87/ton; thus providing a net profit gain $182/ton for the end user.

Waxed and/or PE coated or laminated packaging papers, paperboards, box boards and corrugated containers are still widely used for packaging of processed foods, frozen food, detergent, produce, meats, poultry and fish and their transport to distribution centers and onto retail stores. Many are single use or have a limited use life. Ice packed meats; fish and poultry originate in processing plants and are in-use for only a few days in cooler storage and transport to retail stores. For greater length transport times, CO_2 packs are used. Both water resistance and water vapor barrier resistance is required to preserve corrugated container stiffness and strength to slow creep during the shaking and shock of transport to final destination. Since these packaging materials become septic the ability to repulp and recycle into like kind is very important. Conventional cascade waxed corrugated containers for these applications, may contain up to 40% wax by weight. Paraffin based waxes, traditionally, have been nearly a waste product. Packaging companies enjoyed the plentiful supply and low price. New cracking processes in the chemical industry have become much more efficient. The supply of these waxes tightened and prices, more than tripled, during the last major spike in petroleum prices. Wax not only provides water and water vapor barriers but also provide, through a phase change significantly increases in container stiffness. This is important for greater stacking height in coolers, not necessarily, for transport that are normally single pallet height.

Conventional papermaking systems can not repulp (recycle) even low wax content or extruded polyethylene barrier packaging materials[2]. Wax severely effects hydrogen bonding dependent strength and creates paper machine deposits.

Sustainable Packaging: Polymeric Coated Papers, Paperboard or Corrugated Containers

A few suppliers have been able to formulate recyclable coatings. Some have been available in the market place for 10-years[3]. There are many approaches to these coatings as the patent literature reveals, but only a few make economic senses in the market place. Amberg[4] etc identify polymerized inorganic-organic films that provide gas barriers to oxygen, VOCs and water vapor. To displace, paraffin and PE based barriers, containers having recyclable barrier coatings, must be priced close to competitive non-recyclable alternatives in the purchasing agent's analysis. However, purchasing agents probably ignore the cost of disposal.

Development Standards

The non-repulpable packaging products are easily obtained and tested for level of barrier properties and material components. As an example, conventional roll wrap composed of two light weight liner plies laminated together via extruded PE can be selected for this discussion. Its simple construction makes it a good choice for development target properties for a sustainable roll wrap. The process parameters for laminating, quality of PE, weight extruded and properties of liner determine the level physical, mechanical and optical properties. PE extrusion as a barrier coating is also common on the backside of coated or uncoated paperboard, food wraps, etc.

A simple analysis of moisture content, oven dry weight and PE weight per unit area via die cut and thermo-gravimetric analysis reveals the basic product design. Such an analysis would come-up with a design of 2-plies of 119 gsm oven dry (OD) liner, 7.5% moisture and 27 gsm of extruded PE. WVTR determinations under tropical conditions (37.8°C; 100°F, 90% RH) would be normal at or below 45-g/m^2/day.

The laminating bond of PE can be improved by pre-application of a cationic material such as polyethylenimine (PEI). This technology is also common to the Indigo printing process to prevent ink spread, prevent bleed and assure good ink adhesion. A quality control test to keep application rates of PEI in the 7 to 15 mg/m^2 range is readily available from Indigo process literature in the public domain.

Water Vapor Transmission Rates (WVTR)

ASTM E-96 describes a test method for determining WVTR under tropical conditions. The TAPPI test method for determining "WVTR of paper and paperboard at high temperature and humidity" is described in T 464 om-01. WVTR is calculated for steady state conditions and commonly expressed as grams (g) of water vapor transmitted through a known area (m^2) of sample in a specific time (24-hr = 1-day). Steady state conditions are determined by conditioning representative samples for 1, 2, 3, 4 and 6-hours in tropical conditions, weighing and placing them back in a chamber set at tropical conditions additional 24-hours, reweighing for calculation of the average WVTR for 1-day after the initial conditioning. The graph in Figure 1 shows steady-state WVTR values are reached at 2-hours and longer initial conditioning.

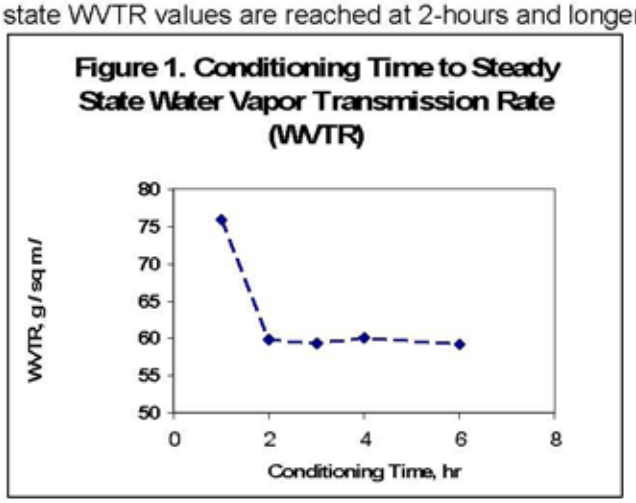

The tray size, (vapor transmission area), edge sealing, desiccant type and amount can be set to accommodate different laboratory situations. In general, the amount of desiccant present has to have a capacity for a 24-hr period to be enough to absorb, for example, the amount of water vapor that would pass through base liner. For example, 126-gsm liner air dried above has a WVTR of about 400 g water vapor /m^2/day. The same, liner with 15 and 30 g/sq m of a very water resistance SB latex, would have a WVTR of 275 and 175 g/m^2/day, respectively. Thus the

quality of the platy pigments is the key component to getting WVTR rate below 50 g water vapor /m^2/day.

Pigments for Water Vapor Barrier

An article by Clive Hare and Roland Beck [5] entitled "Extenders" provides a good review of pigments properties and uses. In particular, they indentify platy pigments as the "work horse" of protective and barrier paint films. Part of Table 1, "Principal Extender Types and Typical Properties" is show below. The *utility* column has chlorite and mica as having barrier and stress mitigation properties. Mica has the additional features of corrosion resistance, hardness and the highest surface area (oil absorption) suggesting a very platy structure and/or higher degree of delaminating. Talc has the benefit of flexibility, slipperiness, nearly hydrophobic surface and lowers blocking tendency.

TABLE 1
Principal Extender Types and Typical Properties

Extender	*Make Up*	*Specific Gravity*	*Lb/gal*	*Particle size, u*	*Oil Abs*	*pH*	*RI*	*Hardness Moh*	*Particle Shape*	*Utility*
Talc	Mg Silicate	2.8	23.3	2 - 15	30 - 45	8-9	1.58	1	Various	Fill, stress mitigation, film reinforcement
Chlorite	Al Mg Silicate	2.8	23.3	2 – 10	35 – 45	8 – 9	1.57	1	Platy	Fill, barrier
Kaolin	Al Silicate	2.6	21.5	0.5 – 3.5	25 – 50	4.5 – 7	1.57	2.5	Platy	Fill, Opacity
Mica	Al K Silicate	2.8	23.5	5 – 20	50 – 70	7.5 – 9.5	1.59	2 – 3	Platy	Fill, Barrier, stress mitigation, corrosion resistance

Latex for Water Vapor Barrier Coatings

Styrene butadiene (SB) latices tend to form coating films that resists penetration by water better than styrene acrylic (SA) or polyvinyl acetate (PVAc) latices. The lack of consistent water penetration[7] has been sited for SB-clay coatings for boxboard to cause inconsistent gluing (less than 95%+ fiber tear) in folding boxboard. SA and PVAc latices provide the consistent gluability allowing the water from the PVAc adhesive to penetrate through the coating into the fiber in the base box board to assure the high fiber tear.

Blocking

Pigmented coatings provide opacity, whiteness, ink receptivity and print fidelity to folding carton and folding boxboard, carrier board and corrugated containers. These coatings typically have pigment to latex binder weight ratios about 85/15. The glass transition (Tg) temperature where polymer chains of adjacent coalesced latex particles inter-migrate after drying to cure, ranges from 4 to 22 °C for most paper, board and corrugated applications. These coatings have sufficient strength for most offset printing and low blocking tendencies. Folding carton for cigarette board is still an exception as PVAc at Tg 39°C is used to provide stiffness, gluing, low odor and excellent rotogravure print fidelity, especially in mid-tones.

Barrier coatings grades have a much greater propensity to block in rolls or when stacked. Pigment to binder weight ratios approach 50/50 while volume ratios (26.6/73.4) show styrene butadiene (ρ = 1.02 g/cc) occupies nearly three times the volume of the much higher density

(ρ = 2.82 g/cc) pigment. The upper half of TABLE 2 provides are quick overview of mica pigment to SB latex weight ratios, the corresponding volume ratios and densities of the dried coating film.

TABLE 2

FILM THICKNESS AS A FUNCTION OF MICA / SB WEIGHT RATIO & COAT WEIGHT

ρ= 2.82, MICA	MICA / SB WEIGHT RATIOS IN DRY FILM									
ρ= 1.02, SB	0/100	10/90	20/80	30/70	40/60	50/50	60/40	70/30	80/20	90/10
Density, g/cc	1.020	1.090	1.17	1.26	1.37	1.50	1.65	1.84	2.08	2.40
SB, vol, %	100	96.1	91.7	86.6	80.6	73.4	64.8	54.2	40.9	23.5
Coat Wt, gsm	FILM THICKNESS, μm = micron									
5	4.90	4.59	4.28	3.96	3.65	3.34	3.02	2.71	2.40	2.09
10	9.80	9.18	8.55	7.93	7.30	6.68	6.05	5.42	4.80	4.17
15	14.7	13.8	12.8	11.9	11.0	10.0	9.07	8.14	7.20	6.26
20	19.6	18.4	17.1	15.9	14.6	13.4	12.1	10.8	9.60	8.34
25	24.5	22.9	21.4	19.8	18.3	16.7	15.1	13.6	12.0	10.4
30	29.4	27.5	25.7	23.8	21.9	20.0	18.1	16.3	14.4	12.5
35	34.3	32.1	29.9	27.7	25.6	23.4	21.2	19.0	16.8	14.6
40	39.2	36.7	34.2	31.7	29.2	26.7	24.2	21.7	19.2	16.7
45	44.1	41.3	38.5	35.7	32.9	30.0	27.2	24.4	21.6	18.8
50	49.0	45.9	42.8	39.6	36.5	33.4	30.2	27.1	24.0	20.9

Latex Stability

Both the mechanical and chemical stability of the SB latex used in functional coatings are important. However, the grooved rod metering coaters used for off-machine coating application or an in-line coater at the corrugator run at speeds normally less than 900 fpm. A highly mechanically stability latex is probably not needed. Some scientists argue lower mechanical stability means quicker film formation. This would also suggest the latex supplier is trying to minimize surfactant costs.

A highly mechanically stability SB is favored, as a uniform dispersion of mica directly in SB latex must be achieved by a high shear disperser to obtain a high solids coating and minimize the drying requirement. To that end, for the functional coating market, latex producers try to maximize coating solids at 52% +/-1%. This is very close to the latex solids, where crowding of adjacent latex particles occurs for narrow particle size distribution latex and viscosity rises rapidly. The mechanical requirements for such are well documented by Morehouse & Cowles[6]. Tip speed for good dispersion in viscosity liquids should be maintained between 4000-6000 fpm. The high shear saw tooth design impellor blade is

good for both dispersing and mixing. The relationship between blade diameter, vessel height and diameter and distance of blade from vessel bottom are well documented.

Coating Design

The lower part of Table 2 is instructive in choosing the *experimental space* of coat weight and mica to SB weight ratios to explore. Coating film thickness is plotted as a function of these two independent variables. Figure 2 plots this relationship. The assumptions are no air voids and a perfectly smooth base paper to calculate a coating film thickness. To further restrict the initial experimental space, two other assumptions were made. That the film thickness would be limited to that required by PE ± 25% and that at least 20% mica would be

required. Thus coat weights from 20 to 32.5-gsm and mica to SB weight ratios of 20/80 up to 60/40 should be initially explored. A check of Table 2 shows that a mica to SB weight ratio of 60/40 has a volume ratio 35/65. This is as very plausible choice for a continuous film SB (65% by volume) and ideally embedded in the film, large thin overlapping platelets of delaminated mica aligned nearly parallel to the machine direction and cross machine directions in many multi-layers thick. Water vapor migration through successive platy pigment layers is normally described as a tortuous path thus dropping transmission rates through the continuous SB film.

Figure 2. COATING (MICA-SB) FILM THICKNESS AS FUNCTION COAT WEIGHT & MICA TO SB WT. RATIO

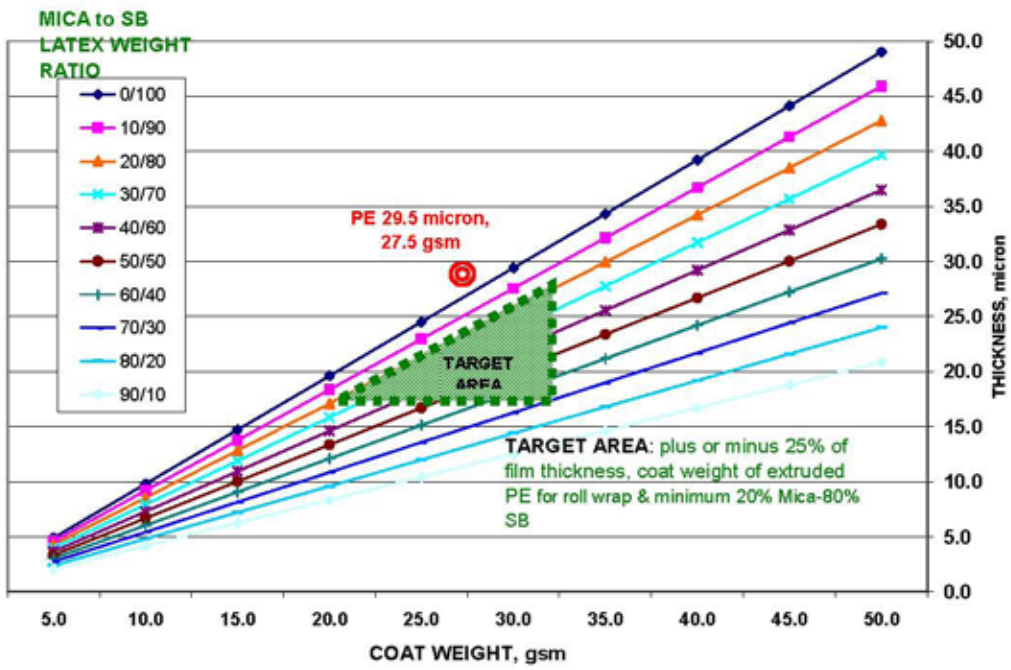

Laboratory Work

A constant speed variable torque lab disperser with initial ramp to speed with setting changes is a good choice with standard high shear blade. The amount SB latex required is weighed, defoamer is added and dispersant if required. An initial dispersant demand curve with the platy pigment of choice at 50 – 60% solids will establish whether dispersant is required. The platy pigment is added slowly at moderate speed to assure pigment wet-out. Rotor speed is kicked-up to give a tip speed of 5000 fpm to assure complete dispersion of pigment agglomerates to individual platelets. A moderately alkaline pH helps stabilize the dispersion and is required if an alkali soluble thicker is used for viscosity adjustment for runnability, metering and lay down

considerations. Ammonia is recommended over a permanent alkali when formulating water or water vapor barrier coatings. Solids, pH and viscosity are checked and adjusted if needed. Drawdowns are done using a series of wire wound rods on automated drawdown equipment having standard three layer backing material. The coated liner is dried at 105 C to check coat weights by weight difference from initial OD liner. The steady-state water vapor transmission rate for the coated samples are determined accord the TAPPI or ASTM methods for tropical conditions.

Raw Material Specifications

If significant grit is present in the functional coating two things occur. Coat weight for a giving wire wound rod size will be higher than expected and WVTR values will be high due to defects in the coating film. Finished coating screening is recommended to eliminate grit. Two issues present themselves: the length of many platy pigments are greater than the coating film thickness and what size screen will remove grit and not very thin large platelets? Orientation of the platy mica pigment in the plane of the SB film is extremely important. A few large platelets oriented nearly perpendicular can provide a path for high water vapor transmission as do holes through the coating film.

Experiments can be done with standard square-hole wire sieves and vibrating, sonic or orbital motion shakers to further define the acceptable platy pigment size distribution that provides the most economical WVTR target. A series of sieves having opening sizes of 150, 125, 105, 90, 75 & 53 micron can be stacked to fractionate platy pigments from various suppliers. The resulting WVTR for each caught fraction and/or all material passing through a given sieve size can be checked for WVTR. Once this work is completed, the most economical means that can be worked out with a specific supplier to obtain the desired platy pigment distribution can be negotiated. If grit can be eliminated up-front at the supplier level and your commercial size dispersing equipment and addition sequence does not create grit, final screen of the functional coating may not be necessary.

Summary

Water and water vapor resistance containers that are repulpable and recyclable into like kind grades can easily be manufactured using coatings made primarily of SB latices and platy pigments. High shear dispersion equipment for make-down of dry platy pigments directly into high solids SB latex is required. An adequate amount of defoamer is required for initial pigment dispersion. A fugitive alkaline maintains water resistance better when alkali swell-able thickeners are used for runnability. The size distribution of the platy pigments, applicator type that aligns platelets in the plane of the coating and lack of grit in the coating are critical parameters to achieve water vapor barriers.

Literature

1. Report found on Michelman, Inc. web site

2. Charles P. Class Recyclable Barrier Coatings Offer Alternative, "The environmentally-friendly coatings can be used to replace wax boxes", Mar 1, 2009

3. John B. Homoelle, General Manager Technology, Michelman, Inc., 9080 Shell Rd, Cincinnati, OH, 45236, USA

4. S. Amberg-Schwab, M. Hoffmann Fraunhofer-Institut für Silicatforschung, Neunerplatz 2, D-97082 Würzburg, Germany & H. Bader and M. Gessler, Fraunhofer-Institut für Lebensmitteltechnologie und Verpackung, Giggenhauser Str. 35, D-85354 Freising, Germany, Journal Sol-Gel Science and Technology ½ 141-146 (1998), Netherlands.

5. Clive Hare, Coating System Design Inc., Lakeville, MA and Roland Beck, Manager, Marketing, NYCO Minerals Inc., Calgary, Alberta, Canada, (nycominerals.com/directories/PDFS/LITE)

6. Modern Dispersion Technology, A primer for dispersers, Chino, CA, www.morehousecowles

7. Quintin Parker, BASF Corp., Charlotte, NC, 2003, personal communication.

This page intentionally left blank.

Session 5
Other Materials

David Vahey, Chair

U.S. Forest Service, Forest Products Laboratory

All cellulose-based composite materials experience reduced strength and stiffness and increased failure strain in high moisture environments, but these changes occur at different magnitudes depending on material. Each species of solid wood has different moisture sensitivity that needs to be accounted for in structural applications. Composite material manufacturers often take advantage of the high strength to weight ratio of cellulose fibers for production of innovative products, using moisture sorption within their design. Other manufacturers need the high strength to weight ratio with very low moisture sensitivity and rely on impervious laminations.

Strength properties of low moisture content yellow-poplar and Southern Pine

David E. Kretschmann, Research Engineer
David W. Green, Supervisory Research Engineer, Emeritus

U.S. Forest Service, Forest Products Laboratory, Madison, Wisconsin

Contemporary engineering design practices in the United States require information on the strength of lumber for moisture contents as low as 4%. Efficient design of experimental studies on lumber properties at low moisture contents requires a better understanding of the basic mechanisms controlling moisture-property relationships. A study is being conducted on the effect of moisture content on strength and stiffness in bending, tension and compression parallel and perpendicular to grain, and longitudinal shear in yellow-poplar (Liriodendron tulipifera L.). Results of this study and one previously conducted on Southern Pine (Pinus taeda) will be compared and there implications on structural performance discussed.

Hygroexpansion of plant-based fiber mats for “green” composites

P.J.J. Dumont[1], J.-F. Bloch[1], L. Orgéas[2], B. Vermeulen[3], P. Vroman[3], S. Rolland du Roscoat[2]

1. Laboratoire de Génie des Procédés Papetiers (LGP2), CNRS / Institut polytechnique de Grenoble (Grenoble INP) - BP 65 - 38402 Saint-Martin-d’Hères cedex9, France

e-mail : pierre.dumont@efpg.inpg.fr

2. Laboratoire Sols-Solides-Structures-Risques (3S-R), CNRS / Université de Grenoble (UJF & Grenoble INP) - BP 53 - 38041 Saint-Martin-d’Hères, cedex 9, France

3. École Nationale Supérieure des Arts et Industries Textiles (ENSAIT), 2 allée Louise et Victor Champier, BP 30329, 59056 Roubaix cedex 1, France

Keywords: composites, plant fibers, dimensional stability, hysteresis, anisotropy, X-ray microtomography

There is a growing interest in making renewable and sustainable composite materials. Plant fibers are suitable to reinforce composites due to their high strength and stiffness with respect to their low density. Nonetheless, they have intrinsic drawbacks such as their poor dimensional stability when subjected to changes in temperature or moisture.

This study aims at describing the microstructural deformation phenomena of plant-based fiber mats that are induced by changes in the relative humidity (RH) of the ambient air. Tested mats were formed with flax fibers of various qualities. They were produced by opening the fiber bales by carding and subsequently orientated to cross-machine direction by using a cross-lapper to form a web of required basis weight. Finally they were needle-punched and hydro-entangled.

At the macroscopic scale, the in-plane dimensional variations of these mats were studied by using a specially developed device. At the microscopic scale, an in situ analysis of the 3D evolution of their microstructure was carried out by using the synchrotron X-ray microtomography (European Synchrotron Radiation Facility, Grenoble, France). In parallel, their sorption properties were studied. During these various experiments, samples were subjected to the same relative humidity (RH) cycles (RH varying between 20 and 80%) at a constant temperature of 23°C.

Results show hysteresis phenomena for the absorption and desorption properties, as well as for the hygroexpansion of these fibrous mats. In this latter case, results emphasize also the influence of the anisotropic structure of the tested fibrous mats. At the microscopic scale, the analysis of the X-ray microtomographies highlights the combined evolutions of the porosity and of the geometry of the fibrous phase during the RH cycles. Accounting for these various observations, a model for the hygroexpansion of these mats is proposed.

Modelled and measured bending stiffness of polyethylene coated multi-layer paperboard at two moisture contents

Sara Paunonen (*), Øyvind Gregersen
Department of Chemical Engineering, NTNU
7491 TRONDHEIM, NORWAY
(*) Sara.Paunonen@chemeng.ntnu.no

1. Abstract

The bending stiffness of the glued multi-layer solid board was modelled using the classical laminate technique. Each layer is considered as a homogeneous elastic medium. SEM pictures were used for thickness determination. The calculated values were compared to measurement values produced by 2-point and 4-point bending techniques. The samples were exposed to standard and high humidity (90 %RH) conditions. The results show that the elasic modulus and thickness of the glue layer joining the paperboard sheets must be taken into account in the model to agree with the measured bending stiffness values.

2. Introduction

Packaging is a key sector for paper-based products. Paper-based transport packages are widely used due to their good performance-weight ratio and high bending stiffness. The material studied is a multi-layer paperboard (solid board). It consists of six layers that are glued together with a polyvinyl acetate (PVA) based glue. The four middle layers are solid board medium. The outermost kraft papers are polyethylene coated. This type of paperboard is used in heavy-duty applications, especially in transport of victuals in humid conditions.

The bending stiffness is a well-known, and still a central structural elastic material property that gives rigidity to the end product. An adequate bending stiffness in MD and CD contributes positively to the usability of paperboard boxes. The box needs to be rigid enough to allow the large panels to resist pressure from the contents and also pressure of box stacking.

The paperboard studied in this work is used as a transport package that is exposed to high humidity levels and liquid water. The aim of the study is to predict the bending stiffness based on elastic properties and thickness of the layers. The modelling will gradually increase in detail to reach the level where the effect of the adhesion layer on the bending stiffness is described. The bending stiffness is studied at the relative humidity levels 50 and 90 %RH. The results are verified by comparing them with results from three different test methods.

3. Calculation of bending stiffness

When a sheet is bent, the concave side is compressed and the convex side is elongated. In the middle, there is a neutral surface that doesn't change in length. The neutral surface occurs in the middle of the sheet only if the sheet is of homogeneous material or if the stacking of layers in a laminate structure is symmetric.

The bending stiffness of a structure is defined as relationship between the applied bending moment and the resulting curvature of the structure. The bending stiffness combines the effect of the material properties and the geometry of the structure. It is the product of the elastic modulus of the material E and the area moment of inertia of the cross-section I. For a homogeneous structure with a constant elastic modulus the calculation formula is simple:

$$S_b = EI = E\frac{h^3}{12} \tag{1}$$

S_b is the bending stiffness for one meter of material [Nm], h is the thickness of the beam [m] and E is the elastic modulus [Pa]. The equation emphasizes the importance of thickness.

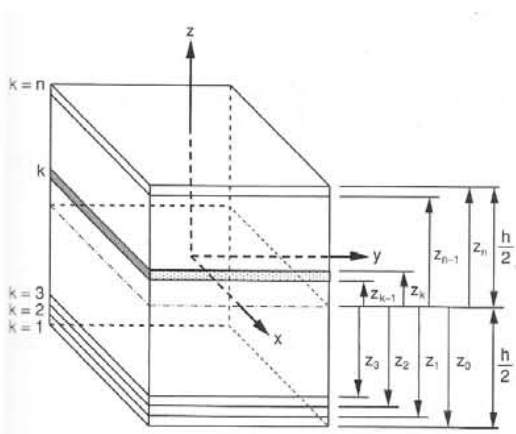

Figure 1. Multidirectional laminate with coordinate notations, Daniel and Ishai (2006).

Figure 1 shows a laminate with n layers. The thickness of the structure is h, z_k and z_{k-1} are the z-coordinates of the upper and lower surfaces of layer k. The total force and moment resultants are obtained by summing the effect of all layers.

The general calculation principle for laminate bending stiffness is given for example in Daniel and Ishai (2006). External forces N, moments M, reference plain strains ε_0 and the curvatures κ can be gathered to a matrix as follows. The bending stiffness S_b is found by solving the relation between moment M and curvature κ when net axial forces are zero (N=0).

$$\begin{bmatrix} N \\ M \end{bmatrix} = \begin{bmatrix} A & B \\ B & D \end{bmatrix} \begin{bmatrix} \varepsilon^0 \\ \kappa \end{bmatrix} \text{ where} \tag{2}$$

$$A_{ij} = \sum_{k=1}^{n} Q_{ij}^{k} \left(z_k - z_{k-1} \right), \; B_{ij} = \frac{1}{2} \sum_{k=1}^{n} Q_{ij}^{k} \left(z_k^2 - z_{k-1}^2 \right),$$
$$D_{ij} = \frac{1}{3} \sum_{k=1}^{n} Q_{ij}^{k} \left(z_k^3 - z_{k-1}^3 \right) \text{ with i,j = x,y,s(shear)} \tag{3) – (5}$$

$$S_b = D - \frac{B^2}{A} \tag{6}$$

The elastic moduli of the layers can be used instead of the stiffness matrix Q_{ij}^{k}. The three laminate stiffness matrices A, B and D are functions of the geometry, material properties and stacking sequence of the layers. For symmetric laminates, the B is zero and thus the bending stiffness reaches its maximum. The outermost layers of a multi-layer structure play an important role due to the effect of geometry. The high elastic modulus of these layers comes into effective use as they lie far from the neutral axis and thus possess high area moment of inertia value. The basic function of the intermediate layers is to keep the outermost layers separated. Hamelink (1963) and Luey (1963) were the first authors that point out these geometrical facts for paper materials.

Ranger (1967) made several laboratory multi-ply sheets and studied how their bending stiffness could be predicted. He noticed how the results are easily affected by the thickness determination and bending the samples beyond the elastic region. A detailed calculation schema where the position of the neutral surface did not need to be calculated was first presented by Carlsson and Fellers (1980). They got excellent agreement between calculated and measured values when using specific elastic modulus values for 3-layer sheets. Yang (1981) adopted a plate formulation for a layer, and the laminate bending model was thus capable of handling more versatile loading situations like in-plane compressions, shear loads and distributed transverse loads.

The results of five different bending stiffness testers were compared by Koran and Kamden (1989). For comparison they used laboratory hand-sheets that were far thinner than the paperboards used in the present study. Fellers and Carlsson (2002) gave an excellent overview on different tester principles and their applicability ranges especially for paperboard. Fellers (1997) studied the reproducibility of four bending stiffness measurement techniques: Lorentzen & Wettre, Taber and two testers using resonance methods. He concludes that for paper and boards grammage ranging from 100 to 400 g/m^2, the variation decreases with increasing grammage. The Taber tester gave highest variation.

The bending stiffness is a key parameter for paperboard materials used as transport boxes. It is used for, e.g., calculation of buckling load of panels. In the literature results are reported on layered papers and paperboards, but little work is reported on glued, heavy-weight solid board materials. In addition, the effects of humid conditions have not been considered.

4. Experimental

The material studied is a heavy-duty solid board (1220 g/m^2). It constitutes of six unidirectionally stacked paper or paperboard layers. The four centre solid board medium layers are made of 100 % recycled fibre (OCC). The outer two layers are made of bleached kraft paper that has double extrusion coated polyethylene layer on one side. The paper and polymer are regarded as one material in the following experiments.

The layers are glued together with an industrial laminator to produce the commercial solid board. In the lamination, 18-33 g/m^2 of liquid glue (solids content 24 %) per adhesion layer is applied with roll applicators. The gluing process introduces an extra amount of water into the solid board. For five adhesion layers the total amount of water is approximately 70 – 120 g/m^2. The lamination compresses the solid board sheets with the pressure 3-5 bar. The lamination temperature 50 °C is only due to the temperature of the heated glue.

First, the solid board and its constituting paperboard layers (before lamination) were characterized by measuring grammage and thicknesses (ISO 534:1988) and the stabile moisture contents of the individual layers in standard climate and in high humidity (90 %RH/27 °C). The moisture content of a 15x210 mm size solid board sample stabilises in 17 hours when transferred from 50 to 90 %RH.

Thicknesses of the laminated solid board layers were determined also form SEM micrographs. Ten SEM pictures were taken from two board samples and thicknesses were determined manually. With an image analysis program, a rectangle was drawn around each paperboard layer so that the horizontal edges were placed in the middle of the adhesion layer that bonds two materials. The height of the rectangle was recorded in pixels and transferred to SI units. The sample was dried before taking SEM pictures.

The in-plane force-elongation curves were measured with a Zwick universal tensile tester according to ISO 1924:1994. The speed of the tensile testing was 25 %/min, the test length 100 mm and each result is an average of 9 test pieces. The moisture content of the test pieces were allowed to stabilize 3 days in 90 %RH before measuring. The test pieces were taken out from a plastic bag just before the testing. The time between consecutive tests is approximately 45 seconds. The elastic moduli E_x and E_y were manually determined from the curves as the steapest slope of the stress strain curve.

The bending stiffness of the solid board was measured with three testers at standard climate and at high humidity (90 %RH/27 °C). Taber type tester and Lorentzen & Wettre (L&W) testers are 2-point bending testers. The test piece is clamped at the one end and concentrated load is applied to the other end (two-point bending). The tests were carried out according to Tappi 489 (Taber) and ISO 2493 (L&W). The test piece width was 38 mm, and the moment arm 50 mm. Samples were cut with a knife because the Taber cutter was not able to cut the thick test pieces. Both testers deflected the samples to 7.5°. The Lorentzen & Wettre 4-point bending test was carried out according to ISO 5628. The distance between two inner supports was 150 mm. The 4-point samples were allowed to stablise 27 days after the the step change in relative humidity. The stabilisation time for the 2-point bending samples was 5 days.

5. Data and results

Table 1 shows the grammage and the single sheet ISO thicknesses for stable material moisture contents at two relative humidity levels.

Table 1: Grammage, thickness (ISO 534:1988) and stable moisture contents of the solid board and its constituents.

	Grammage [g/m2]	Stdev [g/m2]	ISO Thickness [mm]	Stdev [mm]	Moisture content	
					[%] 50 %RH	[%] 90 %RH
SolidBoard	1219	4	1.73	0.03	8.0	11.5
OuterLayer1	78	1	0.104	0.003	2.6	5.8
Layer1	260	2	0.45	0.02	6.0	9.4
Layer2	256	2	0.43	0.02	5.7	10.1
Layer3	257	2	0.43	0.02	6.2	10.1
Layer4	244	2	0.42	0.02	5.8	10.5
OuterLayer2	78	1	0.104	0.003	2.6	5.8

Table 2 shows the elastic moduli based on ISO thicknesses. A similar set of elastic moduli was calculated using SEM thicknesses.

Table 2: Elastic modulus of the layers in MD (x) and CD (y) direction in two relative humidity levels using ISO 534:1988 thicknesses.

	50 %RH				90 %RH			
	Ex [MPa]	std [MPa]	Ey [MPa]	std [MPa]	Ex [MPa]	std [MPa]	Ey [MPa]	std [MPa]
SolidBoard	2 970	90	1 420	50	2 280	40	1 080	30
OuterLayer1	5 700	300	2 150	80	3 800	200	1 350	60
Layer1	3 420	40	1 610	30	2 380	50	1 000	30
Layer2	3 720	20	1 680	40	2 250	40	1 040	20
Layer3	3 430	50	1 450	60	2 450	60	970	50
Layer4	3 730	20	1 520	30	2 600	100	980	30
OuterLayer2	5 700	300	2 150	80	3 800	200	1 350	60

Figure 2 shows a SEM picture of the solid board. The extruded polymer coating is seen as a black layer on top and bottom of the laminate structure. Beneath the polymer there is the layer of chemical pulp. The four paperboard layers in the middle have almost even thickness. The white particles are fillers. The five bonding layers are clearly seen in the picture. The glue is seen as white thin layers on the contacting paperboard surfaces. The bonding layers have long segments where the glue doesn't bridge the surfaces, and the total amount of glue varies. At places where the surfaces are in contact, the thickness of the glue layer is approximately 10 μm (see the arrows in the figure). The glue on the paperboard surface, which is not in contact with the other board surface, is approximately 3 μm thick.

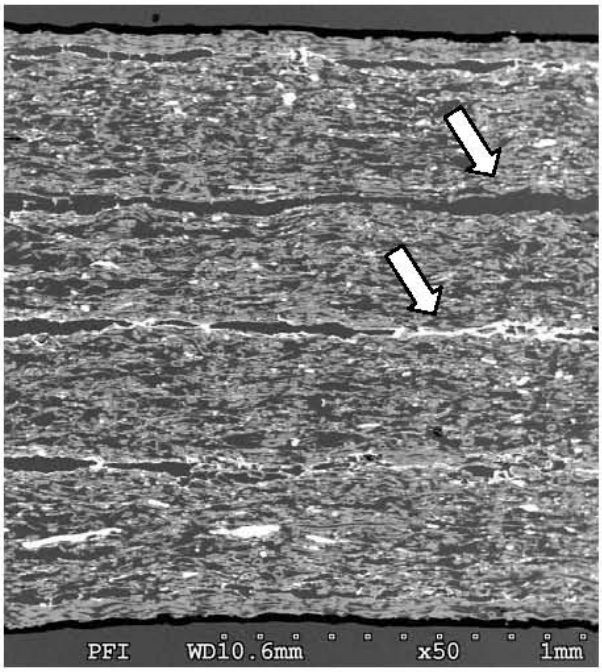

Figure 2: SEM picture of the solid board.

Table 3. Layer thicknesses from SEM pictures.

	Thickness [mm]	Stdev [mm]
SolidBoard	1.55	0.04
OuterLayer1	0.077	0.007
Layer1	0.34	0.04
Layer2	0.33	0.04
Layer3	0.36	0.03
Layer4	0.36	0.04
OuterLayer2	0.080	0.005

Table 3 shows the layer thicknesses measured from ten SEM pictures. The layer thicknesses sum up to the thickness of the solid board.

The measured bending stiffnesses of the solid board in two relative humidities are shown in Figure 3.

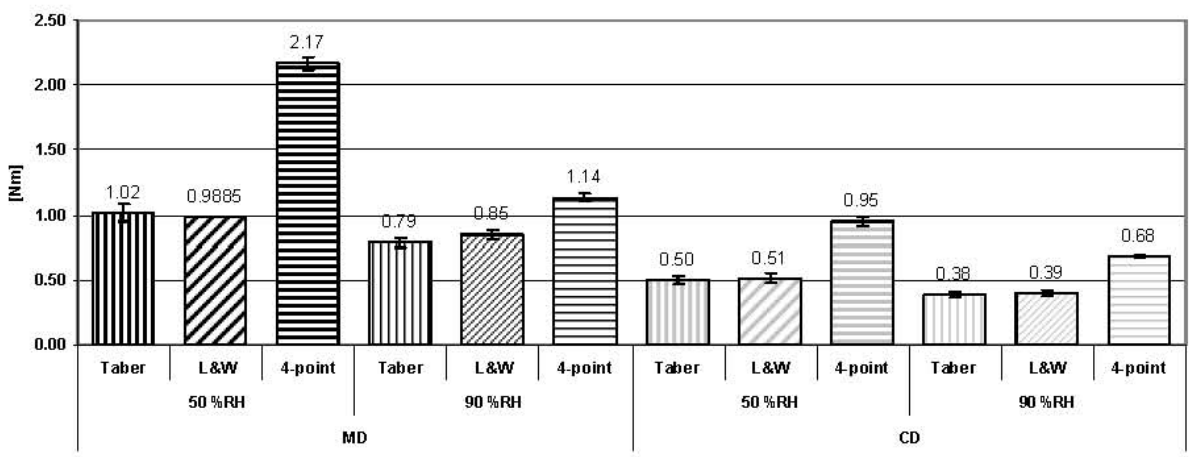

Figure 3. Measured bending stiffness of solid board [Nm].

Modelling of bending stiffness

The bending stiffness was modelled according to equations 3-6. The calculation uses either the ISO thicknesses or the SEM thicknesses and elastic modulus based on either of these thicknesses. The results are calculated for two material moisture contents.

Three cases were studied. First, the bending stiffness was calculated for a structure that is considered homogeneous through the thickness. The next step was to calculate the bending stiffness of a layered structure, but disregarding the properties of the five bonding layers. Finally, the bending stiffness was calculated for the solid board that had eleven distinctive layers; six paperboard layers and five glue layers. All the layers are modelled with two parameters; thickness and elastic modulus. Preliminary experiments show that the dried glue film has elastic modulus 3.7 GPa in standard climate and 3.2 GPa in high humidity. The glue layer thickness is set to 10 μm, as was measured from the SEM pictures. These parameters are used to calculate the bending stiffness of the layered structure including the glue. Table 4 represents the data corresponding these three cases.

Table 4. Calculated bending stiffness of solid board.

			Homogeneous		Layered no glue		Layered with glue	
Direction	**% RH**	**Method**	**S_b [Nm]**	**t [mm]**	**S_b [Nm]**	**t [mm]**	**S [Nm]**	**t [mm]**
MD	50	ISO	1.28	1.729	2.58	1.948	2.78	1.998
		SEM	1.04	1.555	1.66	1.555	1.81	1.605
	90	ISO	0.98	1.729	1.77	1.948	1.92	1.998
		SEM	0.80	1.555	1.14	1.555	1.25	1.605
CD	50	ISO	0.61	1.729	1.07	1.948	1.18	1.998
		SEM	0.50	1.555	0.69	1.555	0.77	1.605
	90	ISO	0.47	1.729	0.67	1.948	0.77	1.998
		SEM	0.38	1.555	0.43	1.555	0.50	1.605

Figure 4 gathers all the so far presented bending stiffness values into one figure. The three different calculated cases are presented together with the 4-point bending stiffness measurement results.

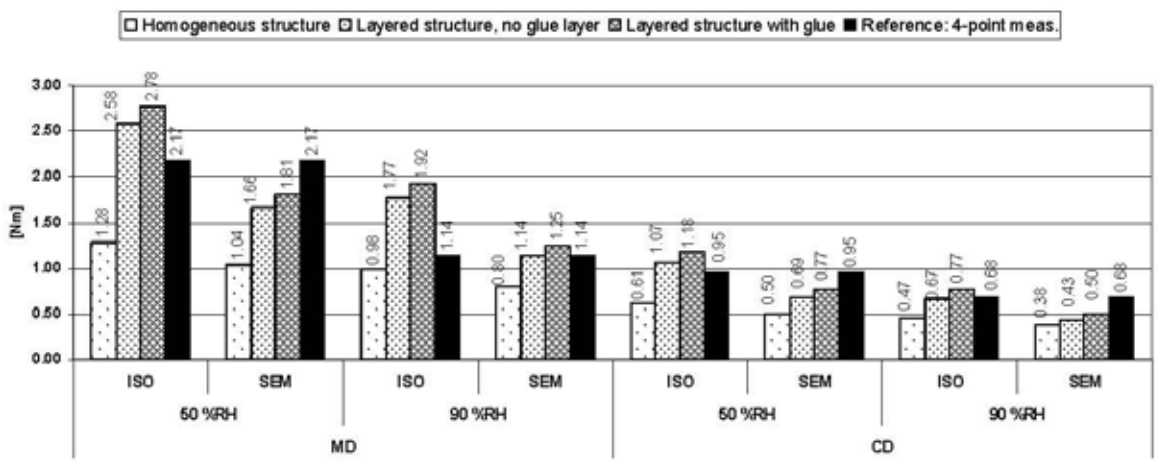

Figure 4. Bending stiffness of solid board [Nm] modelled as a homogeneous or a layered structure.

6. Discussion

When measuring bending stiffness it is essential to keep the deformation small so that the maximum slope of the force deformation curve can be recorded. The geometrical conditions of the test should be under certain limits to keep the deformation in the elastic

range. The 2-point methods (Taber and Lorentzen & Wettre tester) deflected the 38 x 50 mm test piece to 7.5° angle and the maximum force was recorded for bending stiffness calculation. The angle was considerably larger than the elastic limit at about 1.1° for MD and 2.2° for CD for the material and geometry in question. The 100 mm width 4-point test piece had the free test length 150 mm, and maximum deflections were 1.1 mm for MD and 1.6 mm for CD. These values are clearly below the maximum allowable deflections 3.3 mm and 6.5 mm respectively. In the following discussion, the 4-point results are considered as the correct reference values. The 2-point methods give lower bending stiffness values compared to 4-point method, as expected. This is true for all the studied cases; MD and CD bending in two moisture contents. In CD, the 2-point results are approximately 55 % of the 4-point results. In MD, the measurement results in normal conditions are 46 % and in high humidity conditions 72 % of the 4-point results.

The thicknesses determination has a crucial role in the bending stiffness calculation. With the ISO 534:1988 method, the thickness is recorded when the applied pressure on the material studied is 100 kPa. The thicknesses determined from SEM pictures are more real in a sense that no pressure is applied and surface roughness is not included in the thickness measurement. On the other hand the areas studied are very small. In addition, the moisture content affects the thickness of the material. The ISO 534:1988 single sheet thickness of the solid board increases 2.4 % from standard to high humidity conditions. Samples are dried before taking SEM micrographs. The material is most probably thinner than in normal or high humidity conditions which lead to lower bending stiffness values.

Generally a structure that has a homogeneous cross section is less stiff than a designed layered structure with the same thickness. If the solid board is considered homogeneous structure, the modelled values are too low compared to value measured with 4-point technique in each case (see Figure 4). Modelling the solid board as a layered structure gives too large values when ISO thicknesses are used. The exaggeration is bigger for MD than for CD. Assigning E modulus and thickness values for the glue layer, the deviation is even higher from the 4-point results in each case.

If the thicknesses from SEM pictures are used in the calculations, the layered model gives too low values compared to 4-point results in both moisture contents in CD and also in MD in standard climate. Probably the characteristics of the thickness measurement technique have a large effect on the results. The thickness measurements from dried samples give so low bending stiffness values, that the measured value can't be reached. The laminate model gives values that correspond to the 4-point measurements if the properties of the glue layer are tuned. For example, if each glue layer is 35 μm thick and has an elastic modulus of 3 GPa, the following bending stiffness values [Nm] are obtained: MD/50%RH 2.18; MD/90%RH 1.54; CD/50%RH 0.99; CD/90%RH 0.68. With the glue layer thickness 35 μm, the thickness of the structure is equal to the ISO thickness of solid board.

The glue doesn't occur as distinctive solid layers with a certain thickness and elastic modulus in the solid board. The SEM pictures reveal that the bonding layers contain air filled voids. There are several explanations for the lack of contact between the glued paper surfaces. The amount of applied glue is not enough to fill the pockets between two

uneven paperboard surfaces. The mixing and transport of the liquid glue during the lamination can introduce air to the glue layers.

The high humidity treatment reduces the measured (4-point) bending stiffness approximately 47 % for MD and 28 % for CD compared to the standard conditioned samples. For the layered structure (without glue) the reduction is 31 % in MD and 37 % in CD. The effect of moisture is introduced to the calculations as diminished elastic modulus of the solid board and the layers. The hygroexpansion in thickness direction is not taken into account.

7. Conclusion

High humidity treatment reduces the measured bending stiffness values 47 % (MD) and 28 % (CD). As expected, the homogeneous model underestimates the bending stiffness. Better results were obtained using a layered laminate model. The ISO thicknesses overestimate the bending stiffness as surface roughness is included in the measurement. The thickness measured using SEM underestimate the bending stiffness. The samples were bone dry and then thinner than at the studied humidities. Parameters need to be assigned to the glue layer joining the paperboard sheets to improve agreement with the measured bending stiffness values.

8. Acknowledgement

Ms Gunvor Haga Levang (Peterson Emballasje AS, Ranheim Norway) and Fiber-Based Packaging project lead by Ms Marianne Lenes at the Paper and Fiber Reseach Institute (PFI) are acknowledged for providing the materials and the insight into this work. The Research Council of Norway, Peterson AS, Eka Chemicals AB, and the Foundation of Paper and Fiber Reserch Institute are greatfully acknowledged for the financial support. Mr Per Olav Johnsen at PFI is acknowledged for taking the SEM pictures.

9. References

CARLSSON, L. A. & FELLERS, C. N. (1980) Flexural Stiffness of Multi-Ply Paperboard. *Fibre Science and Technology,* 13(3), 213-223.

DANIEL, I. M. & ISHAI, O. (2006) *Engineering mechanics of composite materials,* New York, Oxford University Press.

FELLERS, C. (1997) Bending stiffness of paper and paperboard - a round robin study. *Nordic Pulp and Paper Research Journal,* 12(1), 42-44.

FELLERS, C. N. & CARLSSON, L. A. (2002) Bending stiffness, with Special Reference to Paperboard. IN MARK, R. E., HABEGER, C. C., BORCH, J. & LYNE, M. B. (Eds.) *Handbook of physical testing of paper, volume 1*. New York, Marcel Dekker.

HAMELINK, J. (1963) The Effect of Fiber Distribution upon Stiffness of Paperboard. *Tappi,* 46(10), 151A - 153A.

KORAN, Z. & KAMDEN, D. P. (1989) Bending stiffness of paperboard. *TAPPI Journal,* 72(6), 175-179.

LUEY, A. T. (1963) Stiffness of Multi-Ply Boxboard. *Tappi,* 46(11), 159A - 161A.

RANGER, A. E. (1967) Flexural stiffness of multi-ply boxboard. *Paper Technology,* 8(1), 51-56.

YANG, C. F. (1981) Predicting Structural Rigidity of Multi-Ply Paperboard. *Tappi,* 64(11), 73-76.

This page intentionally left blank.

Session 6
Modeling and Creep Response

Sergiy Lavrykov, Chair

Empire State Paper Research Institute (ESPRI), Syracuse, New York

Recent advances in corrugated container modeling incorporate nonlinear, viscoelastic behavior of medium and linerboard along with sophisticated geometry. Powerful numerical analysis is now possible on desktop computers. These developments allow box designers to analyze multiple, non-related failure mechanisms while optimizing container weight and cost.

Corrugated board box design using full detailed FEM modelling

M.E. Biancolini, C. Brutti, S. Porziani
Department of Mechanical Engineering, Tor Vergata University, Rome
Contact: biancolini@ing.uniroma2.it

Due to its large use in shipping and keeping goods, interest in corrugated board box design is grown in the last period. The main request for a box is to support its own weight and of any other box stacked on it without damage.

The performance can be predicted by means of design formula or complex structural models. An accurate prevision allows an optimisation of the product that can be achieved finding the best composition (i.e., number of layers, corrugation type and materials). Furthermore a local analysis of the stress field allows the optimisation of ventilation holes and handles holes shape and position.

Finite Elements Modelling (FEM) allows to estimate the local stress field an can be conducted at two level of complexity. The first one consists in the modelling each wall of the container with shell elements, condensing the internal structure by means of the lamination theory or homogenisation, the second one consists in the complete modelling of each layer of paper material representing its actual shape. The last approach is very difficult to implement for two reasons: the numerical cost of the calculation, and the complexity of the model. For this reason such kind of analysis is still confined to research field.

This paper is focused on the full detail modelling of corrugated board containers. A dedicated software has been developed for FEM model preparation (Fig.1). The tool allows to generate a detailed mesh of a generic container. Starting parameters include: paper materials (selected from a database), number of wave (single or double wall, Fig.5), box dimensions (including flaps, Fig.3), creasing shape (Fig.4) and adhesive stiffness (adhesive joining is represented by single node to node connectors), meshing parameters (local refining can be prescribed in the critical areas, Fig.2).

Proposed tool allows to quickly set-up parametric analysis with a minimum man effort (of course a lot of CPU is required for the non linear analysis completion). Numerical previsions are discussed from different perspective:

- a detailed modelling allows to better understand the structural behaviour of the container and its failure mechanism;
- a wide parametric analysis allows to define design maps that would be very expensive to obtain experimentally;
- a comparison between experiments and numerical prediction can be performed to understand the differences between the FEM model (representative of an ideal container) and reality;
- full detail modelling can be used as a reference for the tuning of simplified models based on design formula or shell based FEM.

References

[McKee1963] - McKee, C.; Gander, J. W. & R., W. J. “Compression strength formula for corrugated boxes” - Paperboard Packaging, 1963, 55, 149-159

[Baum1981] - Baum, G.; Brennan, D. & Habeger, C. “Orthotropic elastic constants of paper” - TAPPI Journal, 1981, 64, 97-101

[Bronkhorst2003] - Bronkhorst, C. “Modelling paper as a two-dimensional elastic-plastic stochastic network” - International Journal of Solids and Structures, 2003, 40, 5441-5454

[Campbell1961] - Campbell, J. “The in-plane elastic constants of paper” - Australian Journal of Applied Sciences, 1961, 12, 356-357

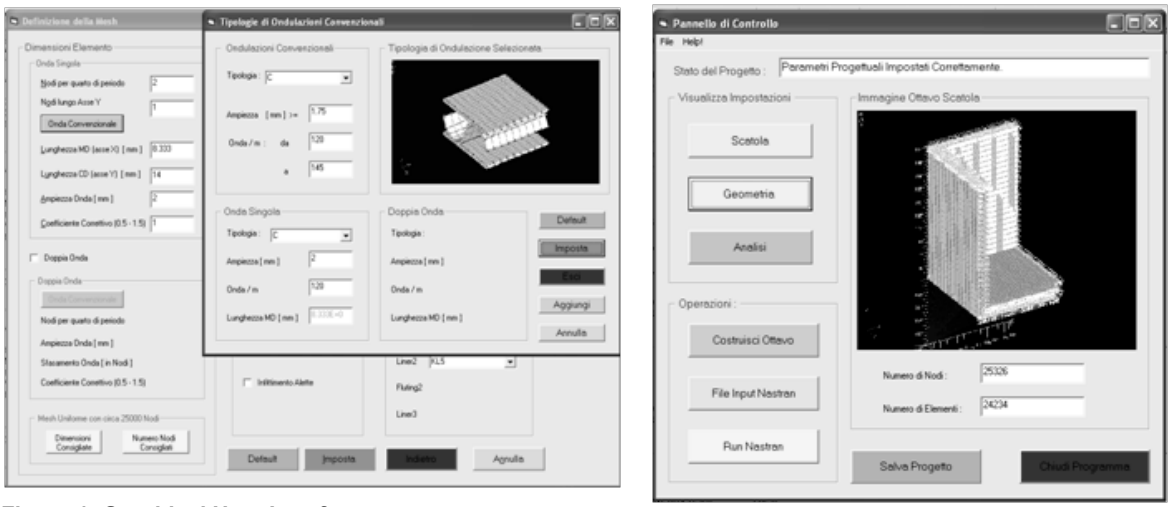

Figure 1. Graphical User Interface

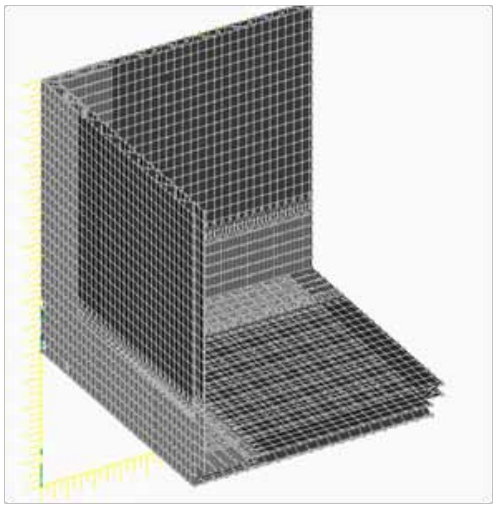

Figure 2. Box FEM model

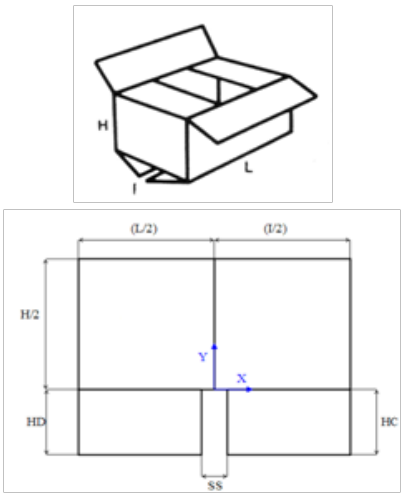

Figure 3. Real box and symmetrical model.

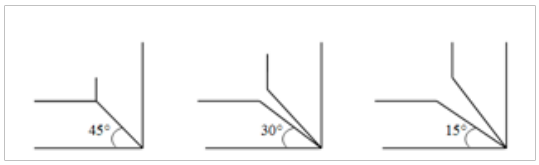

Figure 4. Implemented creasing shapes.

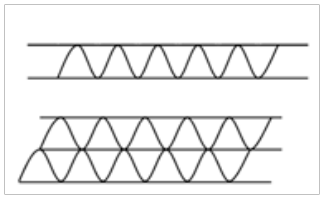

Figure 5. Single and double wall corrugated board profiles.

Note: Travel difficulties prevented Professor Guo from presenting his paper.

Mechanical model on creep properties of double-wall corrugated paperboard

Yanfeng Guo, Jingjing Zhang, Wei Zhang, Yungang Fu
Department of Packaging Engineering, Xi'an University of Technology,
Xi'an 710048, Shaanxi Prov., P. R.China

Abstract: This paper deals with mechanical model on creep properties of double-wall corrugated paperboard by using theory of viscoelastic mechanics. The main feature of this paper is the establishment of mechanical model and mathematical relationship of creep properties of double-wall corrugated paperboard, the analysis and calculation of model parameters. Two mechanical models of creep properties have been established, the first mechanical model includes four parameters, the second mechanical model consists of with three parameters, and the second mechanical model is simpler and more convenient than the first one. By comparing the theoretical and experimental results, the validity of two mechanical models is verified. These two mechanical models may also reflect the creep properties of double-wall corrugated paperboard, and the first mechanical model is better to describe the creep properties of double-wall corrugated paperboard at different combined conditions of relative humidity and constant compression load than the second one. The work provides mechanical models and mathematical relationships relevant to design applications for protective packaging for transportation and storage of goods.

Keywords: Double-wall corrugated paperboard, creep properties, mechanical model

Introduction

Corrugated paperboard is a kind of environmental-friendly package cushioning material with corrugated sandwich structure, holds lightweight, high strength-to-weight and stiffness-to-weight ratios, and more heavily loaded boxes, pads and pallets may be made of double-wall corrugated paperboards. In addition, it is made of reusable paper and water-based glue, and these materials are recyclable, reusable and biodegradable. So it has economic and environmental advantages over plastic foams, and there is an increasing interest in utilizing it in protective package for precise equipment and instrument, household appliance and fragile goods etc.[1] The compression strength, crush strength, bending defection, flexural stiffness were investigated by Hahn, Urbanik, Hahn, Biancolini, Lee, Bronkhorst.[2-6] In the reference [7], Guo et al evaluated the creep properties of double-wall corrugated paperboard by a series of experimental studies, analyzed the effects of relative humidity and constant compression load on creep property, established the piecewise experimental formulas of creep and time curves. Yet there is lack of a further study on mechanical model of creep properties. So, on the basis of previous experimental research on creep properties of double-wall corrugated paperboard at different combined conditions of relative humidity and constant compression load, the aim of this paper is to establish the mechanical model and mathematical relationship of creep properties, and verify the validity of mechanical models.

Four-Parameter Mechanical Model

In this part, the first mechanical model with four parameters is developed by using theory of viscoelastic mechanics, and the model parameters are calculated by using coefficient method.

When subjected to a constant compression load for a period of time, corrugated paperboard tends to lose thickness, and this phenomenon is referred to as creep properties. The creep properties of double-wall corrugated paperboard have been obtained by a series of experimental studies on creep testing apparatus at twenty different experimental conditions.[7] The creep and time curves of double-wall corrugated paperboard are more complicated, in the initial stage of loading, the deformation rate of double-wall corrugated paperboard increases similarly with a linear function. From 1 hour to 168 hours, the creep properties are obvious, and the creep rate increases with an exponential function during the creep stage of loading. The mathematical model of creep and time curves of double-wall corrugated paperboard is described as piecewise experimental formulas as follows

$$\varepsilon = \begin{cases} a_0 t & (t \le 1) \\ a_0 + 1 - e^{-\alpha(t-1)} & (1 < t \le 168) \end{cases} \tag{1}$$

Where, t is loading time, a_0 and α are the characteristic factors (see Table.1), the symbol σ_0 represents the constant compression load, and the character 'RH' is the abbreviation of relative humidity.

Table.1 Characteristic factors of creep and time curves

RH/%	σ_0 /10kPa	a_0	α /10^{-4}
	1.688	0.1594	4.4188
	1.842	0.1601	6.1308
60	1.996	0.1763	4.3385
	2.150	0.3041	11.9450
	2.304	0.4613	6.9852
	1.688	0.2181	12.314
	1.842	0.2313	11.6650
70	1.996	0.2987	10.5420
	2.150	0.3712	5.7302
	2.304	0.4173	4.9058
	1.688	0.2855	21.922
	1.842	0.3681	11.8750
80	1.996	0.3951	19.4810
	2.150	0.4636	2.1771
	2.304	0.5007	3.4963
	1.688	0.3557	30.5780
	1.842	0.5363	7.7698
90	1.996	0.7068	3.0668
	2.150	0.7085	3.6041
	2.304	0.8683	2.5009

During the initial stage of loading ($t \le 1$), the strain $\varepsilon_1 = a_0 t$ is a linear function of loading time, and the expression of strain is in conformity with the deformation rule of damper. During creep stage of loading ($1 < t \le 168$), the expression of strain or creep rate may be written as

$$\varepsilon = \varepsilon_2 + \varepsilon_3 = (a_0 + 1 - e^{\alpha}) + e^{\alpha}(1 - e^{-\alpha t}) \tag{2}$$

Where, the first term of right side of Eq.(2) $\varepsilon_2 = a_0 + 1 - e^{\alpha}$ is a constant and conforms to the

transient elastic deformation rule of spring, yet the second term $\varepsilon_3 = e^{\alpha}(1-e^{-\alpha t})$ is an exponential function and accords with the deformation rule of Kelvin Model.[8] By the above analysis, the first mechanical model may be established as the combined model of damper, spring and Kelvin Model, which is shown in Fig.1, and it consists of four parameters such as viscosity factor η_1, elastic modulus E_2, viscosity factor η_3 and elastic modulus E_3 of Kelvin Model.

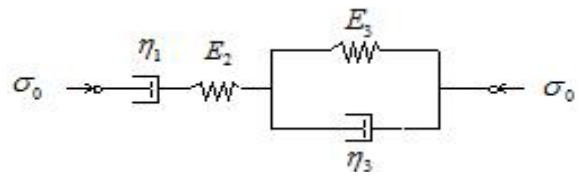

Fig.1 The first mechanical model with four parameters

Calculation of model parameters

For the first mechanical model with four parameters, the stress strain constitutive relations of damper, spring and Kelvin Model are respectively described as follows:

$$\begin{cases} \varepsilon_1 = \dfrac{\sigma_0}{\eta_1} t \\ \varepsilon_2 = \dfrac{\sigma_0}{E_2} \\ \varepsilon_3 = \dfrac{\sigma_0}{E_3}(1-e^{-t/\tau}) \qquad (\tau = \dfrac{\eta_3}{E_3}) \end{cases} \tag{3}$$

So, by using coefficient method, the four parameters of mechanical model may be calculated according to the following procedure:

(1) During the initial stage of loading ($t \le 1$), by comparing the strain $\varepsilon_1 = a_0 t$ with the first expression of Eq.(3), the viscosity factor of damper is derived as $\eta_1 = \dfrac{\sigma_0}{a_0}$. Then substituting the characteristic factor a_0 and constant compression load σ_0 at twenty different experimental conditions in Table.1 into η_1, the viscosity factor of damper η_1 are calculated and shown in Table.2.

Table.2 Viscosity parameter of damper η_1 (10^4Pa·s)

RH/%	Constant compression load σ_0 /10kPa				
	1.688	1.842	1.996	2.150	2.304
60	10.5897	11.5053	11.3216	7.0700	4.9946
70	7.7396	7.9637	6.6823	5.7920	5.5212
80	5.9124	5.0041	5.0519	4.6376	4.6016
90	4.7456	3.4346	2.8240	3.0346	2.6535

(2) During the creep stage of loading ($1 < t \le 168$), by comparing $\varepsilon_2 = a_0 + 1 - e^{\alpha}$ with the second expression of Eq.(3), the elasticity parameter of spring is obtained as $E_2 = \dfrac{\sigma_0}{a_0 + 1 - e^{\alpha}}$. Then substituting the characteristic factors a_0 and α, and constant compression load σ_0 at twenty

different experimental conditions in Table.1 into E_2, the elastic modulus of spring is calculated and given in Table.3.

Table.3 Elasticity parameter of spring E_2(10kPa)

RH/%	Constant compression load σ_0/10kPa				
	1.688	1.842	1.996	2.150	2.304
60	10.5897	11.5496	11.3495	7.0979	5.0022
70	7.7835	8.0041	6.7060	5.8010	5.5277
80	5.9582	5.0203	5.0769	4.6398	4.6048
90	4.7868	3.4396	2.8252	3.0361	2.6542

(3) During the creep stage of loading ($1 < t \le 168$), by comparing $\varepsilon_3 = e^{\alpha}(1-e^{-\alpha t})$ with the third expression of Eq.(3), the two characteristic parameters of Kelvin Model are respectively derived as $E_3 = \frac{\sigma_0}{e^{\alpha}}$ (elastic modulus) and $\eta_3 = \frac{E_3}{\alpha}$ (viscosity factor). Then substituting the characteristic factor α and constant compression load σ_0 at twenty different experimental conditions in Table.1 into E_3 and η_3, the elastic modulus and viscosity factor of Kelvin Model are calculated and provided in Table.4.

Table.4 Characteristic parameters of Kelvin Model

RH/%	σ_0/10kPa	E_3/10kPa	η_3/10^8Pa·s
60	1.688	1.6887	0.3822
	1.842	1.8431	0.3006
	1.996	1.9969	0.4603
	2.150	2.1526	0.1802
	2.304	2.3056	0.3301
70	1.688	1.6901	0.1372
	1.842	1.8441	0.1581
	1.996	1.9981	0.1895
	2.150	2.1512	0.3754
	2.304	2.3051	0.4699
80	1.688	1.6917	0.0772
	1.842	1.8442	0.1553
	1.996	1.9999	0.1027
	2.150	2.1505	0.9878
	2.304	2.3048	0.6592
90	1.688	1.6931	0.0554
	1.842	1.8434	0.2373
	1.996	1.9966	0.6510
	2.150	2.1508	0.5968
	2.304	2.3046	0.9215

Three-parameter Mechanical Model

In this part, the second mechanical model with three parameters has been established by using theory of viscoelastic mechanics, and the parameters of mechanical model have been calculated by using the differential form of constitutive relation.

For the experiential formula of creep and time curves of double-wall corrugated paperboard, during the initial stage of loading ($t \le 1$), the differential equation of strain may be written as

$$\dot{\varepsilon}_1' = a_0 \tag{4}$$

Because a_0 is a constant, $\dot{\varepsilon}_1'$ is in conformity with the deformation rule of damper. During the creep stage of loading ($1 < t \le 168$), the differential equation of strain or creep rate is derived as

$$\dot{\varepsilon}_2' = \alpha e^{-\alpha(t-1)} \tag{5}$$

Which accords with the deformation rule of Kelvin Model.[8] So, according to the characteristics of differential equations of classical mechanical model such as damper and Kelvin Model, the second mechanical model may be developed and given in Fig.2. It comprises three parameters such as viscosity factor η_1', viscosity factor η_2' and elastic modulus E_2' of Kelvin Model.

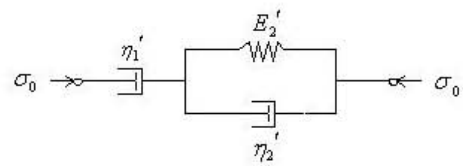

Fig.2 The second mechanical model with three parameters

For the second mechanical model with three parameters, the differential equations of damper and Kelvin Model are respectively described as follows:

$$\sigma_0 = \eta_1' \dot{\varepsilon}_1' \tag{6}$$

$$\sigma_0 = E_2' \varepsilon_2' + \eta_2' \dot{\varepsilon}_2' \tag{7}$$

Substituting Eq.(5) into Eq.(7), the differential equation of Kelvin Model is again written as.

$$\sigma_0 = E_2' \varepsilon_2' + \eta_2' \dot{\varepsilon}_2' = E_2'(a_0 + 1 - e^{-\alpha(t-1)}) + \eta_2' \alpha e^{-\alpha(t-1)} \tag{8}$$

Calculation of model parameters

According to the differential form of constitutive relation, the three parameters of mechanical model may be calculated by using the following procedure:

(1) During the initial stage of loading ($t \le 1$), substituting Eq.(4) into Eq.(6), the stress is derived as $\sigma_0 = \eta_1' \dot{\varepsilon}_1' = \eta_1' a_0$, so the viscosity factor of damper is $\eta_1' = \frac{\sigma_0}{a_0}$. Then substituting the characteristic factor a_0 and constant compression load σ_0 at twenty different experimental conditions in Table.1 into η_1', the viscosity factor of damper η_1' is calculated and shown in Table.5.

(2) During the creep stage of loading ($1 < t \le 168$), Eq.(8) describes the differential equation of Kelvin Model, and it may be written as

$$\sigma_0 = E_2'(a_0 + 1) - E_2' e^{-\alpha(t-1)} + \eta_2' \alpha e^{-\alpha(t-1)} \tag{9}$$

By combining Eq.(7) with Eq.(9), it should satisfy the following relation

$$\begin{cases} \sigma_0 = E_2'(a_0+1) \\ 0 = -E_2' e^{-\alpha(t-1)} + \eta_2' \alpha e^{-\alpha(t-1)} \end{cases} \tag{10}$$

So, the two characteristic parameters of Kelvin Model are derived as $E_2' = \frac{\sigma_0}{a_0+1}$, $\eta_2' = \frac{E_2}{\alpha}$.

Then substituting the characteristic factors a_0 and α, and constant compression load σ_0 at twenty different experimental conditions in Table.1 into E_2' and η_2', the elastic modulus and viscosity factor of Kelvin Model are obtained and given in Table.5.

Table.5 Characteristic parameters of mechanical model

RH/%	σ_0/10kPa	η_1'/10^4Pa·S	E_2'/10kPa	η_2'/10^8Pa·s
	1.688	10.5897	1.4559	0.3295
	1.842	11.5053	1.5878	0.2590
60	1.996	11.3216	1.6968	0.3911
	2.150	7.0700	1.6486	0.1380
	2.304	4.9946	1.5767	0.2257
	1.688	7.7396	1.3858	0.1125
	1.842	7.9637	1.4960	0.1282
70	1.996	6.6823	1.5369	0.1458
	2.150	5.7920	1.5680	0.2736
	2.304	5.5212	1.6256	0.3314
	1.688	5.9124	1.3131	0.0599
	1.842	5.0041	1.3464	0.1134
80	1.996	5.0519	1.4307	0.0734
	2.150	4.6376	1.4690	0.6747
	2.304	4.6016	1.5353	0.4391
	1.688	4.7456	1.2451	0.0407
	1.842	3.4346	1.1990	0.1543
90	1.996	2.8240	1.1694	0.3813
	2.150	3.0346	1.2584	0.3492
	2.304	2.6535	1.2332	0.4931

Verification of Mechanical Models

In this part, the deference of these two mechanical models is analyzed, and the validity of them is verified. The first mechanical model includes four parameters such as η_1, E_2, E_3, η_3, yet the second mechanical model consists of three parameters such as η_1', E_2', η_2', and the second model is simpler and more convenient than the first model. For the parameters of spring in these two models, there is the mathematical relationship

$$\frac{1}{E_2'} = \frac{a_0+1}{\sigma_0} = \frac{a_0+1-e^{\alpha}}{\sigma_0} + \frac{e^{\alpha}}{\sigma_0} = \frac{1}{E_2} + \frac{1}{E_3} \tag{11}$$

It is clear that the effect of two springs (E_2, E_3) in the first mechanical model is the same as the

spring ($E_2^{'}$) in the second mechanical model. So the second mechanical model has less computation and complexity than the first one, and is convenient to analyze the mechanical properties of double-wall corrugated paperboard.

In the reference [7], the experimental studies for creep properties of double-wall corrugated paperboard have twenty different experimental conditions. According to these experimental conditions, by using the stress and strain relation equations of these two mechanical models, the creep and time curves may be respectively obtained. Then comparing the theoretical and experimental results, the validity of these two mechanical models would be verified. For example, the theoretical and experimental curves for four kinds of experimental condition are given in Fig.3. Due to the limited space, other comparisons are omitted. By comparing the experimental results and theoretical values of these two mechanical models, it is obvious that, these two mechanical models may also reflect the creep properties of double-wall corrugated paperboard, yet the first mechanical model would be better to reflect the creep properties of double-wall corrugated paperboard at different combined conditions of relative humidity and constant compression load than the second one.

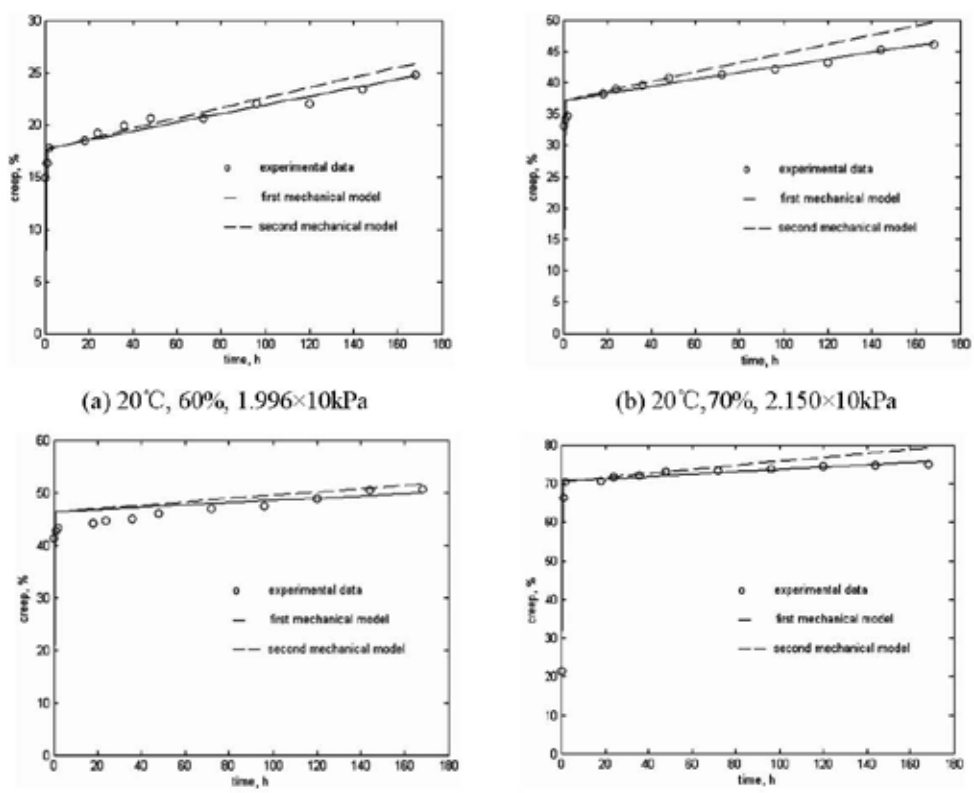

(a) 20℃, 60%, 1.996×10kPa (b) 20℃,70%, 2.150×10kPa

(c) 20℃, 80%, 2.150×10kPa (d) 20℃, 90%, 1.996×10kPa

Fig.3 Comparison of experimental and theoretical results

Conclusions

The work provides mechanical models and important mathematical relationships relevant to design applications for protective packaging for transportation and storage of goods. By using

theory of viscoelastic mechanics, two mechanical models of creep properties are established, and the validity of them are verified by comparing with the experimental results. The first mechanical model includes four parameters, the second mechanical model holds three parameters, and the second mechanical model is simpler and more convenient than the first one. These two mechanical models may also reflect the creep properties of double-wall corrugated paperboard, and the first mechanical model is better to describe the creep properties of double-wall corrugated paperboard at different combined conditions of relative humidity and constant compression load than the second one.

Acknowledgments

This research work is supported by the Scientific Research Foundation of Science and Technology Department of Shaanxi Province under the Grant 2007K07-21 and the Scientific Research Foundation of Printing & Packaging Material and Technology Beijing Area Major Laboratory under the Grant KF200705. We would like to thank Northwest Corrugated Paperboard Limited Company for providing the test specimens of double-wall corrugated paperboard.

References

1. Kirkpatrick, J. and Sek, M., "Replacement of Polymeric Cushioning with Corrugated Fiberboard-case Study", Proceedings of 10th IAPRI World Conference on Packaging, Australia, Melbourne, 267-276(1997).
2. Hahn, E. K., Rudo, A. D., Westerlind, B. S., Carisson, L. A., "Compressive Strength of Edge-Loaded Corrugated Board Panels", Experimental Mechanics,32(3):259-265(1992).
3. Urbanik, T. J, "Effect of Corrugated Flute Shape on Fiberboard Edgewise Crush Strength and Bending Stiffness", Journal of Pulp and Paper Science, 27(10):330-335(2001).
4. Biancolini, M. E. and Brutti, C., "Numerical and Experimental Investigation of the Strength of Corrugated Board Packages", Packaging Technology and Science,16(2): 47-60(2003).
5. Lee, M. H. and Park, J. M., "Flexural Stiffness of Selected Corrugated Structures", Packaging Technology and Science,17(5):275-286(2004).
6. Bronkhorst, C. A. and Riedemann, J. R., "The Creep Deformation Behavior of Corrugated Containers in a Cyclic Moisture Environment", Proceedings of the Symposium on Moisture Creep Behavior of Paper and Board, Stockholm, Sweden, 249-273(1994).
7. Guo, Yanfeng, Fu, Yungang, Zhang, Wei, "Creep Properties and Recoverability of Double-Wall Corrugated Paperboard", Experimental Mechanics, 48(3):327-333(2008)
8. Christensen, R. M., "Theory of Viscoelasticity (Second edition)", Dover Publication, New York, 2002

Compression fatigue creep of paperboard

C. Tim Scott and Roland Gleisner

U.S. Forest Service, Forest Products Laboratory, Madison, Wisconsin

Mechanical fatigue creep is the imposition of a cyclic stress on a structural element causing irreversible deformation. Fatigue is typically characterized by a mean stress level about which a periodic stress is imposed whose amplitude and frequency can vary with time. Considerable effort has been made to characterize the fatigue properties of materials, principally metals, since catastrophic failures are often associated with cyclic fatigue stresses, particularly when defects are present. Both tension and compression fatigue stresses are present in many paper processes and applications. In the papermaking process itself, the paper web experiences periodic tensioning as it winds through the machine. It may again experience more cyclic stress as it is unwound and converted. The core on which it is wound and unwound may also experience considerable cyclic stresses which have been known to cause failures, particularly near the chuck.

In a specific structural application of paper, corrugated boxes are designed to carry considerable stacking loads but may also experience cyclic compression stresses in the shipping environment. Even humidity variations can lead to considerable cyclic stresses in warehouse environments. Attempts have been made to measure the stacking strength of boxes exposed to various vibration loads and under cyclic humidity conditions. Likewise, attempts have been made to measure the compression creep response of linerboard and medium under cyclic humidity conditions. However, little is known about the fatigue strength of the paperboard exposed to cyclic compression stresses or how fatigue cycling may be used to predict moisture hysteresis.

This paper will present an overview of the instrumentation and experimental approach developed to evaluate cyclic compression fatigue of paperboard. A heavy linerboard sample (BW = 260gsm), cut for cross-machine direction specimens, was selected for initial tests. Four cyclic frequencies were evaluated (.2, 2, 20, and 200 Hz). The mean compressive stress was chosen not to exceed 80% of the “static” compressive fail load. Specimens were subjected to cyclic fatigue for at least 1-hour or until they failed. The cyclic creep portion of the data was fit to a power-law function and creep rates were determined at various time intervals.

Session 7
Moisture and Time Response

M.E. Biancolini, Chair

University of Rome, Rome, Italy

Cellulose materials have hierarchal structure, and various degrees of viscoelastic behavior occur at all structural levels, but measuring these effects becomes particularly challenging when approaching microstructures. Improvements in test equipment allow more complete analysis of these behaviors. Recent work on cellulose fiber mechano-sorptive behavior helps define a range of performance in fiber webs, where continuum behavior is measured. The vast spectrum of time, temperature, and moisture behavior of cellulose materials provides an important area of future research.

Use of ultrasonic velocity measurement to investigate moisture-induced stress relaxation in paper

David Vahey, John Considine, Roland Gleisner

U.S. Forest Service, Forest Products Laboratory, Madison, Wisconsin

Introduction

Convenient, non-destructive ultrasonic velocity testing is useful for studying the influence of moisture treatments on paper performance. Ultrasonic testing is sensitive to internal stresses developed during paper manufacture and responds to the loss of such stresses induced by moisture treatments. The goal of this work is to characterize the internal stresses in paper by monitoring their degradation under moisture cycling.

The present approach uses ultrasound to characterize the stiffness of a set of commercial papers covering a wide range of grammage and function. The papers were subjected to repetitive cycles of soaking, preconditioning at 30% RH, and reconditioning at 50% RH, all done without drying restraint. Following each cycle, the stiffness anisotropy and orientation-angle (the "peanut curve") were determined ultrasonically. Both shear and tensile stiffnesses were measured. Dimensional changes in the samples were also measured.

This approach to study the relation between drying stresses and stiffness orientation is the reverse of that commonly taken. Wahlström and Mäkelä (2005) and Hess and Brodeur (1996) both related handsheet stiffness properties to fiber orientation and the degree of drying restraint [1,2]. They found that stiffness and fiber-orientation anisotropy were the same for sheets dried under full restraint. For sheets that were freely dried or dried under partial restraint (wet straining), they found that the stiffness anisotropy was higher than the fiber-orientation anisotropy. Hess and Brodeur (1996) also showed that the fiber misalignment angle was invariably larger than the stiffness misalignment angle. However, a theoretical basis for the observations was not provided.

A heuristic model suggested by the findings is

$$E(\theta) = E_B F(A_F, \theta - \theta_F) S(A_S, \theta - \theta_S) \qquad \text{Eq. (1)}$$

where $E(\theta)$ is the sonic modulus at orientation angle θ, E_B is the (isotropic) modulus contribution from bonding, F is the contribution from fiber orientation anisotropy A_F and orientation θ_F, and S is the contribution from stress orientation anisotropy A_S and orientation θ_S. The analysis of our experiments will be based on this model, using the assumptions that (1), the fiber orientation distribution F is unchanged as a result of moisture cycling, and (2) the isotropic bonding contribution E_B is unchanged by moisture cycling. This leaves stress orientation S as the variable to be characterized by repeated soaking-drying cycles.

Samples and Tests

The samples used in the study were four boards and four office papers. The samples have had an extensive measurement history in connection with previous work on z-direction fiber orientation [3]. As part of previous work, two specimens from each sample were measured on commercial ultrasonic testing equipment offered by SoniSys Corporation, Atlanta, Georgia. Measurements included the "peanut curve" associated with the in-plane propagation of longitudinal sound waves. In addition, shear propagation was measured in the cross-machine direction (CD) and at 45º to the CD. In the current work, the same specimens were measured after each of five wetting/drying cycles using two Sonic Sheet Testers model SST-250, made by Nomura Shoji Corporation, Japan. One of the testers was used as produced. The other was modified to measure in-plane shear waves. Calibration of the shear velocity measurement was done by comparison to the shear measurements provided by SoniSys on the same samples.

Specimen shrinkage in the MD and CD was also measured after each moisture cycle. Measurement resolution was 0.25 mm. corresponding about 0.1%. After five moisture cycles, typical total shrinkage was about 1.0%, corresponding to 10 resolution elements.

Analysis

Measurements from the two specimens for each sample were averaged prior to processing. While the full peanut curve complete with angle is produced by each ultrasonic test, the angles tended to be small and were not a major focus of the analysis. The major focus was the trend in the maximum (~MD) and minimum (~CD) longitudinal and shear stiffness values following each wetting-drying cycle. A simplified form of Equation (1) used to track the trend is

$$E_{MD} = E_B \left(\frac{N_{MD}}{N_{CD}} \right)^n S_{MD}, \qquad \text{Eq. (2)}$$

and

$$E_{CD} = E_B \left(\frac{N_{CD}}{N_{MD}} \right)^n S_{CD}. \qquad \text{Eq. (3)}$$

The generalized form of the fiber orientation distribution F in Eq. (1) is replaced by a very specific form; namely, F is the ratio of the number of fibers N parallel to a direction of interest (MD or CD, above) divided by the number of fibers perpendicular to that direction, raised to a power n. This relationship is known to hold for the case of full drying restraint with $n = 0.5$ [1,2]. That the relation may hold for other conditions is an assumption made for convenience, since it leads to the following simplifications:

$$E_{Geo} = \sqrt{E_{MD} E_{CD}} = E_B \sqrt{S_{MD} S_{CD}}, \qquad \text{Eq. (4)}$$

and

$$\frac{E_{MD}}{E_{CD}} = \left(\frac{N_{MD}}{N_{CD}} \right)^{2n} \frac{S_{MD}}{S_{CD}}. \qquad \text{Eq. (5)}$$

For this work, the correctness of the form of the fiber orientation distribution is less important than the assumption that it doesn't change with repeated wetting-drying cycles. Therefore, Equations (4) and (5) allow us to track the changes in internal stress with moisture cycling. At the same time, measurements of the shrinkage of the samples with each cycle allow correlation of the loss of internal stress with dimensional change.

Some Results

Figure 1 shows the parallel relationship between the loss of ultrasonic modulus and the shrinkage in the sheet after each of five moisture cycles. The results are averaged for the four board samples, but a very similar curve also pertains to the four office papers. Shrinkage and ultrasonic modulus track very closely for the first two cycles. Since our measurement of ultrasonic modulus characterizes the sheet at 25 kHz, and shrinkage is a very low-frequency phenomenon, the early agreement between the two measurements is more surprising than their eventual divergence.

Note that two results are plotted for the fourth soaking cycle. In all other cycles, testing was done following soaking, preconditioning and moisture absorption to equilibrium at 50% relative humidity (RH). After the fourth soaking, the preconditioning room was not immediately available. Measurements plotted at the abscissa "Soak 4D" were made following soaking and desorption to 50% RH without preconditioning. Samples were then preconditioned and measured again after moisture absorption to 50% RH. These results are plotted at the abscissa "Soak 4". The extent to which the difference in drying history following the fourth soak might have influenced results is not known. Apart from this

uncertainty, the stability of the ultrasonic modulus between soaks 3-5 supports the basic assumption that the bonding modulus E_B is stable throughout the testing.

In other analysis, the anisotropy of internal stress S is compared to the anisotropy of shrinkage. Parallel treatments are performed on shear as well as extensional modulus. Observed anisotropy of the shear modulus, in contrast to expectations of the orthotropic theory, are presented and discussed.

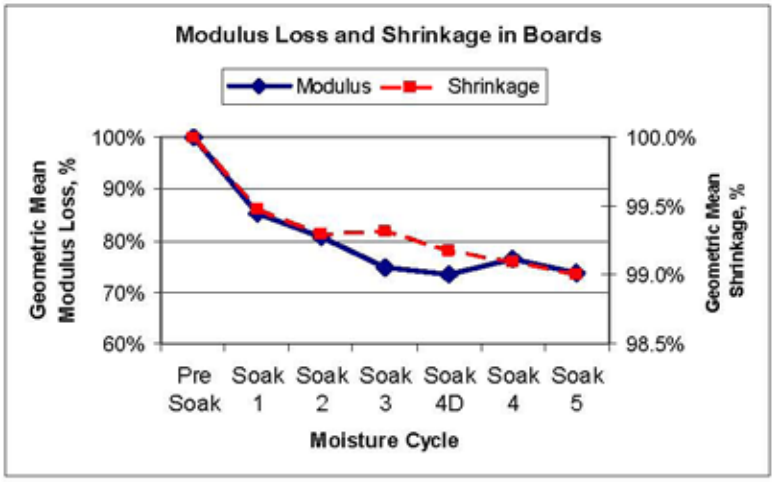

Figure 1. Geometric means of ultrasonic modulus loss and shrinkage in boards after repeated cycles of soaking, preconditioning and re-equilibration at 50% RH. (See text for exception 4D.)

References

1. T. Wahlström and P. Mäkelä, Predictions of Anisotropic Multiply Board Properties Based on Isotropic Ply Properties and Drying Restraints, 13th Fundamental Research Symposium, Cambridge, pp 241-281, September, 2005

2. TR Hess and PH Brodeur, Effects of Wet Straining and Drying on Fibre Orientation and Elastic Stiffness Orientation, J Pulp and Paper Sci. **22,**5, pp J160-J163, 1996

3. D. W. Vahey, and J. M. Considine, "Tests for Z-direction fiber orientation," in 61st Appita Annual Conference and Exhibition, Gold Coast, Australia, 2007, pp. 53-59.

Wood fibres do indeed show mechano-sorptive creep.

Lennart Salmén, Anne-Mari Olsson, Christer Fellers
STFI-Packforsk
Box 5604,
SE 114 86 Stockholm,
Sweden

Abstract

The phenomenon of increased creep during changing moisture has been observed for long, both for wood and paper products. This accelerated creep, termed mechano-sorptive creep, is a complex phenomenon that has been extensively studied from the time of its discovery in the late 1950ties. At a time it was argued that wood fibres did not show this mechano-sorptive creep and therefore the effect was sought in the structure of the paper and the bonding between the fibres. The claims for this arguing were mainly based on measurements of holocellulose fibres. However later studies to some extent questioned this result, as being a consequence of inadequate moisture sorption rates, but also due to observations that regenerated cellulose fibres did show mechano-sorptive creep.

In order to clarify the behaviour for wood and pulp fibres a fibre testing methodology was adopted enabling single fibre testing under climatic variations. For this purpose single wood and pulp fibres were prepared either by careful microscopic isolation of native wood fibres from a single annual ring of a spruce tree or as holocellulose spruce pulp fibres isolated by maceration of the wood. These fibres were one by one glued, using a stiff moisture insensitive glue, to a tensile stage of a dynamic mechanical analyser, DMA, and tested. Each single fibre was first exposed to a tensile stress at a constant climate of 80% relative humidity, RH, followed by a cycling environment varying between 80 and 30 %RH. A number of fibres were measured in this way at different stress levels.
Contrary to earlier claims it was by these measurements demonstrated that single wood and pulp fibres exposed to a cyclic relative humidity indeed show a considerably higher creep than that corresponding to the highest RH experienced in the humidity cycle, i.e. showing a mechano-sorptive creep behaviour. The cyclic creep rate was also shown to be a function of the constant creep rate and to be an apparent linear function of the applied stress.
The ratio between the cyclic creep rate to the constant creep rate was about 2 for the wood fibres and around 2.9 for the holocellulose fibres. This should be compared to a ratio of 5 shown to be the case for papers. If this discrepancy is related to influence of fibre-fibre bonds or to the fact that transverse fibre properties play a role have to be further investigated.

Hygroexpansivity of thermally aged papers

J.M. Considine[1*], M.J. Wald[2], R.E. Rowlands[2], and K.T. Turner[2]

1 U.S. Forest Service, Forest Products Laboratory, Madison, Wisconsin
2 University of Wisconsin, Madison, Wisconsin
*contact author: jconsidine@fs.fed.us

Confidence in the performance of engineered paper products can be increased through knowledge of how mechanical properties, such as strength, stiffness, and hygroexpansivity change with exposure to various conditions. Environmental effects present during storage of paper products can greatly degrade and change the mechanical performance. The primary aim of the present work is to characterize changes of mechanical properties, including tensile response and dimensional stability, with aging and to develop time-dependent models to describe the behavior. Specifically, this research evaluates the effects of thermal aging on the properties of two different papers using tensile testing and hygroexpansivity measurements. The change in stiffness, strength, and hygroexpansivity was measured for papers aged at different temperatures for various lengths of time. An Arrhenius relationship was used to shift the data collected at various temperatures to a master curve where possible. Full details of experimental results as well as insight into the underlying mechanisms of aging will be presented in this talk.

Participants

Johan Alfthan
Senior Research Associate
Innventia AB
Box 5604
Stockholm, Sweden
SE-11486
+46-8676-7268
johan.alfthan@innventia.com

Marco Evangelos Biancolini
Researcher
Mechanical Engineering
University of Rome
Via Politecnico 1
Rome, Italy
RM-000133
biancolini@ing.uniroma2.it

Ian Chalmers
Scientist
Scion
Private Bag 3020
Rotorua, New Zealand
Rotorua Mail Centre 3046
Ian.Chalmers@scionresearch.com

Douglas W Coffin
Professor
Paper and Chemical Engineering
Miami University
64 N Engineering Building, PCE
Oxford, OH 45056
513-529-0771
coffindw@muohio.edu

Jessica Coher
Quality Department
RockTenn
53 Industrial Drive
Syracuse, NY 13204
315-703-9376
jcoher@rocktenn.com

John Considine
Research Engineer
U.S. Forest Service, Forest Products Laboratory
One Gifford Pinchot Drive
Madison, WI 53726
608-231-9525
jconsidine@fs.fed.us

Nicola Dooley
Paper Scientist
Scion
Private Bag 3020
Rotorua, New Zealand
Rotorua Mail Centre 6046
Nicola.Dooley@scionresearch.com

Pierre Dumont
LGP-PAGORA
461 Rue De La Papeterie
St. Martin D'heres, France
38-38402
Pierre.Dumont@grenoble-inp.fr

Christer Fellers
Innventia AB
Box 5604
Stockholm, Sweden
SE-11486
christer.fellers@innventia.com

Benjamin Frank
Manager, Materials Optimization
Packaging Corporation of America
250 South Shaddle Avenue
Mundelein, IL 60060
847-482-2094
bfrank@packagingcorp.com

Terry Gerhardt
VP Technology & IP
Sonoco
125 West Home Avenue
Hartsville, SC 29550
843-383-7303
terry.gerhardt@sonoco.com

Samuel V Glass
Research Physical Scientist
U.S. Forest Service, Forest Products Laboratory
One Gifford Pinchot Drive
Madison, WI 53726
608-231-9401
svglass@fs.fed.us

Barry Hojjatie
Adjunct Associate Professor
Institute of Paper Science and Technology
Valdosta State
50 10th Street NW
Atlanta, GA 30332
404-894-6363
bhojjati@valdosta.edu

Ronald E Hostetler
Research Fellow
US Paper Consulting
2909 SE Blairmont
Vancouver, WA 98683, USA
803-517-9720
ronald.hostetler@gmail.com

James W Huerta
Manager Materials Program Manager
Materials Engineering
Solo Cup Company
4444 West Grace Avenue
Mequon, WI 53092
847-405-2240
jim.huerta@solocup.com

Pasi Kekko
Senior Product Development Engineer
Metso Paper, Inc.
Kontinperänpolku 120
Toivakka 41660
Finland
+358-4054-56129
Pasi.Kekko@Metso.com

David E Kretschmann
Research Engineer
U.S. Forest Service, Forest Products Laboratory
One Gifford Pinchot Drive
Madison, WI 53726
608-231-9307
dekretsc@wisc.edu

Sergiy Lavrykov
PBE - SUNY ESF
409 Walters Hall
1 Forestry Drive
Syracuse, NY 13210
315-470-6516
lavrykov@esf.edu

Walter Li
Norampac, Inc.
525 Abilene Drive
Mississauga, ON
L5T 2H7
Canada
walter_li@norampac.com

Rick Markson
Director of Design
Sonoco CorrFlex
555 Aureole Street
Winston Salem, NC 27107
201-424-2102
rebecca.white@sonoco.com

Monica McCarthy
Senior Professional Scientist
Sonoco
455 Science Drive, Suite 150
Madison, WI 53711
608-231-3060
monica.mccarthy@sonoco.com

Ron M McInnis
CTS
Interstate Resources
111 Constitution Avenue
Reading, PA 19606
484-333-1878
ronm@interstatecontainer.com

Alan Neel
Lab Technician
Paper, Packaging and Distribution Test Lab
International Paper
4140 Campus Drive
Aurora, IL 60504
630-585-3392
Alan.Neel@ipaper.com

Tom A Newell
T&D Lab Analyst
Technology and Development
Huhtamaki Americas
9201 Packaging Drive
DeSoto, KS 66018
913-583-8665
tom.newell@us.huhtamaki.com

Lawrence C Nykwest
Customer Technical Service Mgr
Interstate Resources
44 PLeasant Drive
Bernville, PA 19506
610-662-9773
lnykwest@unitedcorrstack.com

Sara Paunonen
PhD Stipendiat
Department of Chemical Engineering
NTNU
Høgskoleringen 6B
Trondheim
NO-7491
Norway
sara.paunonen@chemeng.ntnu.no

Roman E Popil
Senior Research Scientist
Institute of Paper Science and Technology
Georgia Institute of Technology
500 10th Street NW
Atlanta, GA 30332
404-894-9722
roman.popil@ipst.gatech.edu

Robert Ramsay
Technical Manager
Liquid Ink
INX International
410 West 34th Street, Apt 306
Steger, IL 60475
708-799-1993 x3922
bob.ramsay@inxintl.com

Diana Russell
Lab Supervisor
Paper, Packaging, & Distribution Test Lab
International Paper
4140 Campus Drive
Aurora, IL 606504
630-585-3570
Diana.Russell@ipaper.com

Javad-Reza Saberian
Scientist
Product Performance Program
FPInnovations
570 Saint-Jean Blvd.
Pointe-Claire
QC
H9R 3J9
Canada
+1-514-630-4100 x2364
javad.saberian@fpinnovations.ca

Michael Schaepe
Technical Manager-Corrugating
Cargill
7425 Hobgood Road
Fairburn, GA 30213
michael_schaepe@cargill.com
C Tim Scott
U.S. Forest Service, Forest Products Laboratory
One Gifford Pinchot Drive
Madison, WI 53726
tscott@fs.fed.us

Michael R St. John
Research Associate
Pulp & Paper Research
Nalco Company
1601 West Diehl Road
Naperville, IL 60563
630-305-2349
mstjohn@nalco.com

Joshua Tinch
Sales Representative
Humidity Control
Key Scientific for Parameter Generation & Control
1054 Old US Highway 70 West
Black Mountain, NC 28711
sales@humiditycontrol.com

Kevin T Turner
Professor
UW-Madison
1513 University Avenue
3031 Mechanical Engineering
Madison, WI 53706
608-890-0913
kturner@engr.wisc.edu

David Vahey
Materials Research Engineer
U.S. Forest Service, Forest Products Laboratory
One Gifford Pinchot Drive
Madison, WI 53726
dvahey@fs.fed.us

Yiming Wang
Sonoco
455 Science Drive, Suite 150
Madison, WI 53711
608-231-2992
yiming.wang@sonoco.com

Angelica Wikström
Development Engineer
Packaging Boards
Billerud AB
Storjohanns Väg 4
Grums
SE
66428
Sweden
+46-73-025-1033
angelica.wikstrom@billerud.com

Junyong Zhu
U.S. Forest Service, Forest Products Laboratory
One Gifford Pinchot Drive
Madison, WI 53726
jzhu@fs.fed.us

Index of Authors

Alfthan, J. 12
Biancolini, M. E. 35, 82
Bloch, J.-F. 30, 69
Brutti, C. 35, 82
Chalmers, I. R. 19
Coffin, D. 5
Considine, J. 33, 94, 98
Decker, J. 33
Desloges, I. 30
du Roscoat, S.R. 30, 69
Dumont, P.J.J. 30, 69
Fellers, C 32, 97
Fu, Y. 84
Glass, S.V. 28
Gleisner, R. 92, 94
Green, D.W. 68
Gregersen, Ø. 70
Guo, Y. 84
Hansson, T. 12
Hojjatie, B. 24
Hostetler, R. 59
Kekko, P. 49
Kouko, J. 49
Kretschmann,D.E. 68
Lason, L. 32
Lavrykov, S. 29
Mähler, A. 32
Mauret, E. 30
Ohlsson, A.-M. 32, 97
Orgéas, L. 69
Paunonen, S. 70
Popil, R.E. 24
Porziani, S. 35, 82
Ramarao, B.V. 29
Rutulainen, E. 49
Rowlands, R. 33, 98
Salmén, L. 97
Schaepe, M.K. 24
Scott, C.T. 92
Timonen, J. 49
Turner, K. 33, 98
Vacher, P. 30
Vahey, D. 33, 94
Vermeulen, B. 69
Viguié, J. 30
Vroman, P. 69
Wald, M. J. 98
Wikström, A. 40
Zhang, J. 84
Zhang, W. 84

Appendix
5th International Symposium

courtesy of

Dr. Ian Chalmers

5th Symposium, April 2001 Victoria Australia. Coordinated by Dr. Ian Parker, Monash University, Victoria, Australia

The bending response of corrugated fibreboard to a cycling relative humidity environment.

I.R. Chalmers[*], *A.D. McKenzie*[+] *and B.I.Johnson*[*]

[*]PAPRO - New Zealand Forest Research Limited, Rotorua, New Zealand
Tel: + 64 7 343 5899 Fax +64 7 348 0942 e-mail: Ian.Chalmers@forestresearch.co.nz
Barbara.Johnson@forestresearch.co.nz
[+]Carter Holt Harvey Pulp & Paper Limited, Kinleith Mill, Tokoroa, New Zealand.
Tel:+64 (0) 7 8863543 Fax: +64 7 8863514 e-mail: andrew.mckenzie@chh.co.nz

Summary:

Corrugated fibreboard packaging is a major cost to New Zealand growers and exporters of fruit. Reducing the cost and weight of packaging requires a better understanding of the effects of the high relative humidity found in coolstores on corrugated fibreboard. In practice boxes are also exposed to changing humidity conditions as, for example, during defrost cycles and when stores are loaded and unloaded. However compression and bending stresses on boxes stacked in coolstores causes compression creep and sidewall bulge. If the bulging is too severe boxes may fail and collapse.

An apparatus was built to measure the bending creep performance of corrugated fibreboard in high and cyclic relative humidity conditions. The bending creep strain was found to consist of cyclic bending in response to cyclic relative humidity superposed on a long-term creep deformation. A model was fitted to strain data to describe the non-cyclic creep deformation. Isochronous creep curves could be generated for samples tested using a range of stress levels to allow the creep performance of packaging materials to be compared.

Using coated board samples and small humidity sensors that can fit between flutes, the effect of WVTR on the performance of corrugated board cyclic humidity bending creep was also studied.

INTRODUCTION

Fresh fruit and produce is packaged for the primary reason of selling. Maintaining its eating and visual qualities and providing an attractive display achieve this. When the markets are distant, as for New Zealand growers, the packaging must withstand the rigors of weeks of cool storage and shipping while still protecting the contents and maintaining appearance. Corrugated fibreboard is widely used as a packaging material because it has many attributes that make it a good choice for the task. However, perhaps its greatest limitation is that the high relative humidity (RH) environment best suited for the storage of fresh produce weakens the packaging by raising the moisture content of the paperboard components. Weakened corrugated fibreboard causes stacked boxes to bulge and compress resulting in poor appearance and possibly damaged contents This paper presents a method for evaluating the bending creep performance of corrugated fibreboard under high humidity conditions. The effect of reducing the hygroscopicity of linerboard by coating was also investigated, and preliminary results are described.

BACKGROUND

When corrugated packaging is subjected to compressive load, such as a box on the bottom layer of a loaded pallet, it deforms over time. This can result in damaged contents and unstable stacks. Initially the compressive load on a box is supported mostly in a column compression mode. However, over time the sides and ends bulge, so more of the load is supported in a bending mode. The sides are then weaker than in column compression (Thorpe and Choi, 1992). There is evidence to suggest that box bulge may be a critical element in determining the length of time corrugated boxes can withstand compressive loads (Kirkpatrick and Ganzenmuller, 1997; Haraldsson *et al.*, 1997).

These two modes of support are also used in the McKee equation, where the two material factors in the model are compression strength and bending stiffness of the corrugated fibreboard.

Add to this that many produce coolstores operate at 85 – 95% RH, often with considerable fluctuations due to operating conditions such as defrost cycles. This leads to high and fluctuating moisture levels in the corrugated paperboard boxes which increases the rate of collapse due to the phenomenon called 'mechanosorptive creep'[1] (Söremark and Fellers, 1993; Urbanik, 1995).

Characterising the high / cycling RH performance of corrugated board would best be done by measuring the compression and bending performance over long periods of time, hence the programme to develop testing capabilities to measure this.

Bending creep of corrugated board in cyclic relative humidity has been measured before (Laufenberg, 1991; Söremark and Fellers, 1993) but it had not been described mathematically. Models have been developed to describe the tensile creep of paper in cyclic relative humidity (Haslach *et al.*, 1991) and corrugated board in compression (Urbanik 1995). Because a beam structure under bending stress has elements of

[1] Mechanosorption is the non-linear creep response caused by the combined effects of applied stress and changing moisture content. (Fridley, Tang and Soltis, 1992)

compression and tension inside and outside the neutral plane, respectively, it was thought these models would provide a starting place for developing a model for corrugated board under bending stress.

One of the difficulties of modelling cyclic relative humidity creep is modelling the cyclic response due to swelling and shrinkage caused by the periods of increasing and decreasing relative humidity. Haslach *et al.* (1991) fitted a constant moisture content creep model proposed by Pecht (1985) to the strain minima of paper under tensile stress in a cyclic relative humidity environment [Eq. 1]. This is shown in Figure 1.

$$\text{Creep displacement} = c \ln[1 + Bt^n] \qquad [1]$$

where c = constant, B = time shift factor, t = time and n = constant.

The model was fitted to the cyclic minima because at these points during the experiment the relative humidity returned to a minima and the moisture content of the specimen would have been close to the starting moisture content. This made these points of 'constant' moisture content displacement. It was suggested that although there was considerable cyclic deformation due to expansion and contraction during increasing and decreasing relative humidity respectively, there would be no swelling component in the strain at the points of constant moisture content. Interpolating between these points would give 'pure' creep without swelling.

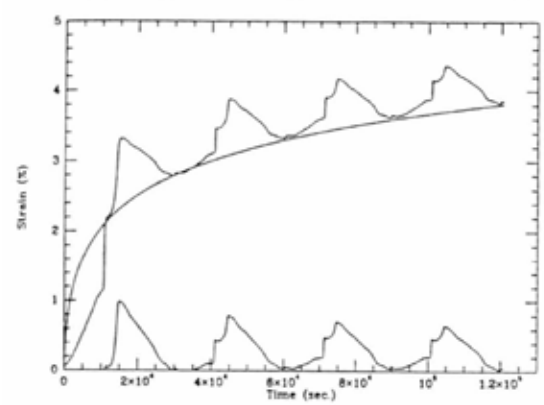

Figure 1 Cyclic RH tensile creep strain response with Pecht model fitted to cyclic minima and model subtracted to show peaks. (Haslach *et al.*, 1991)

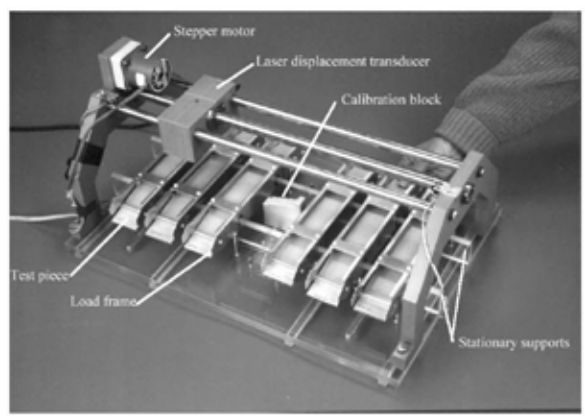

Figure 2 Forest Research bending creep tester

EXPERIMENTAL PART 1

Bending Creep Apparatus

A creep apparatus (Figure 2), based on a test apparatus at the U.S.D.A. Forest Products Laboratory (Gunderson and Laufenberg, 1994), was designed and built at Forest Research to allow automated testing of up to 6 test pieces over extended periods of time. The creep apparatus measured the deflection (creep) of test pieces subjected to four point bending stress. Four point bending was chosen to remove any effect of shear. The outer span of the load frame was 230mm and the span of the inner stationary supports was 114mm. Deflection of each test piece was measured in the centre of the zero shear

region between the inner supports. Measurements were made with a non-contact laser displacement transducer (LDT) by moving it over each test piece. A PC controlled the LDT position and also recorded the deflection measurements and the time when they were taken. Data were recorded at intervals of approximately 3 minutes. The LDT resolution was 0.05mm and displacement measurements were calibrated against an internal reference block during each measurement cycle. The creep apparatus was placed inside an environmental cabinet which controlled the temperature at 23±0.2°C while cycling the relative humidity from 50% to 90% RH in a sinusoidal profile with a 12 hour period.

The corrugated board used in this study was made from kraft linerboard and semi-chemical corrugating medium combined with water resistant adhesive and was representative of material used in horticultural packaging. Test specimens were cut to 50±0.5mm wide by 280mm long in the CD direction. The specimens were subjected to a constant bending moment with the flutes running the length of the specimen. This orientation was chosen because it was the weakest direction of outer liners of the corrugated fibreboard. Test pieces were preconditioned at less than 35% relative humidity then stored at 23°C and 50% RH prior to testing in accordance with standard paper testing procedures. Test pieces were then conditioned in the cycling relative humidity environment for at least 4 relative humidity cycles immediately prior to commencing measurements to relieve any stresses within the paper prior to testing. Testing was started when the relative humidity reached 50% RH. Test specimens were subjected to 4 levels of bending load, see Figure 4.

Data from creep tests were smoothed using a 5 point moving mean to remove high frequency noise. Cyclic minima were found from the smoothed data. The model was fitted to the cyclic minima using the least squares method of non-linear curve fitting.

RESULTS

Deflection - Time (Creep) Curves

Figure 3 shows typical creep curves from samples loaded under 50 – 90 % RH cyclic and constant 90% RH conditions. The deflection of the sample in the cyclic RH increased rapidly at the beginning of the test when the relative humidity was increasing during the first RH cycle. This was followed by a reduction in deflection as the specimens straightened when the relative humidity reduced. Throughout the test during periods of increasing relative humidity the deflection increased and during periods of reducing relative humidity the deflection reduced. This was characteristic of all tests carried out under 50-90% RH cyclic conditions. The cyclic variation of the deflection was approximately sinusoidal superposed on a longer-term trend of increasing deflection.

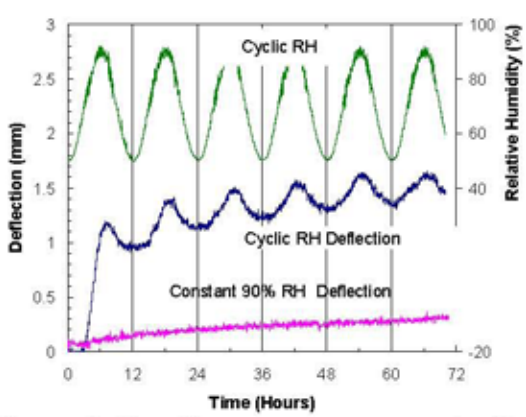

Figure 3 Bending creep response to 60 mN.m bending moment under cyclic RH and constant RH

The samples tested under constant RH conditions were conditioned at 90% RH prior to testing to avoid any RH cycling. Its deflection increased over time, but not as rapidly as the sample under cyclic RH conditions.

DISCUSSION

Curve fitting

The Pecht model [Eq. 1] (Haslach *et al.*, 1991) was chosen because it had been shown to fit the cyclic creep minima of paper subjected to tensile loads in a cyclic relative humidity environment. The Pecht model was fitted to the cyclic minima as done by Haslach *et al.* (1991). It was found that the model was not always stable and would not necessarily converge using least squares fitting techniques. Haslach *et al.* (1991) commented on this.

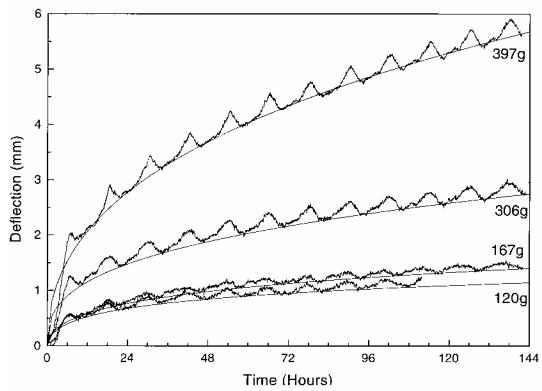

Figure 4 Pecht model fitted to creep data minima from four levels of load (0.034, 0.048, 0.087, 0.113 N.m bending moment). The smooth curve is the fitted Pecht model. The cyclic line is the raw creep data.

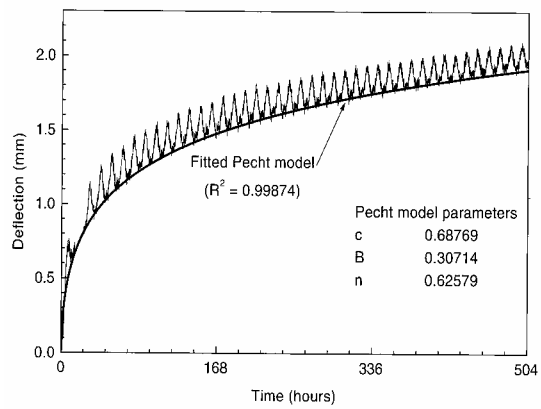

Figure 5 Pecht model fitted to 21 day creep data cyclic minima (0.048 N.m bending moment). The smooth curve is the fitted Pecht model. The cyclic line is the raw creep data.

The Pecht model was found to fit creep data over a range of loads, although the asymmetric cyclic deflection of the specimens at higher loads made it difficult to find minima (Figure 4). For these creep curves the deflection which corresponded with the relative humidity minima was used to fit the Pecht model. This model does not describe primary and secondary creep zones but there was no evidence of these regions or of the specimens failing, even after more than 500 hours (Figure 5). This is further confirms that corrugated fibreboard is capable of large plastic strains under cyclic RH (Bronkhorst, 1997).

Although the model parameters did not have physical significance the fitted model was useful, since the creep at a given time, or the time taken to reach a given level of deflection could be estimated using the Pecht model. This is useful for generating isochronous and isometric curves that can be used to compare the creep performance of different corrugated boards (Haraldsson, *et al.* 1997). The model may also be useful if it can be shown that long-term creep can be predicted from short-term tests.

EXPERIMENTAL PART 2

Coated Corrugated Fibreboard

Background

Following on from the work described in Part1, and as part of a wider 'smart packaging' study, the bending creep performance of corrugated board that had been treated with WVTR coatings was evaluated.

The aim of this work is to eventually be able to specify component performance for corrugated board to enhance the boards cyclic humidity performance in trays or cases in coolstores. It is hoped that cyclic humidity four point bending creep performance is an indicator of likely coolstore performance as this would allow for selection of components for cyclic humidity bending creep performance in the lab which is much simpler than trying to measure TTB cyclic humidity creep performance in the coolstore.

Experimental:

The four point bending creep apparatus, as previously described, was used under the suggested Creep Symposium cyclic RH conditions of 50 to 90% RH at 23° C with 12 hour cycle times in a Thermoline Environmental Cabinet using a sinusoidal profile. All the preliminary work was done with a four point bending moment load of 48 mN.m. Commercial Polyacrylate emulsion coatings (probably also contains wax) were applied to corrugated board using 12µm Meyer rods with either one or two coats on different or both sides. WVTR measurements (75% RH at 25°C/anhydrous Calcium Chloride) on the various combinations showed the following results:

Table 1 WVTR performance of coated corrugated boards

Sample	**WVTR (g/m²/day)**
Uncoated	800
1/s single coat	700
2/s single coat	500
1/s double coat	130
2/s double coating	40

On several of the runs a small humidity sensor was inserted between the flutes to measure the internal board humidity. The corrugated board samples made from a 205/160/205 g/m² 'C' flute were 50 mm wide by 300 mm long parallel to the flute direction (CD) with the edges sealed using a rubber cement on gladwrap film.

A computer running Labview software was used to control the environmental cabinet, run the bending stiffness device and collect data.

Results:

Eight runs of 6 samples were achieved in this investigation. Figure 6 shows run #5 (010214) where one sided and two sided coatings were run with uncoated samples. These results are typical of all the runs carried out.

To be able to develop isochronous curves and compare strain rates, curves were fitted to the data through the strain minimum of each cycle as carried out by McKenzie. However it was very difficult to fit the Pecht model using SAS as the non-linear regression would not converge. The simple exponential function:

$$\text{Strain} = at^{b} \qquad [2]$$

where t = time, and a and b are constants

as used by Chalmers for previous cyclic humidity creep studies (4th Symposium Proceedings) was found to fit quite satisfactorily. By eye it can be seen that after the first couple of RH cycles there is very little difference in secondary strain rate. A simple straight line was fitted to the 2-side coated sample data.

Apart from the 2/side coated sample, the slopes of the curves at 60 hours are similar:

Uncoated	0.0094 mm/hr
1/ide coated up	0.0089 mm/hr
1/side coated down	0.0088 mm/hr
2/side coated	0.003 mm/hr

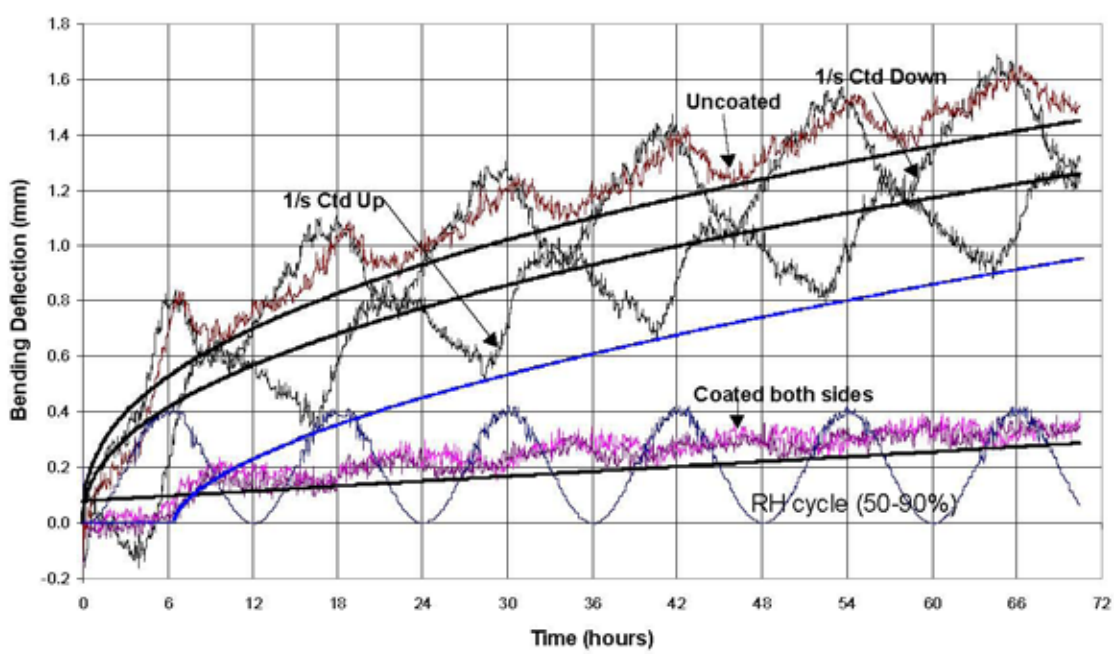

Figure 6. Loaded cyclic humidity bending creep samples with exponential curves fitted to strain at bottom of RH cycle.

The effect of the coating on the stiffness of the board was thought to be a major factor in the bending performance of the corrugated board but bending stiffness tests on the two side double coated board at 50% RH showed an insignificant difference between coated and uncoated board.

In Figure 6 there is an effect noticed on the first cycle where it can be seen that with the coated side down there is little difference in the initial strain compared to the uncoated board. However when the coated side is up the hygroexpansive strain of the uncoated liner overwhelms the effect of the load and the sample bends up instead of down producing a negative deflection for the first four hours. After this time the stiffness of the board is reduced enough by the moisture to be overcome by the bending load and the board bends down. The double side coated board barely moves until the RH cycle maximum is reached, develops some primary strain then settles into a comparatively low secondary strain.

Figure 7 shows a similar run to Figure 6 but with a much longer time period. The slope at 60 hours for the 1/s coated sample is also very similar to other data at 0.0092 mm/hour.

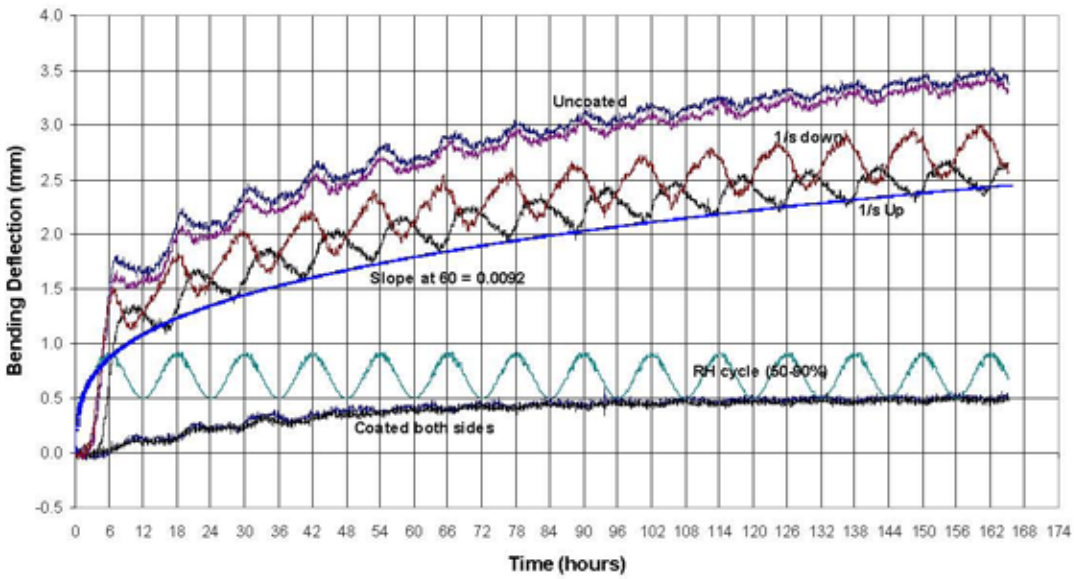

Figure 7 Data from run #4 (010205) showing same form as previous runs.

Figure 8 shows the RH of internal probes vs the cabinet RH. In the uncoated board the RH cycle is in phase with the cabinet, the one side coated board shows a small phase lag of about 45 minutes, the double coated board however cycles only from about 65% RH to 80% RH in the external 50 to 90% RH with a longer phase lag of about 2 hours.

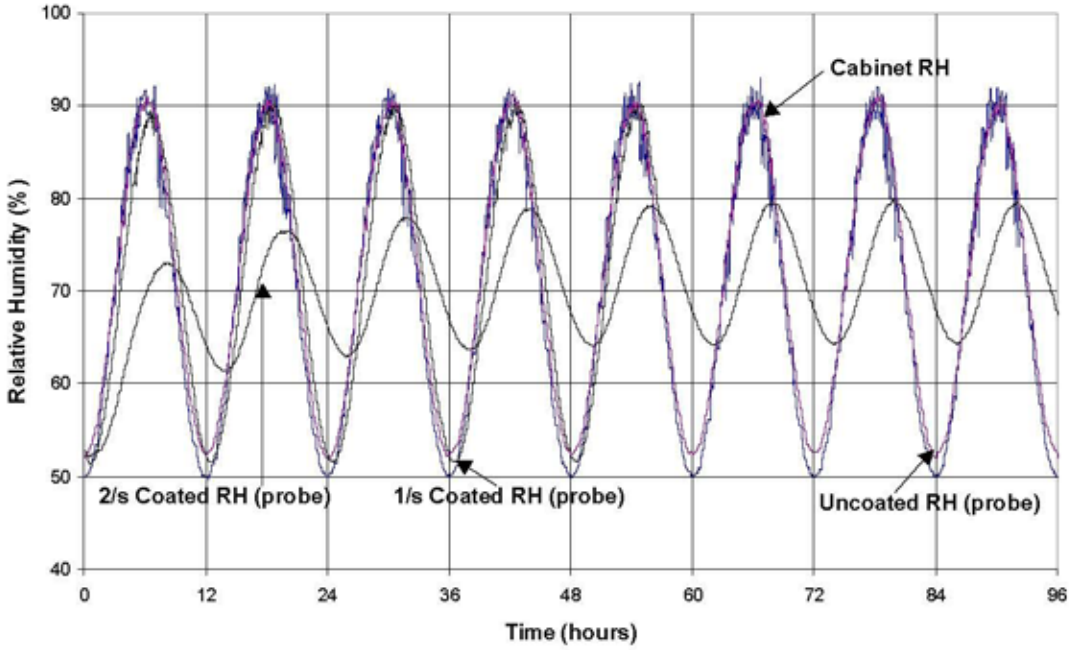

Figure 8. Internal corrugated board RH vs cabinet RH

The internal RH of the two side coated board exhibits a large damping effect from the coatings with the 50 to 90% RH cycles reduced to 65 to 80% cycles under these conditions. These results explain the significantly enhanced performance of the two side coated boards because it appears the moisture content in the board is not getting high enough to reduce the bending stiffness below the applied load in the bending apparatus.

Other runs were completed with single coatings to one side and both sides but the reduction in WVTR (see Table 1) was not enough to significantly influence the performance of the corrugated board compared to the uncoated board and the significantly improved performance of the double coated boards.

All the results obtained so far on uncoated board showed the maximum deflection to coincide with the maximum of the humidity cycle. This is contrary to the results obtained by Soremark and Fellers in 1991 where they found the maximum deflection to coincide with the RH cycle minimum. There are a few major differences between this work and their work however which include the corrugated board orientation (cd vs md of Fellers) and the RH cycle amplitude of 90% vs 80% for Fellers. At 80% RH the moisture content is about 11%, whereas at 90% RH it is about 15% moisture, quite a large difference. Soremark and Fellers used steel ribbons in place of one liner to investigate a stress-induced hygroexpansion. Because our board orientation did not allow the use of ribbons we used a fine wire mesh of the type typically used on BS sheet machines. The mesh was glued to the flute tips of a 118g/125g 'C' flute single facer. Figure 9 shows typical results for the first 4½ cycles for this setup. The deflection was so large on the mesh-down sample that the centre of the sample started to contact the frame of the sample holder and the run had to be stopped.

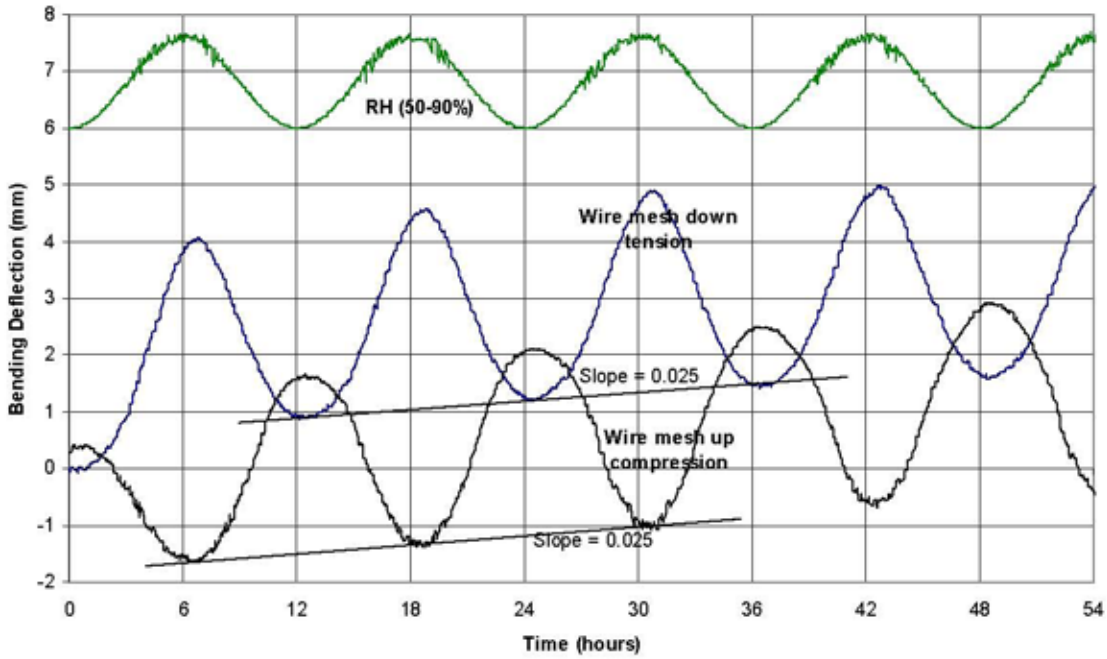

Figure 9. Bending deflection of single facer backed with fine wire mesh vs time with cyclic humidity.

In Figure 9 the single liner produces a hygroexpansive strain under both tension "wire mesh down" and compression "wire mesh up" with a creep component added as well. As expected, the two samples are completely out of phase with each other. Examining the cycle at 42 hours for the mesh down sample we find the size of the hygroexpansive strains to be 0.9596% and at 48 hours for the mesh up sample the strain is 0.9552%. There does not appear to be any difference in hygroexpansive strain between tension and compression. The cyclic humidity creep strains do not follow an exponential function but it can be seen from the straight line visually fitted to the first three cycles in Figure 5 that the bending deflection creep rates of both compression and tension are the same at about 0.025mm/hour

Discussion

The mechano-sorptive creep phenomenon has been demonstarted for corrugated board under bending and low strains. Creep data minima were fitted to the Pecht model, which can be used for comparative and predictive purposes. Preliminary work on corrugated boards treated with WVTR reducing coatings has shown a significant difference in performance for cyclic humidity bending creep. The results of board orientation studies has also revealed that the board hygroexpansion strain and bending creep deflection rate in tension and compression are similar. However it is still "work in progress" and the moisture protective elements of the WVTR coatings need to be probed further.

The four point bending stiffness technique has its limitations but in conjunction with cyclic humidity edgewise compression creep on corrugated board there should be a suitable regime that can be developed to predict the cyclic humidity performance of corrugated board in the lab instead of in the field.

ACKNOWLEDGEMENTS
Carter Holt Harvey Pulp and Paper Limited and New Zealand Forest Research Institute Limited are thanked for their financial assistance. The authors wish to thank Dr W.W. Sampson for his help in modelling, Drs C.J. Studman and R.K. Steadman for their guidance during the development of the technique and Reiner Hensel for the construction of the creep apparatus.

REFERENCES

Bronkhorst CA (1997). Towards a more mechanistic understanding of corrugated container creep deformation behaviour. Journal of Pulp and Paper Science **23**(4), J174-J181

Fridley KJ, Tang RC, Soltis LA (1992). Creep behaviour model for structural lumber. Journal of Structural Engineering **118**(8), 2261-2277

Gunderson DE, Laufenberg TL (1994). Apparatus for evaluating stability of corrugated board under load in cyclic humidity environment. Experimental Techniques **18**(1), 27-31

Haraldsson T, Fellers C, Söremark C (1997). Creep properties of paper - principles of evaluation. Proceedings: 3rd International Symposium, Moisture and Creep Effects on Paper, Board and Containers, 20-21 February 1997, Rotorua, NZ. (Chalmers I R ed.) pp237-246 : PAPRO NZ, Appita, US Forest Products Laboratory United States Department of Agriculture/Forest Service.

Haslach Jr. HW, Pecht MG, Wu X (1991). Variable humidity and load interaction in tensile creep of paper. Proceedings: 1991 TAPPI International Paper Physics Conference, 22-26 September 1991, Kona, HI, USA pp.219-224: Tappi Press, Atlanta, GA

Kirkpatrick J, Ganzenmuller G (1997). Engineering corrugated packages to survive cyclic humidity environments - a case study. Proceedings: 3rd International Symposium, Moisture and Creep Effects on Paper, Board and Containers, 20-21 February 1997, Rotorua, NZ. (Chalmers I R ed.) pp.257-264 : PAPRO NZ, Appita, US Forest Products Laboratory United States Department of Agriculture/Forest Service.

Laufenberg, TL (1991). Characterisation of paperboard, combined board, and container performance in the service moisture environment." *Proceedings: 1991 TAPPI International Paper Physics Conference, 22-26 September 1991, Kona, HI, USA* pp.299-30: Tappi Press

Norimoto M, Gril J, Rowell RM (1992). Rheological properties of chemically modified wood: relationship between dimensional and creep stability. Wood and Fiber Science **24**(1), 25-35

Pecht MG (1985). Creep of regain-rheologically simple hydrophilic polymers. Journal of Strain Analysis **20**(3), 179-181

Salmén L (1993). Responses of moisture properties to changes in moisture content and temperature. Products of Papermaking - Tenth Fundamental Research Symposium, Oxford, UK, 20-24 Sept. 1993 pp.369-430

Söremark C, Fellers, C (1993). Mechano-sorptive creep and hygroexpansion of corrugated board in bending. Journal of Pulp and Paper Science **19**(1), J19-J26

Thorpe J, Choi D (1992). Linear image strain analysis details corrugated container compression failure modes. TAPPI Proceedings of 1992 Corrugated Containers Conference 11-15 October 1992, Washington DC, USA. pp.71-76

Urbanik TJ (1995). Hygroexpansion-creep model for corrugated fiberboard. Wood and Fiber Science **27**(2), 134-140

Chalmers IR (1999) A comparison between static and cyclic humidity compression creep performance of linerboard. Proceedings 4th International Symposium 'Moisture and creep effects on paper, board and containers' EFPG, Grenoble Fr 1999

The bending response of corrugated fibreboard to a cycling relative humidity environment.

I.R.Chalmers	PAPRO
A.D.McKenzie	CHH Pulp and Paper
B.I.Johnson	PAPRO

Carter Holt Harvey

papro NEW ZEALAND
Pulp and Paper Research Organisation of New Zealand

forest research

Corrugated Board Bending Creep Performance

- **Background**
- **Approach**
- **Experimental Part 1**
  - Apparatus
  - Results
  - Model
- **Experimental Part 2**
  - Background
  - Samples
  - Results

Background

- NZ apple exports in 1996 used $70M of packaging.
- Poor understanding of the fundamental drivers of corrugated packaging performance in the field.

Background

First part of study to look at
- bending creep and
- column creep

- Little in the literature

Approach - Experimental Part 1

- Build an apparatus to measure bending creep
- Model the response
- Use isochronous graphs for comparison of modified samples

Apparatus

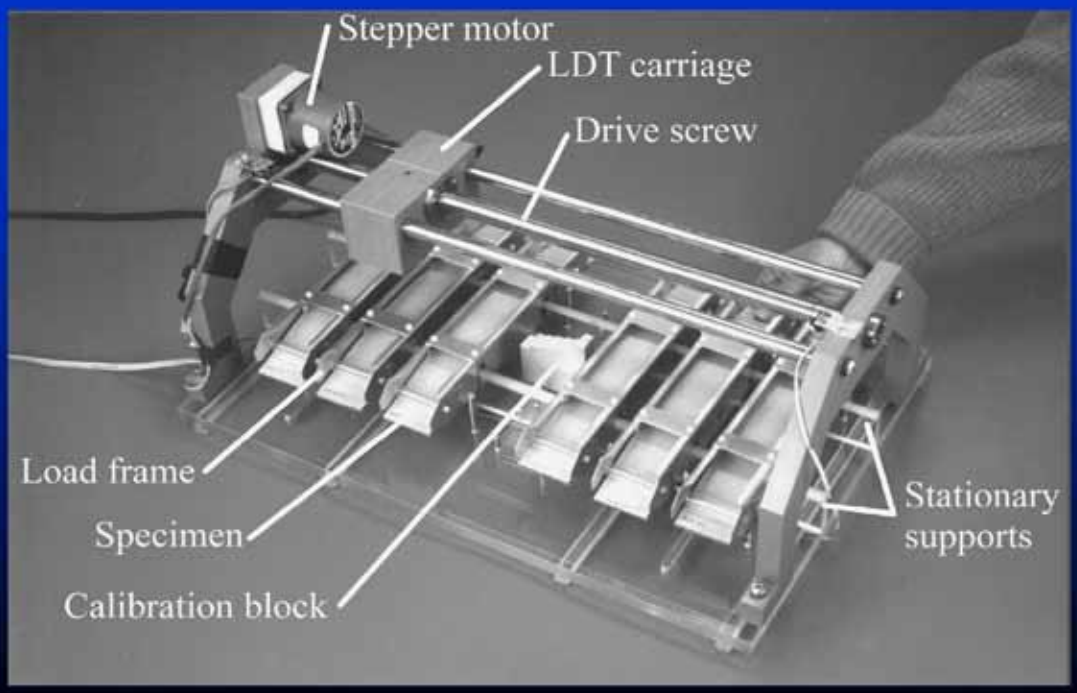

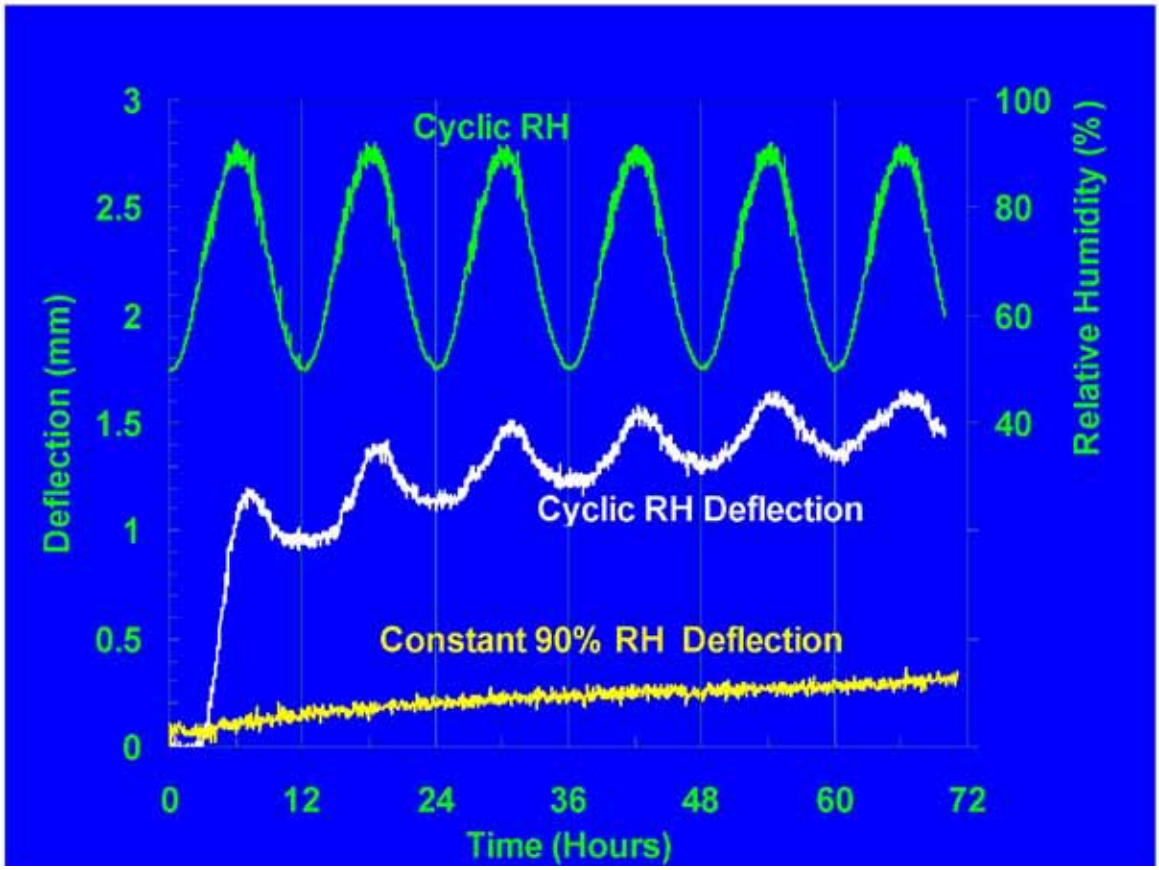

Pecht Model

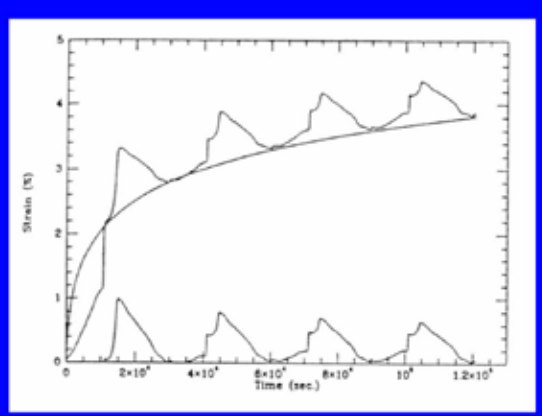

- Haslach et al
- Tension model
- Combines logarithmic and exponential functions
- Strain = a ln(1+bt^c)

Pecht Model Fitted to Minima

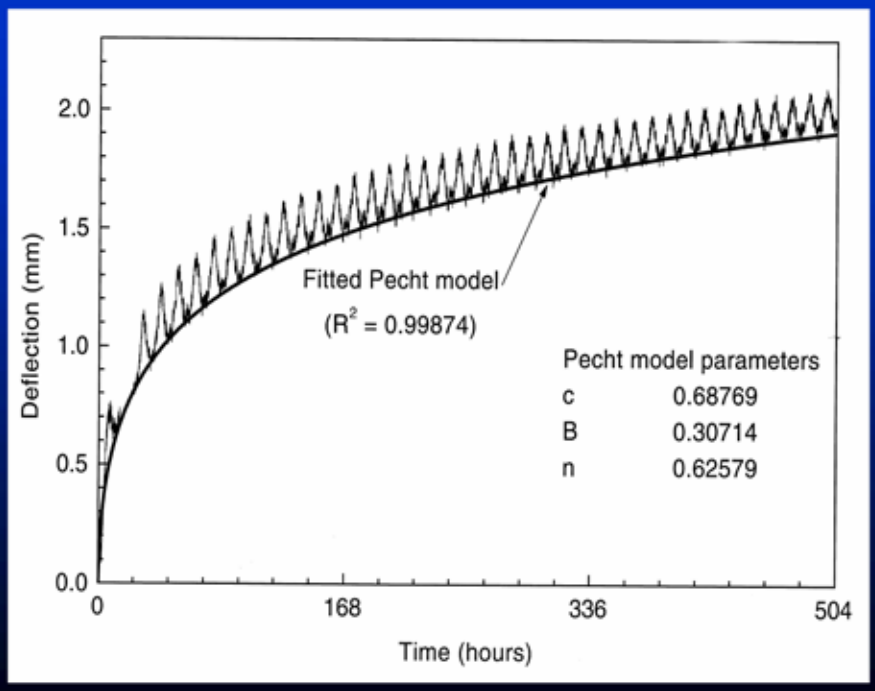

Range of loads for Isochrones

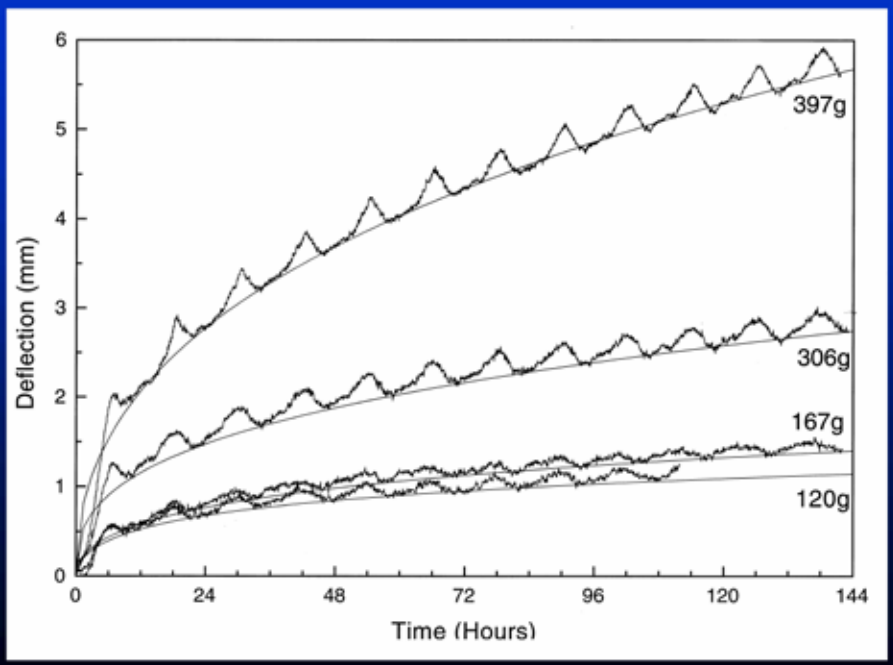

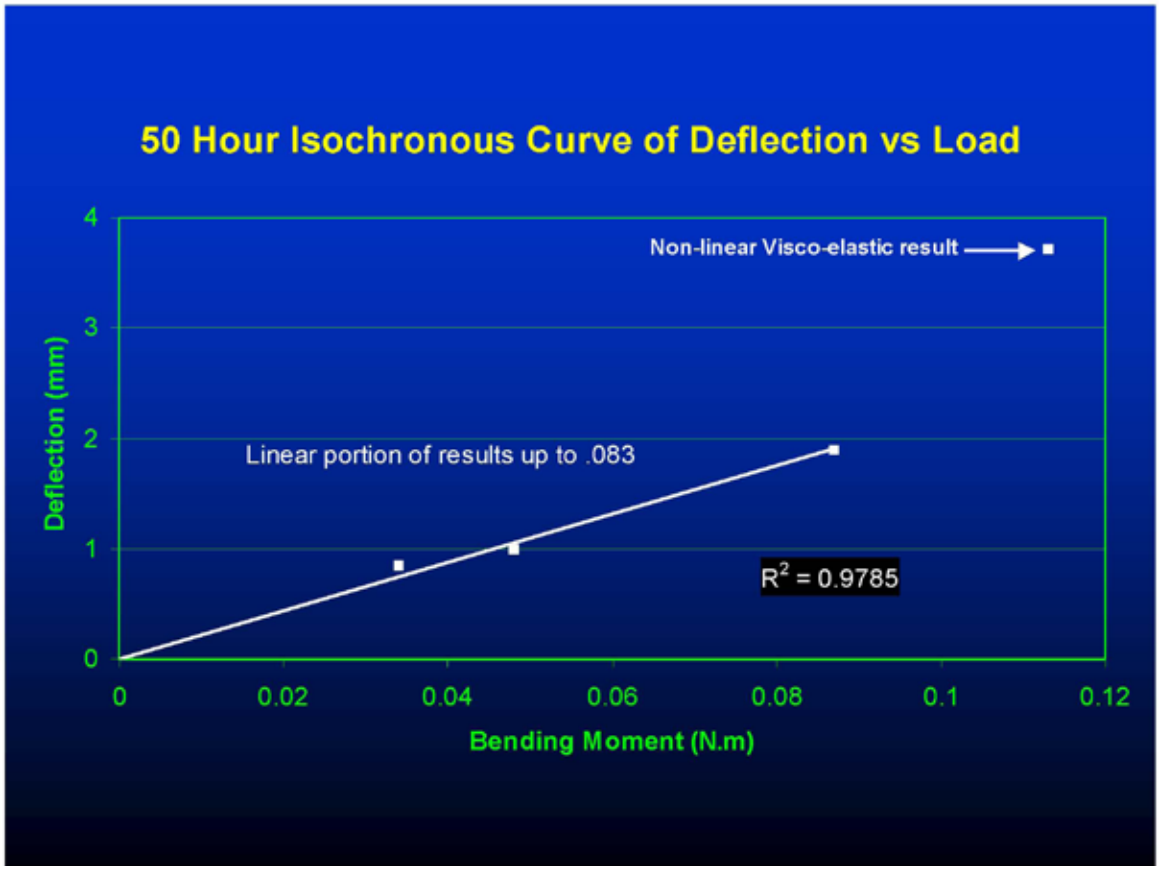

Experimental Part 2 - Background

- Evaluate the usefulness of coatings on corrugated board that reduce WVTR
- Use McKenzies apparatus
- Model the response
- Develop the method to be able to simulate case performance in coolstores

REAL TTB COMPRESSION TESTS
IN COOLSTORES ARE POSSIBLE

BUT TOUGH ON STAFF RESOURCES

WVTR reduction coatings

- Commercial Polyacrylate applied by a 12µm drawdown bar

Sample	WVTR
Uncoated	800
1/s single coat	700
2/s single coat	500
1/s double coat	130
2/s double coat	40

Cyclic Humidity Bending Deflection vs Time
Bending Deflection (mm)
Time (hours)
1/s Ctd Down
Uncoated
1/s Ctd Up
Coated both sides
RH cycle (50-90%)
1.8
1.6
1.4
1.2
1.0
0.8
0.6
0.4
0.2
0.0
-0.2
0
6
12
18
24
30
36
42
48
54
60
66
72

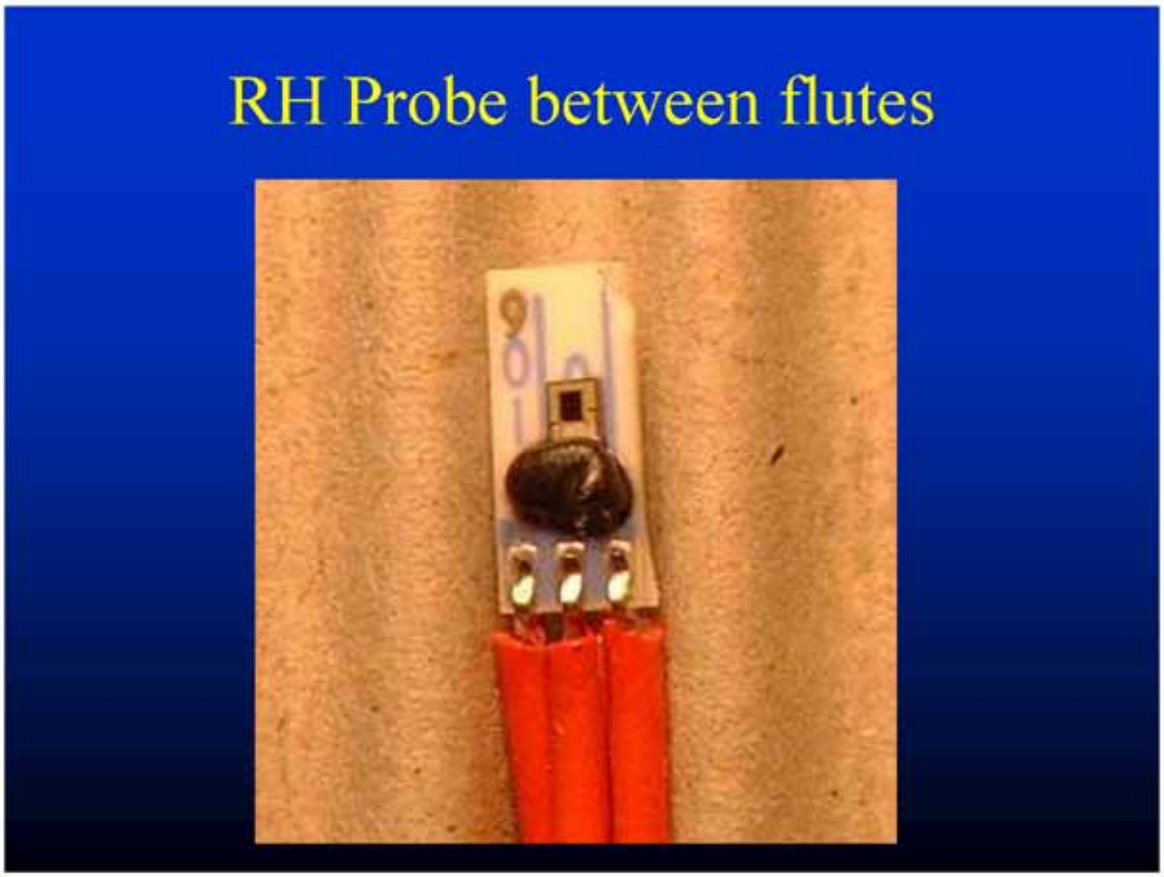
RH Probe between flutes

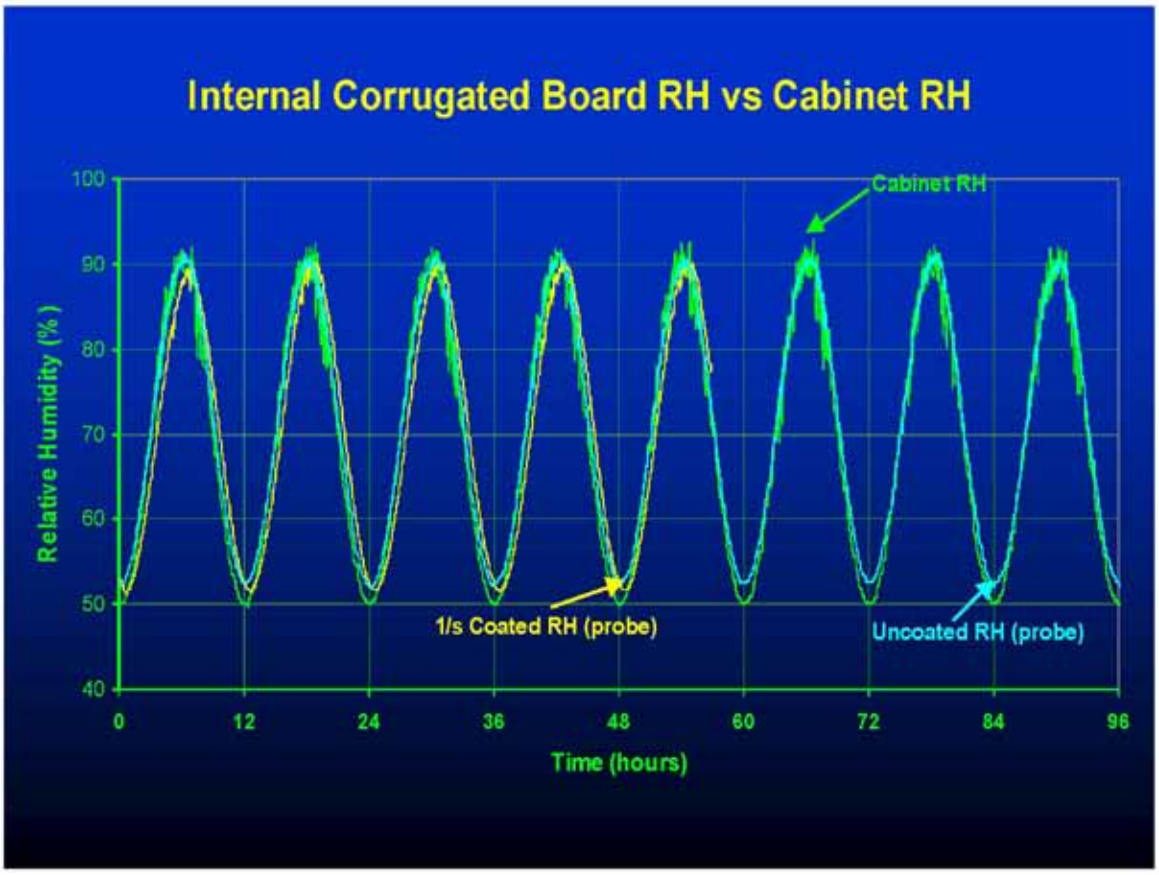
Internal Corrugated Board RH vs Cabinet RH
Cabinet RH
1/s Coated RH (probe)
Uncoated RH (probe)
Relative Humidity (%)
100
90
80
70
60
50
40
0
12
24
36
48
60
72
84
96
Time (hours)

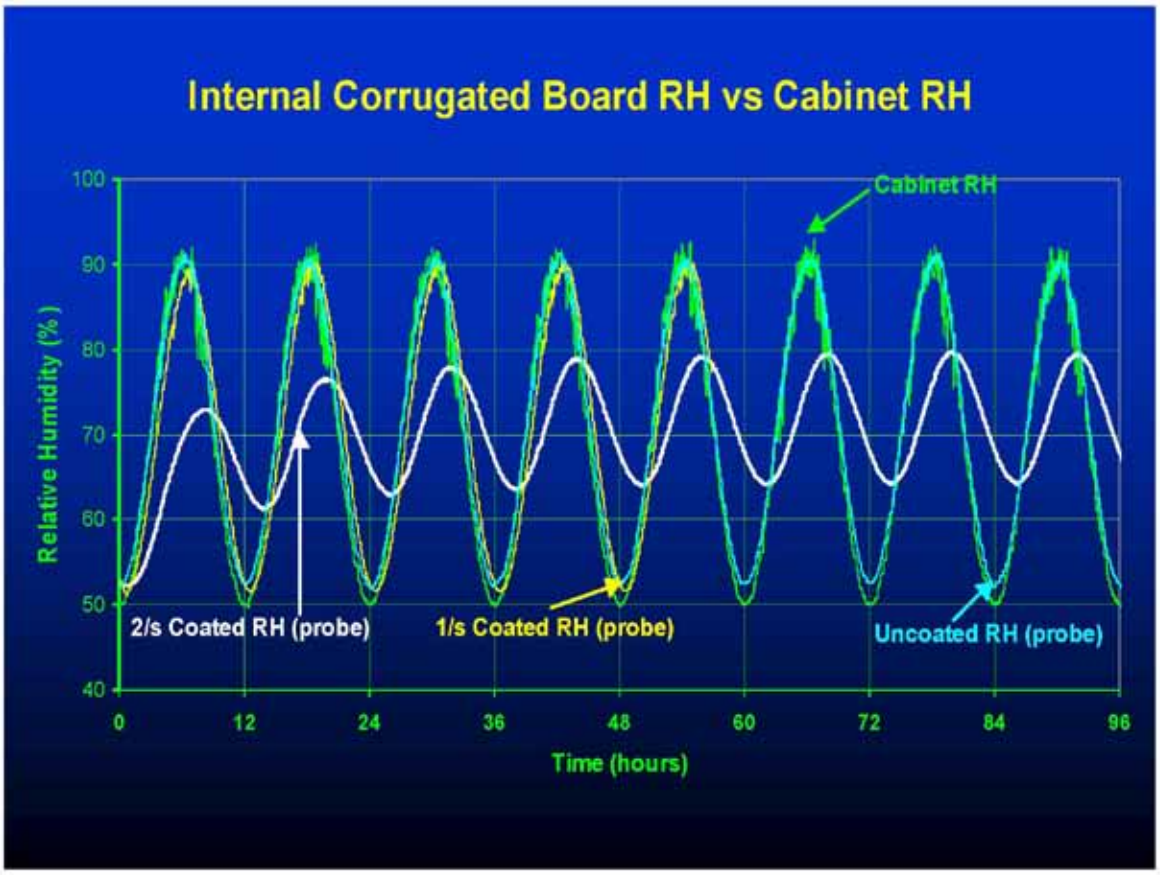
Internal Corrugated Board RH vs Cabinet RH
Cabinet RH
2/s Coated RH (probe)
1/s Coated RH (probe)
Uncoated RH (probe)
Relative Humidity (%)
100
90
80
70
60
50
40
0
12
24
36
48
60
72
84
96
Time (hours)

Wire Mesh Backed Single Facer
NEW ZEALAND'S
BEST LAGER

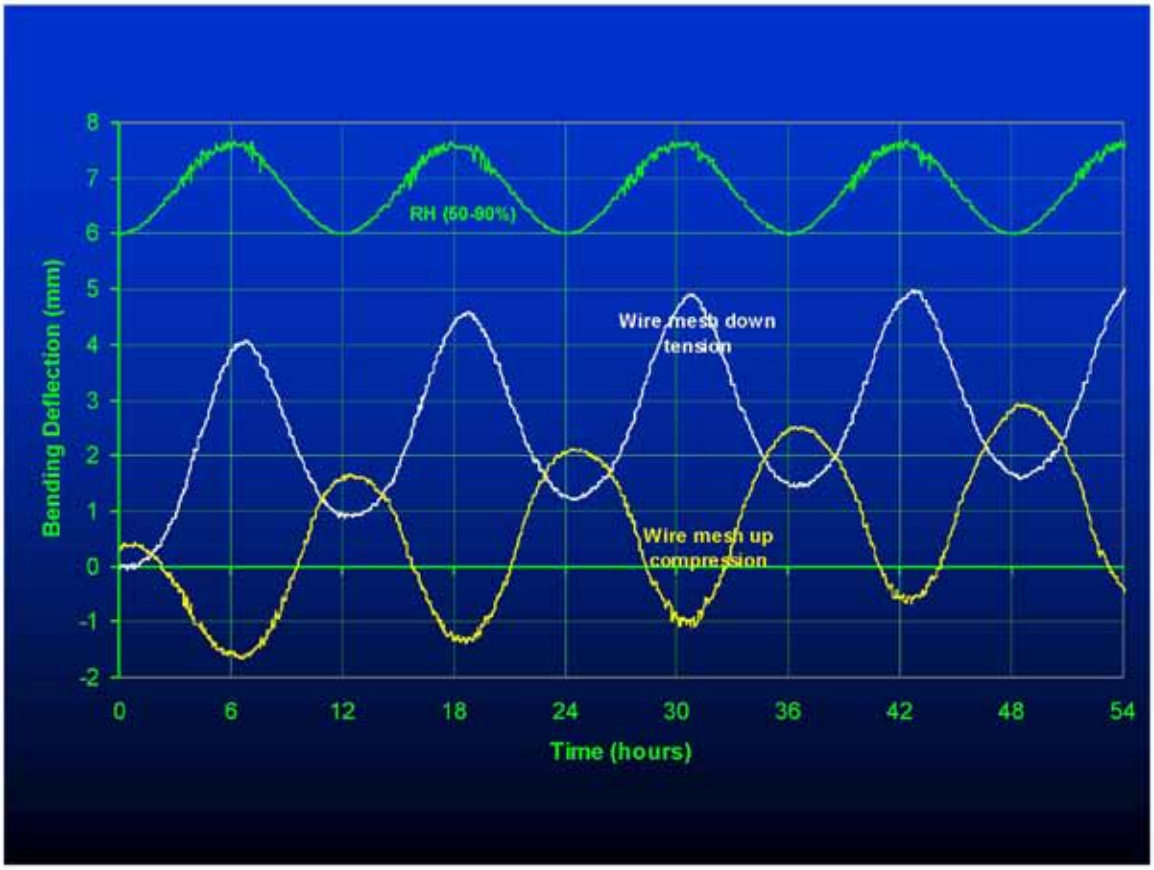
RH (50-90%)
Wire mesh down
tension
Wire mesh up
compression
Bending Deflection (mm)
Time (hours)
8
7
6
5
4
3
2
1
0
-1
-2
0
6
12
18
24
30
36
42
48
54

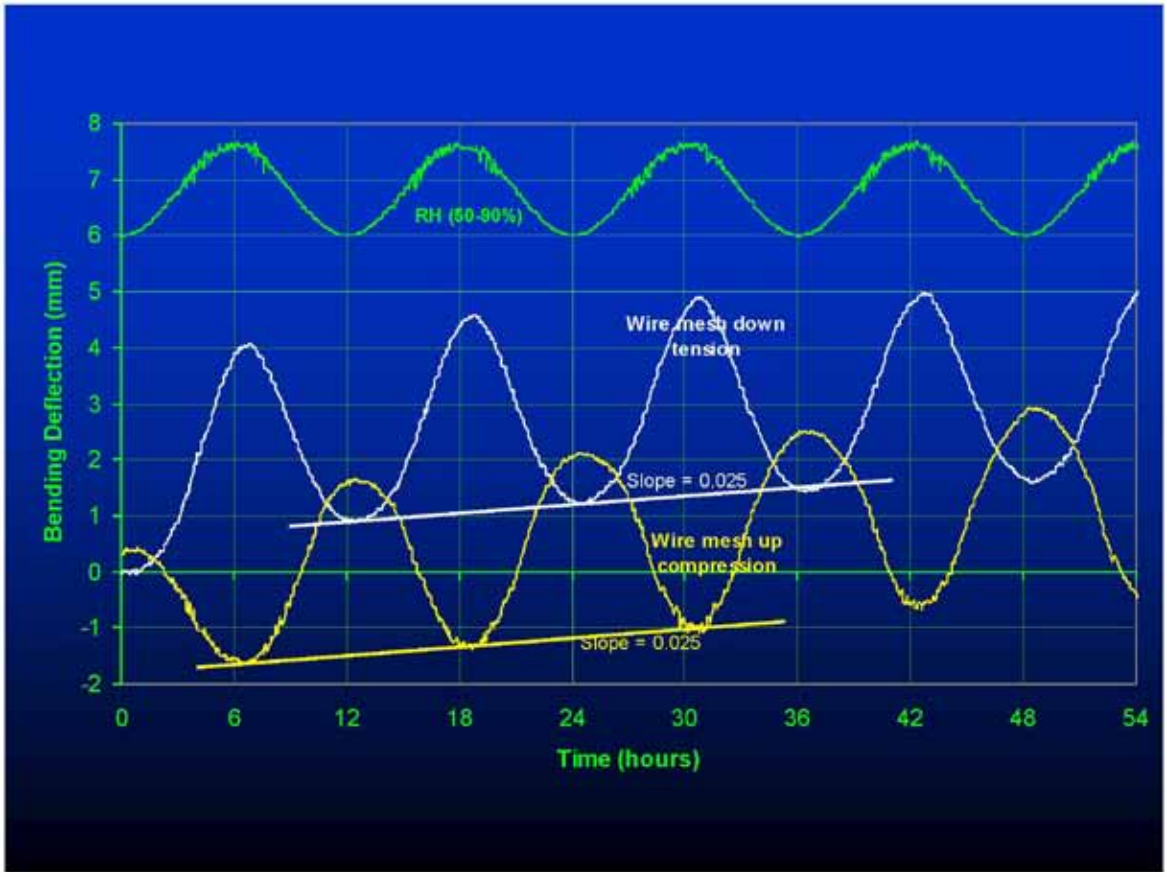
RH (50-90%)
Wire mesh down
tension
Slope = 0.025
Wire mesh up
compression
Slope = 0.025
Bending Deflection (mm)
Time (hours)
8
7
6
5
4
3
2
1
0
-1
-2
0
6
12
18
24
30
36
42
48
54

NEW ZEALAND
apples

fin
I.R.Chalmers PAPRO
A.D.McKenzie CHH Pulp and Paper
B.I.Johnson PAPRO
Carter Holt Harvey
papro
NEW ZEALAND
Pulp and Paper Research Organisation of New Zealand
forest research

A More Mechanistic Model of the Compression Strain-Load Response of Paper

Thomas J. Urbanik
Forest Products Laboratory
1 Gifford Pinchot Drive
Madison, Wisconsin 53705-2398

Proposed for: 5th International Symposium on the Moisture and Creep Effects on Paper, Board and Containers

Abstract

A new strain-load relationship, including elastic strain and primary, secondary, and tertiary phase components of irreversible creep strain is proposed for paper. Expressions for creep rate occurring throughout the successive phases of creep as obtained from experiments on corrugated fiberboard edgewise crush specimens and characterizing constant load data are integrated to determine corresponding expressions for creep strain. A second set of integrated creep strain expressions are obtained by first characterizing the creep rate constants in the model with respect to load increasing linearly with time. Expressions among load level, creep rate, and failure time from former Forest Products Laboratory investigations are incorporated, thereby unifying these studies in the creep of corrugated fiberboard and fiberboard containers, the rate-of-load effect on paper strain response, and the chemical kinetics-based failure of materials.

Physical constants in the creep strain characterizations at a constant load and the accompanying strain characterizations at a linearly increasing load enable the continuous duration-of-load strain response of paper to be predicted from rate-of-load stress-strain curves and vice versa. Fits of the model to data were determined from rate of load experiments on containerboard materials at 50% relative humidity (RH) and at 90% RH. The stress-strain curve at a high loading rate is almost indiscernible from the exclusively elastic characterization. But as loading rate decreases the occurrence of primary creep and secondary creep superimposed upon the elastic response becomes clear and elucidates the importance in differentiating among various creep mechanisms in the experimental stress-strain curve. For the data so far available such tests successfully characterized the primary and secondary phases of creep at the two RH levels but suggest that different experiments appear to be warranted to quantify tertiary creep.

The model has the potential to be extended to creep strain expressions in response to an arbitrary loading profile. Success here would enable researchers to determine all the elastic and creep constants of a paper from a single strain-load test and predict the paper's creep response at any constant load or other loading profiles.

Tom Urbanik

$$\text{Primary Strain } \varepsilon_1 = (R_1 - R_2)e^{-\frac{t}{\tau_1}}$$

$$\text{Secondary Strain } \varepsilon_2 = R_2$$

$$\text{Tertiary Strain } \varepsilon_3 = R_3 e^{-\frac{t_b}{\tau_3}} e^{-\frac{t}{\tau_3}}$$

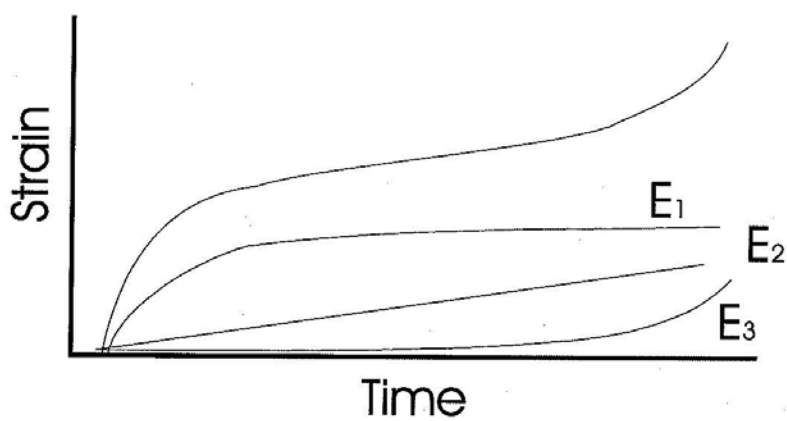

Influence of Heterogeneity on Tensile Accelerated Creep in Paper

Chuck Habeger and Douglas Coffin
Institute of Paper Science and Technology
Atlanta, GA 30318

Many of us have linked material heterogeneity to accelerated creep. Heterogeneity likely gives rise to stress gradients during cyclic moisture, and nonlinear creep properties combine with cyclic stresses to produce elevated creep rates. Therefore, the association of heterogeneity with accelerated creep is warranted. This lead one to question which levels of heterogeneity contribute to accelerated creep. For paper, the obvious heterogeneity on the fiber level comes to mind. Heterogeneity can also be introduced in the ZD direction such as with multi-ply sheets. Finally, one may consider, heterogeneity in the plane of the sheet such as with formation variations.

We have conducted many cyclic humidity creep tests on paper. In some of these tests we have used blends of different fibers, in others we have produced multi-ply sheets using different fiber sources for the individual plies. We have also tested fairly homogenous materials such as cellophane. When we compare and contrast these results we see significant differences. These differences help us understand how material structure influences accelerated creep in tension.

We also have a simple model that captures the important aspects of paper creep. This model exhibits heterogeneity-driven accelerated creep. Thus, we have a way to assess how heterogeneity in swelling, elastic properties, and creep properties can exacerbate accelerated creep.

When we look at all our results, we raise new more interesting questions, answer some practical questions of the papermaker, and better understand the influence of heterogeneity on the accelerated creep of paper.

Does Heterogeneity Influence Tensile Accelerated Creep in Paper?

Chuck Habeger and Doug Coffin

Accelerated Creep

Materials creep more under cyclic humidity conditions than at constant high humidity.

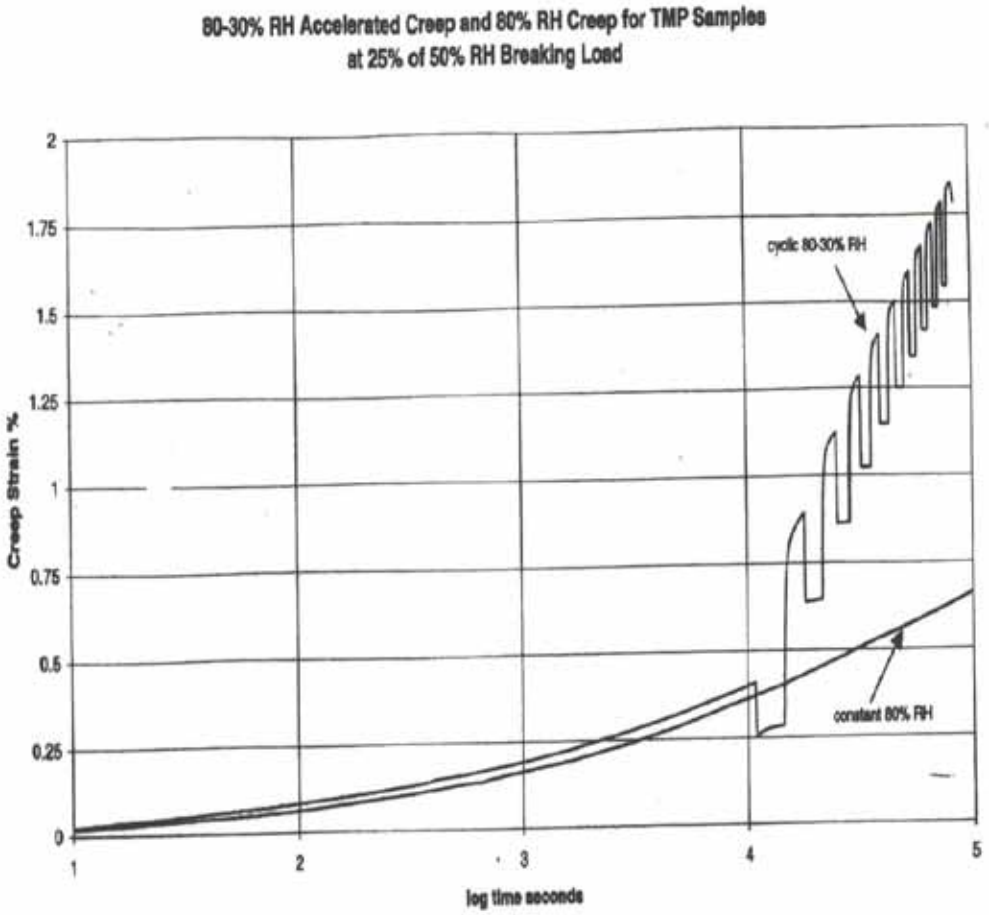

Accelerated Creep

Discovered in concrete by Pickett in 1942

and

in polymers(wood) by Armstrong, Kingston, and Christensen in the 1960s.

After all these years, there remains great controversy over the explanation for accelerated creep.

Talk Outline

1. Sorption-induced stress gradient explanation
   a) moisture-gradient-driven accelerated creep
   b) heterogeneity driven accelerated creep

2. Argue both mechanisms are operative in paper

3. Present paper fiber blend and multi-ply tensile accelerated creep experiments

4. Argue that results are consistent with the sorption-induced stress gradient explanation

Our Preferred Mechanism

Accelerated creep is creep!

The explanation lives in the creep constitutive equation. Accelerated creep is *not* the manifestation of a new phenomenon.

Cyclic sorption results in localized cyclic loading and materials deform more under cyclic load than at a constant average load

Acknowledgements

Our point-of-view is not mainstream, but neither is it original.

"an increase in creep accompanying non-uniform shrinkage or swelling is an natural consequence of the fact that the sustained stress vs. strain curve of concrete is not linear"

Pickett, G. J., Amer. Concrete Inst. 13(4): 33 (1942)

"Changes in moisture can cause rapid transient increases in stress and as the creep rate is a highly non-linear function of stress there can be significant increases in creep rate"

Selway, J., Kirkpatrick, J., Proceedings: Cyclic Humidity Effects on Paperboard Packaging: F.P.L.: 31 (1992)

Cyclic Loading Leads to Extra Creep

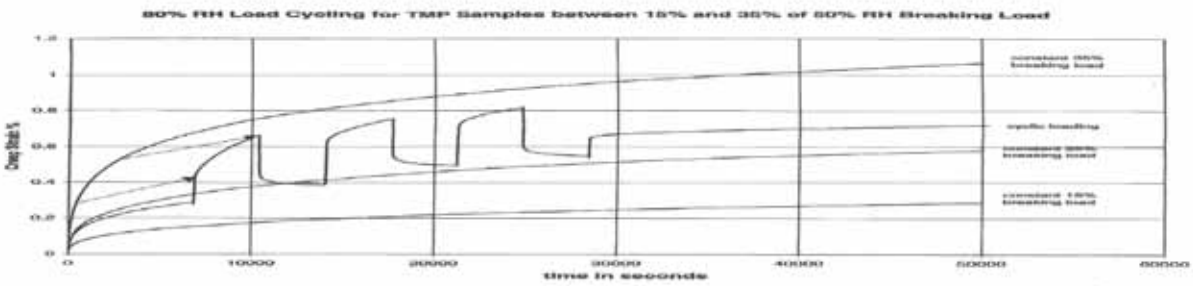

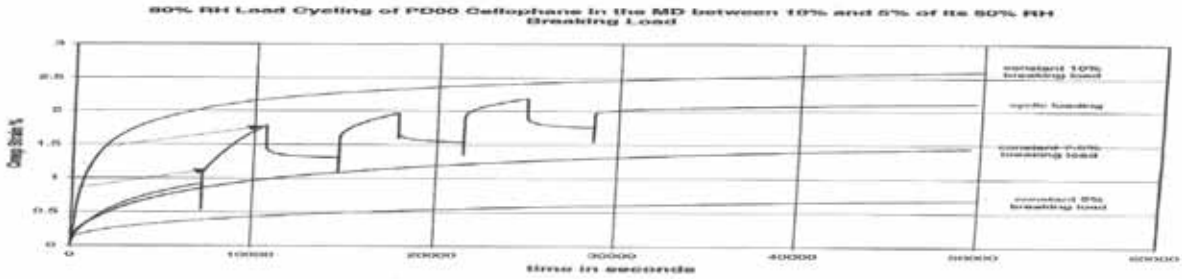

We see two ways that cyclic sorption can cause localized cyclic loading.

If cyclic moisture gradients arise, "Moisture-Gradient-Driven Accelerated Creep" can operate.

or

If the material is heterogeneous in its response to moisture, "Heterogeneity-Driven Accelerated Creep" can operate.

Stress Cycling through Moisture Gradients

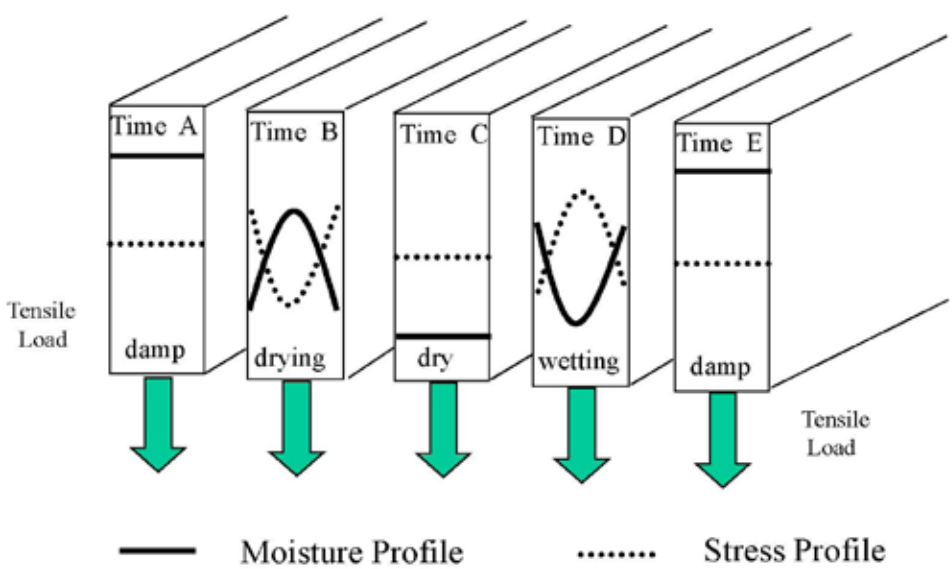

Hypothetical Moisture and Stress Profiles through a Sample Under Tensile Load over a Sorption Cycle

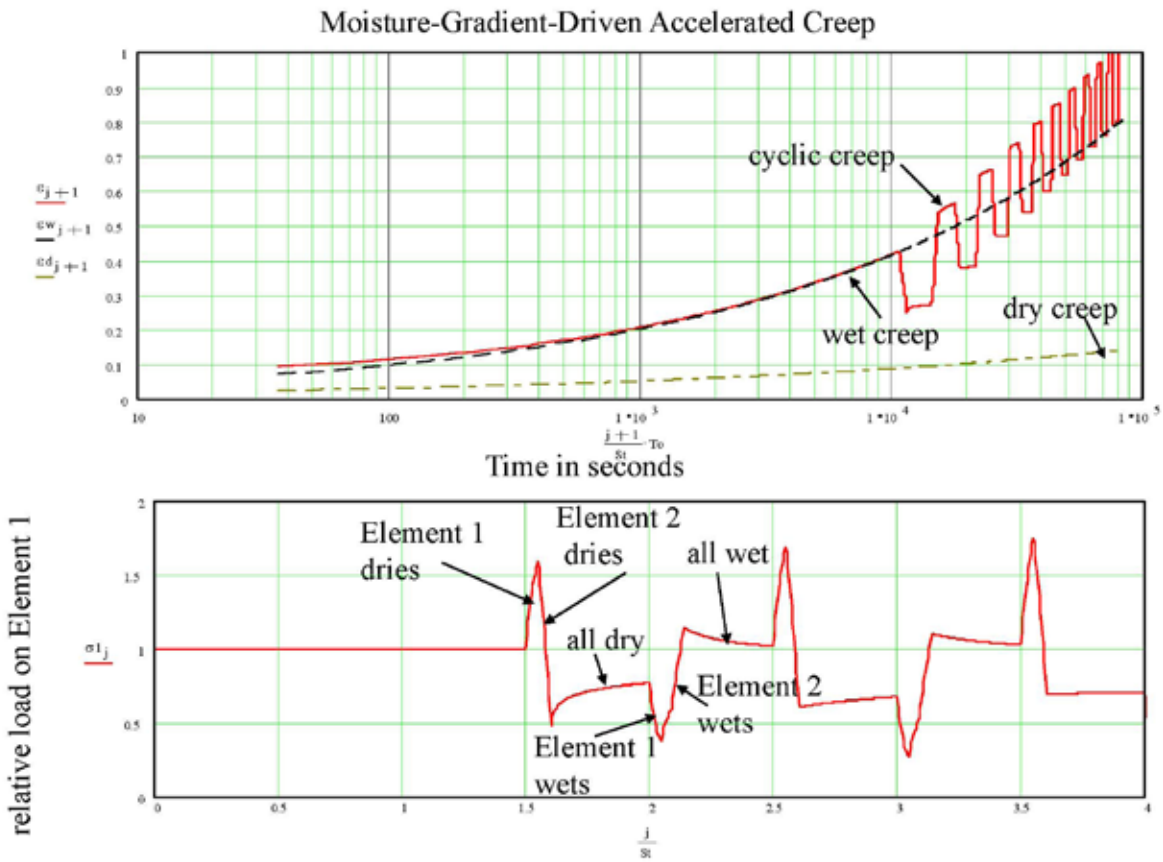

For moisture-gradient-driven accelerated creep to be operative

1. Humidity ramp time must not be long compared to sorption time (no moisture gradients through the sample).

2. Humidity cycle time cannot be very short compared to sorption time (no moisture gradients through the sample).

3. Humidity cycle time cannot be very long compared to sorption time (moisture gradients are too infrequent).

4. Transport boundary condition must be such that moisture gradients are across the sample not in an external convection boundary layer .

Optimum moisture-gradient-driven accelerated creep occurs when cycle time and sorption time are the same order and humidity is changed rapidly.

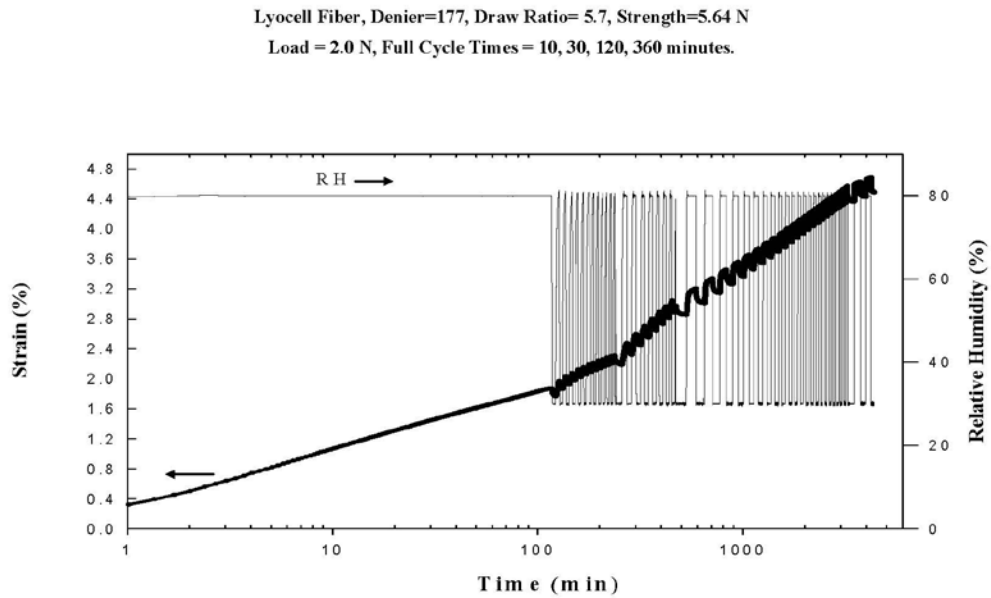

Figure 10

Accelerated creep for a 177-denier lyocell fiber under a 2.0-N load.

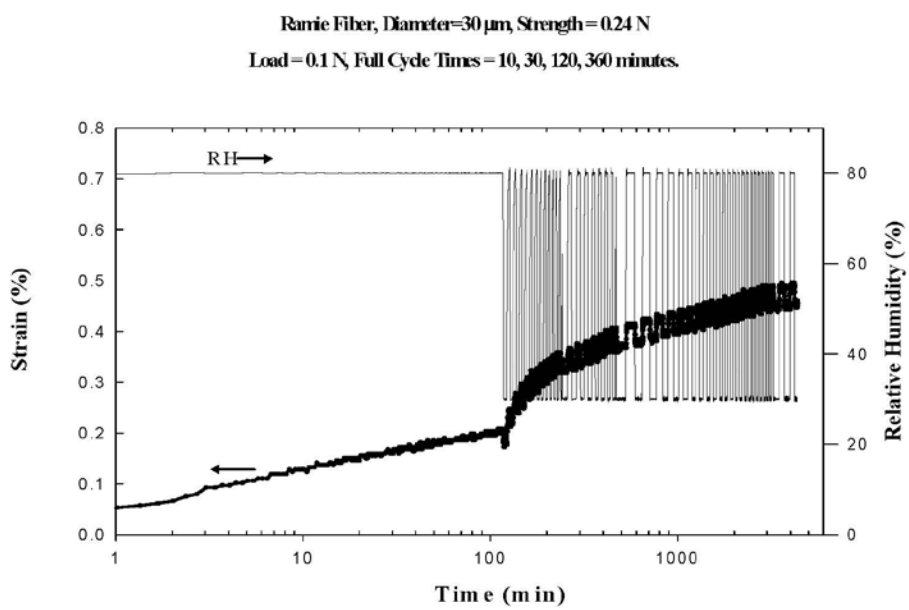

Figure 11

Accelerated creep for 30-μm ramie fiber under a 0.1-N load.

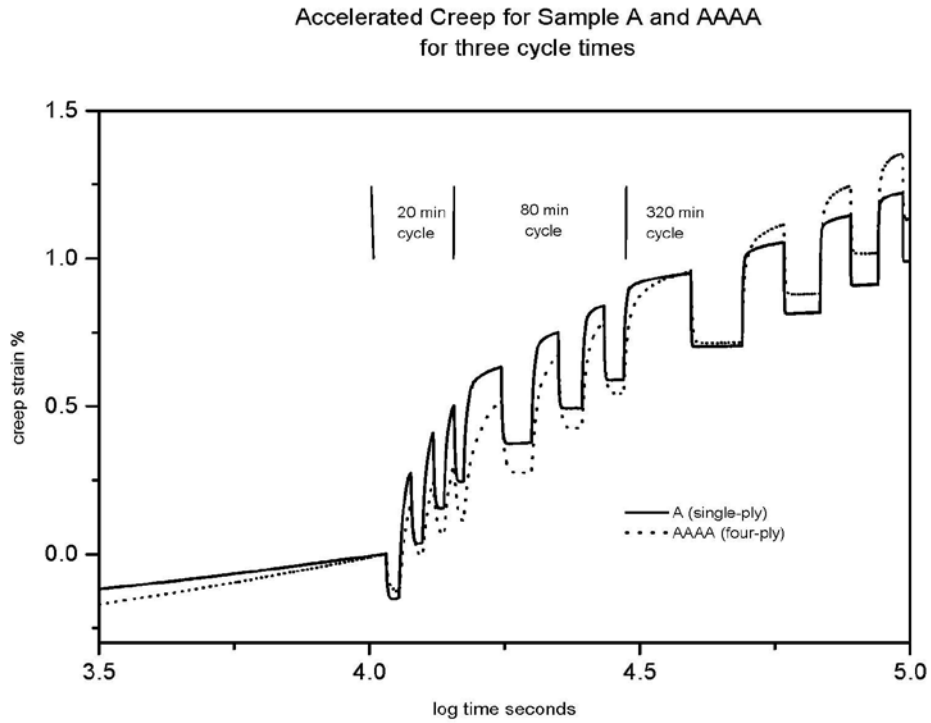

Figure 3

Why is there more accelerated creep in paper than in cellophane?

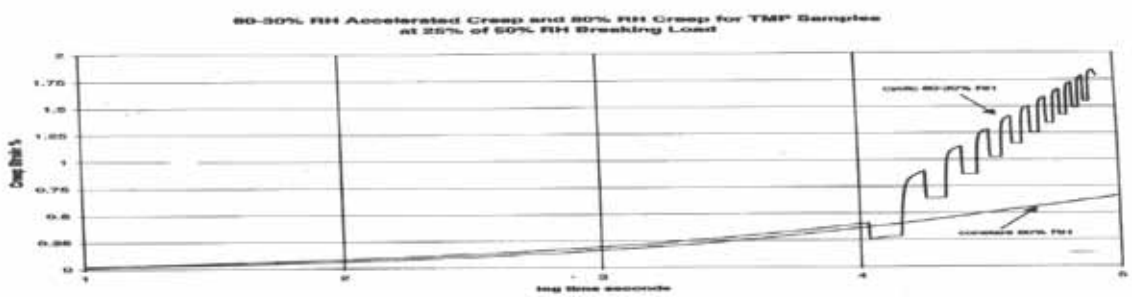

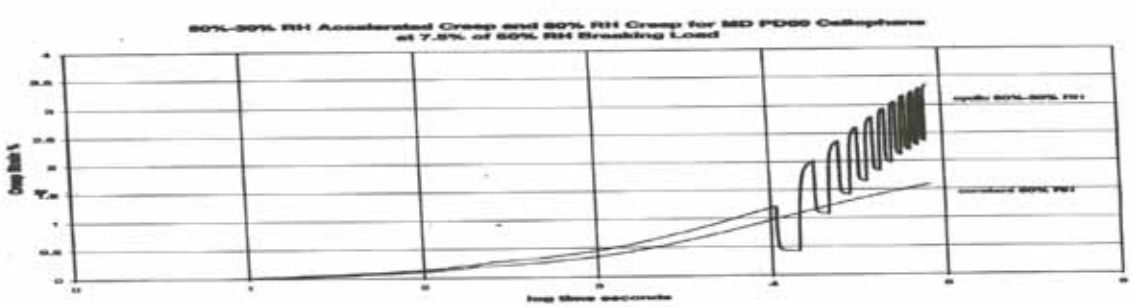

Stress Cycling through Sorption Heterogeneity

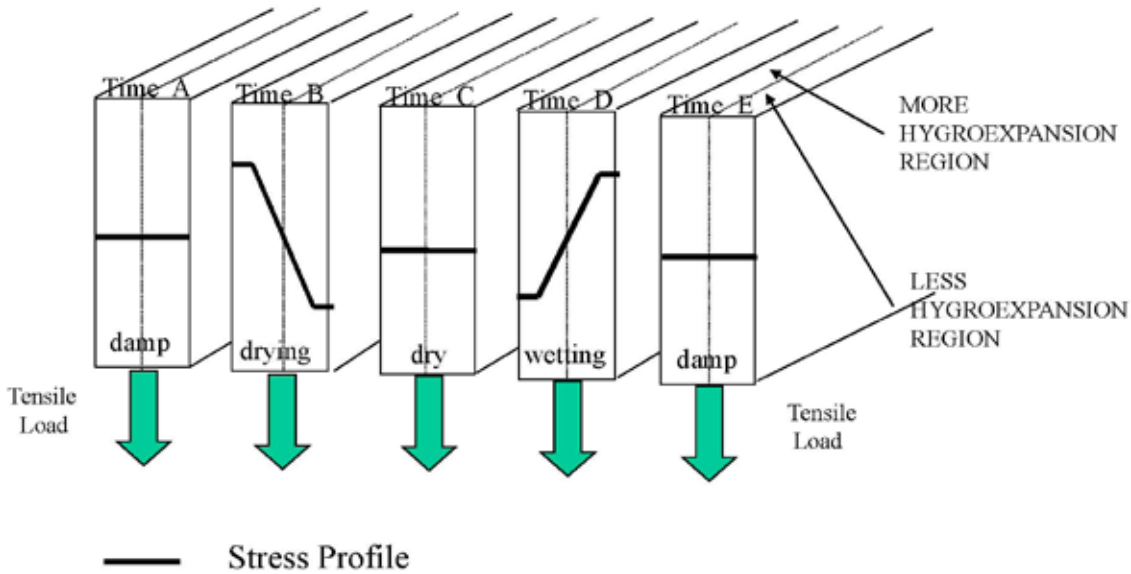

Hypothetical Load Cycling Produced by Moisture Cycling Though Material Heterogeneity in Moisture Sensitivity

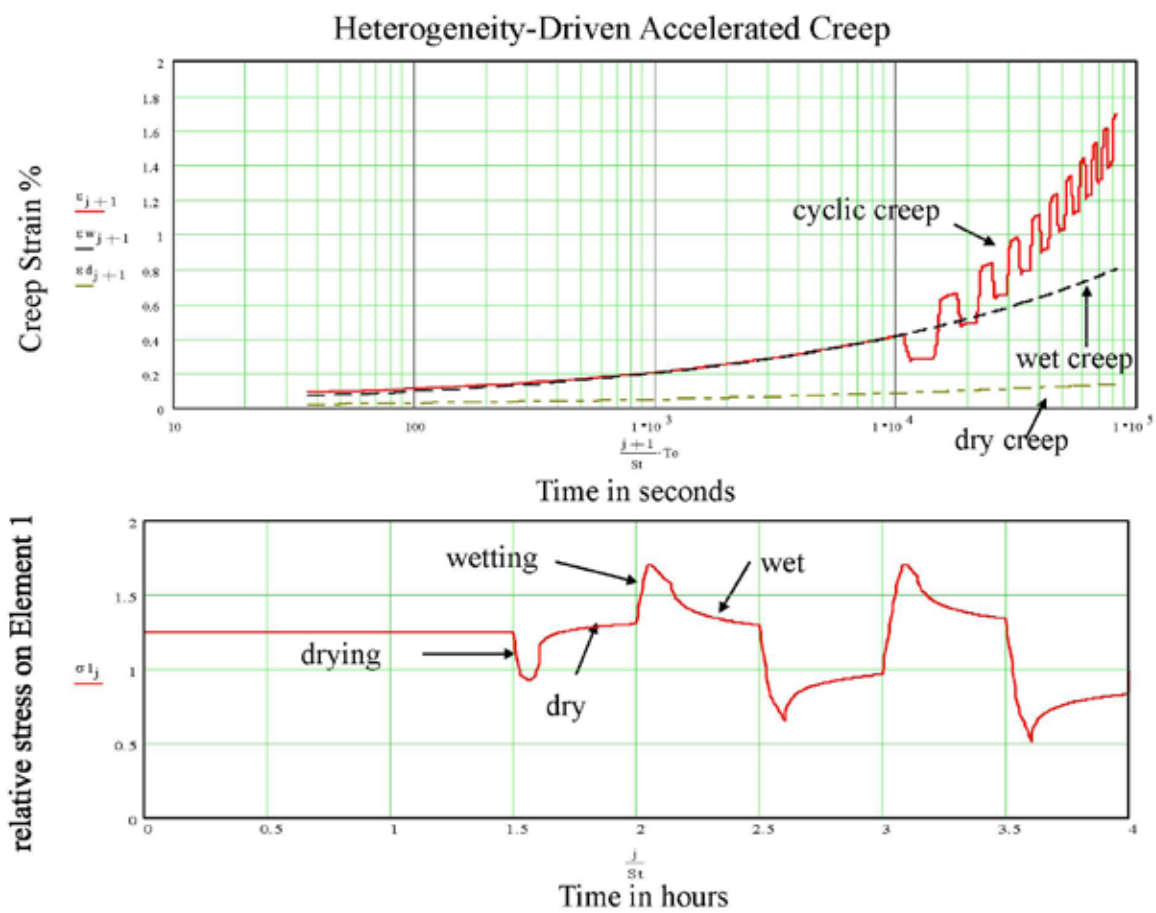

Wood fibers experience anisotropic swelling.

Fibers bonded in paper often have different fiber axis orientations.

Upon cyclic sorption, this leads to heterogeneous moisture responses, extra stress gradients, and extra accelerated creep.

The reason paper shows more accelerated creep than cellophane is probably that it experiences both moisture-gradient-driven and heterogeneity-driven accelerated creep.

Mixture Experiments

Investigate accelerated creep in paper structures with artificial moisture sorption heterogeneity.

High yield pulps have less shrinkage potential, and (dried under equal restraint) high yield pulps have more hygroexpansivity.

50-50 fiber blends of a bleached kraft and a TMP pulp

50-50 multi-ply layer sheets of a bleached kraft and a TMP pulp

Physical Properties of Samples

Sheet Type	Density	Basis Weight	Tensile Strength	Stretch	Specific Longitudinal Sonic Modulus	Hygroexpansion 30-80% RH
	g/cm^3	g/m^2	kN/m	%	km^2/s^2	%
A	0.314	61.9	1.84	1.6	4.98	0.39
B	0.317	61.9	0.68	1.1	3.95	0.32
AB	0.305	59.6	1.41	2.0	4.81	0.36
AAAA	0.332	254	8.41	2.7	5.23	0.34
BBBB	0.356	250	3.36	1.9	4.84	0.30
ABBA	0.333	256	5.58	2.2	4.94	0.32
BAAB	0.347	258	5.81	2.5	4.73	0.33

- **How should one quantify accelerated creep?**
- **What method?**
- **What loads?**

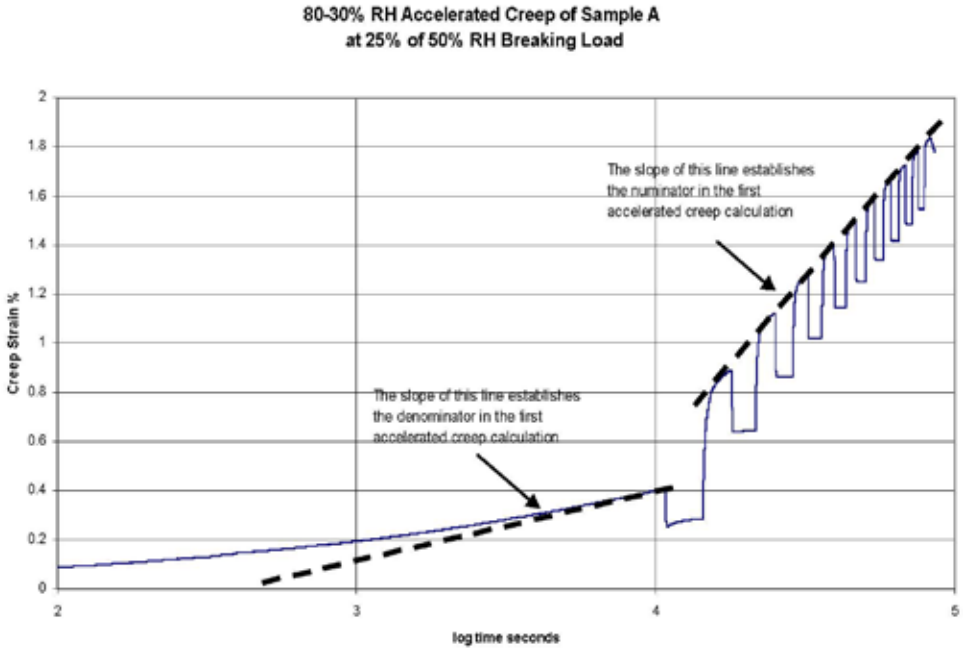
80-30% RH Accelerated Creep of Sample A
at 25% of 50% RH Breaking Load
Creep Strain %
log time seconds
The slope of this line establishes the numinator in the first accelerated creep calculation
The slope of this line establishes the denominator in the first accelerated creep calculation

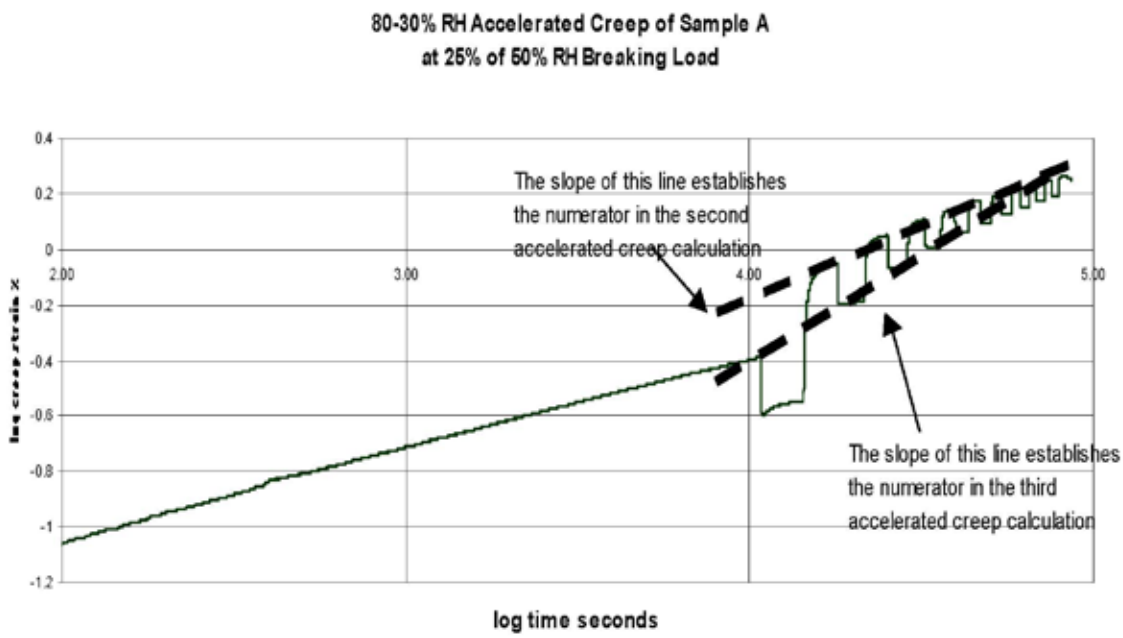
80-30% RH Accelerated Creep of Sample A
at 25% of 50% RH Breaking Load
log creep strain %
log time seconds
The slope of this line establishes the numerator in the second accelerated creep calculation
The slope of this line establishes the numerator in the third accelerated creep calculation

Blend Accelerated Creep Results

semi-log plot

Sheet Type	Accelerated Creep at 25% of Sample's Tensile Strength	Accelerated Creep at 25% of Sample B's Tensile Strength
A	5.1 (.3)	8.3 (.4)
B	4.5 (.1)	4.5 (.1)
AB	4.6 (.1)	6.0 (.3)

log-log plot

Sheet Type	Accelerated Creep at 25% of Sample's Tensile Strength	Accelerated Creep at 25% of Sample B's Tensile Strength
A	1.50	1.55
B	1.45	1.45
AB	1.55	1.51

full log-log plot

Sheet Type	Accelerated Creep at 25% of Sample's Tensile Strength	Accelerated Creep at 25% of Sample B's Tensile Strength
A	2.37	2.86
B	2.26	2.26
AB	2.34	2.52

Average [accelerated creep AB/.5(accelerated creep A + accelerated creep B)]
= 0.99 (.04)

Multiply Accelerated Creep Results

semi-log plot

Sheet Type	Accelerated Creep at 25% of sample's tensile strength	Accelerated Creep at 25% of sample BBBB's tensile strength	Accelerated Creep at 35% of sample BBBB's tensile strength
AAAA	3.8 (.1)	4.2 (.1)	5.2 (.1)
BBBB	3.9 (.1)	3.9 (.1)	3.3
ABBA	4.5 (.2)	5.2 (.1)	4.1
BAAB	4.2 (.2)	4.6 (.1)	3.8 (.4)

log-log plot

Sheet Type	Accelerated Creep at 25% of sample's tensile strength	Accelerated Creep at 25% of sample BBBB's tensile strength	Accelerated Creep at 35% of sample BBBB's tensile strength
AAAA	1.56	1.18	1.24
BBBB	1.40	1.40	1.51
ABBA	1.40	1.44	1.50
BAAB	1.65	2.32	1.57

full log-log plot

Sheet Type	Accelerated Creep at 25% of sample's tensile strength	Accelerated Creep at 25% of sample BBBB's tensile strength	Accelerated Creep at 35% of sample BBBB's tensile strength
AAAA	1.85	1.96	2.03
BBBB	2.13	2.13	2.08
ABBA	2.07	2.34	2.27
BAAB	2.38	3.44	2.18

Average [accelerated creep (ABBA +BAAB)/(AAAA+BBBB)]
= 1.18 (.16)

Fiber blending didn't exacerbate accelerated creep.

We contend this is because the minor increase in swelling heterogeneity introduced through blending is dwarfed by that naturally present from anisotropic fiber swelling.

Multi-ply sheets did show extra accelerated creep because an addition mode (cross-ply) for heterogeneous sorption was introduced.

Effect of relative humidity cycles on the mechano-sorptive creep stiffness

Joel Panek and Christer Fellers
STFI
Box 5604, S-114 86 Stockholm, Sweden
tel: +46 8 67 67 000
fax: + 46 8 21 42 35
email: joel.panek@stfi.se, christer.fellers@stfi.se

The accelerated creep of paperboard under varying relative humidity conditions is a well-known phenomenon. It is a practical problem because it results in a lower load capacity and shorter lifetime of paper-based containers. Further, the total creep deformation cannot be predicted from short-term measurements in static conditions, which leads to uncertainty in product performance. To help solve these problems, we have developed a method to evaluate creep under cyclic relative humidity conditions. This method produces, among other properties, a mechano-sorptive creep stiffness, which quantifies the creep under a constant load and a standard cycling condition of 50-90-50% RH over a 7 hour period. The mechano-sorptive creep stiffness is calculated from the total deformation at the end of each cycle, and is given as a function of the number of cycles. This approach has given valuable information about creep under the standard conditions; additional information is now needed for when the relative humidity is varied in other ways, e.g. 30-90-30% RH. This will give a more thorough picture of the response of paper to relative humidity cycling and improve the ability to predict the creep of paper under any conditions. We propose that the effect of the relative humidity level can be put in terms of the moisture ratio of the sample. In this way, the mechano-sorptive creep stiffness can be described as a function of the number of cycles, the initial moisture ratio, and the maximum difference in moisture ratio during cycling. In the results presented here, the mechano-sorptive creep stiffness was plotted versus the change in moisture ratio during cycling for different relative humidity cycles. The results showed that the mechano-sorptive creep stiffness decreases as the difference in moisture ratio during the cycle increases, and that the MS creep stiffness is the most sensitive to just a small increase in moisture ratio.

Paper Temperature and Moisture Measurement

Ross Chiodo
Product Development Specialist
Visy Technical Centre, 13 Reo Cres., Campbellfield

The issue of "Green" paper and related conversion problems has been somewhat of a "grey" area in the corrugated board industry. To explain why some of these conversion problems occur, a better understanding of the changes to paper properties during this "Green" period, is necessary. Paper Temperature and Moisture Content are often accused as the causes of some of these conversion problems, so this seemed a good place to start. These properties can be monitored by conventional means during conversion of the reels, however this would involve many reels and controlled conversion dates and times, which is impractical if not impossible to organise. To investigate this further, a method of measuring temperature and moisture content of paper, at various points in one reel, whilst in storage, was developed. The method uses fine wire temperature thermocouples for temperature measurement and fine gauge copper wires measuring electrical resistance through paper, for moisture measurements. A combination of several of these probes were made in the form of "tapes" which were then inserted into a trial reel during the mill rewinding stage, soon after manufacture. The reel was then placed into storage where Temperature and Moisture content were tracked over time.

The Difference between Static and Sonic Moduli of Paper and the Effect of Moisture Content on this Difference

D. W. Coffin IPST, Atlanta, GA
J. Lif and C. Fellers, STFi, Stockholm Sweden

ABSTRACT

The motivation for this paper is to address the recent statement [1]

> *....the sonic modulus of paper is larger than the mechanically measured modulus. The reasons for this are not clear.*

We sense that this statement reflects the thoughts of a substantial number of people in the industry. On the other hand, we believe that the phenomenological explanation for the discrepancy is clear. Therefore, we conclude that the conveyance of this message to the industry has not been adequate.

It is emphasized that the material behavior of paper is typical of many polymers and that the fundamental difference in the two measurements is simply a consequence of viscoelastic behavior and the very different time scales involved in the two measurements.

At room temperature, moisture plasticizes paper and the difference between the sonic and static measurements increase. In oriented sheets, increased moisture tends to increase the ratio of MD to CD moduli, but again the magnitude of this change is different for static and sonic measurements. All these effects are easily explained in terms of viscoelastic properties and their sensitivity to moisture. To support our reasoning and show that the behavior is quite normal and expected, sonic and ultrasonic measurements for a wide range of papers and at several moisture contents are presented. The implications of the two measurement techniques on understanding and modeling paper behavior are made.

Reference.

1. NISKANEN K. and P. KARENLAMPI, "In-plane Tensile Properties," Chapter 5 of *Paper Physics*, editor K. Niskanen, p. 142. (1998)

FACTORS INFLUENCING DIMENSIONAL STABILITY IN PAPER AND BOARD

(Authors: M. Ahsan Qureshi*, Ian Parker**)

ABSTRACT

Dimensional Instability, including Curl and Cockle, in paper and/or board produces a number of operational and converting problems for end users. Most common are register problems in multi-colour printing and feeding problems in printing, converting and packaging systems. A range of other problems occurs in electronic printing systems and in the processing of map papers, template papers and punch cards, etc.

Machine made paper is anisotropic in nature, which gives the possibility that the paper sheet is oblique. The anisotropy of paper means there are differences in the dimensional stability in the three directions ie. X, Y, and Z. Anisotropy is affected by a number of parameters and operational variables throughout the paper making process. It is generally accepted that the dimensional stability or instability of paper and board is determined by its fibre furnish and a complex set of variables in papermaking process and converting operations. Variables involved in papermaking are moisture, grammage, refining conditions, wet end variables and drying conditions. Other factors that can cause dimensional instability and curl are internal and external sizing and other chemical additives, which control water absorption behaviour of paper, pigment coating and laminating etc. The problem has also been strongly related to time and to the temperature and relative humidity variations taking place in the external environment during storage and converting operations.

The objective of this work was to investigate the extent to which dimensional changes in paper or board are determined by the environmental effects of time, temperature and relative humidity. Hence, with the quantification of the amount of these effects, the behaviour of paper in a given set of conditions may be predicted. This work also aimed to study common physical and structural properties of the paper and the effect of papermaking variables, to propose solutions to overcome dimensional instability problems.

A special feature of this research work was that whilst, most previous research has been confined to wood fibres, it includes straw (wheat straw fibres) that is also a major source of raw material for paper and board making. In view of this, papers from different fibrous sources were selected and tested for specific properties described above.

From the results it was concluded that when environmental conditions are changing slowly, the dimensional changes in the paper are stable and predictable. On the other hand, with rapid and abnormal changes in the environment, dimensional changes are so abnormal that predictions cannot be made. The effect of furnish was quite obvious in that hardwood was dimensionally the most stable while straw was the least. Among common papermaking and structural variables, conditions that reduce two-sidedness result in a more dimensionally stable paper.

In the light of the results, suggestions were made on how to reduce, and to possibly eliminate environmental shocks to the paper and to optimise papermaking variables that reduce two-sidedness. A good selection / combination of fibrous raw materials as well as chemical additives coupled with machine variables, giving special attention to the forming section, could help produce less variable and dimensionally more stable paper.

Analysis of physical paper behavior subjected to previous compression and tensile strains under different relative humidities

Isabelle Desloges-Vullierme, Jean-Marie Serra-Tosio

Ecole Française de Papeterie et des Industries Graphiques
Laboratoire GP2 – UMR CNRS 5518
B.P. 65 – 38402 Saint Martin d'Hères CEDEX - France

During the use of corrugated board packaging, liners and medium are subjected to creep which gradually affects their physical performance. The aim of this study is to analyze the aging of paper under compression and different moisture conditions, as can be seen during the storage of boxes.

In this investigation we studied the effects of creep and relative humidity on different physical properties of paper. First, we considered the effects of relative humidity variations. We studied the sensitivity of the fiber network to humidity. Properties as thickness, roughness, tensile and compression strength were analyzed. Then, using the Varipress apparatus developed at the EFPG, several kinds of industrial papers for paperboard (kraftliner, testliner, semi-chemical medium) were subjected to different conditions. We applied rates of compression dead-load, leading to a slow creep of papers. This was performed in a constant atmosphere of 50% RH and 85% RH and also under cyclic moisture conditions. The quality of such aged papers was analyzed in terms of strength properties (tensile strength, delamination in Z direction), compression strength (SCT), stiffness, hygro-expansivity. Similar work was done with paper subjected to previous tensile strain. A comparison is made between effects of compression and tensile creeps. Finally, different papermaking operations such as calendering or use of additives can be considered to reduce creep phenomena.

Cyclic Humidity Bending Creep of Corrugated Board. Measurement, Modelling and Effect of WVTR

Creep.papers@eng.monash.edu.au
Andrew D. McKenzie[1] and Ian R.Chalmers[2]
1 Product Development Engineer, CHH Pulp & Paper Kinleith
2 Group Leader, Paper and Packaging Research, PAPRO

Corrugated fibreboard packaging is a major cost to New Zealand growers and exporters of fruit like apples and Kiwifruit. Reducing the weight of packaging for more efficient transportation and lowered cost requires a better understanding of the effects of the high relative humidity found in coolstores on corrugated fibreboard. Some coolstore conditions are very extreme and are likely to get worse. For example, it has recently been found that to prevent shrivel in apples the relative humidity surrounding the fruit should be closer to 98% RH than to say 90%.

Compression and bending stresses on cartons stacked in coolstores causes compression creep and carton bulge. If the bulging is too severe cartons may fail and collapse prematurely. In practice cartons are exposed to changing humidity conditions as coolstores are loaded and unloaded or during coolstore chilling equipment de-icing cycles.

An apparatus was built at PAPRO to measure four point bending creep performance of 50 x 250 mm corrugated fibreboard samples in an environmental chamber under high and cyclic relative humidity conditions. Six samples were tested in a batch with a laser height measuring device used to log bending strain.

The bending creep strain was found to consist of cyclic bending in response to cyclic relative humidity superposed on a long-term creep deformation. An Empirical model first proposed by Pecht in 1985 was fitted to strain data to describe the non-cyclic creep deformation. Isochronous creep curves could be generated for samples tested using a range of stress levels to allow the creep performance of packaging materials to be compared.

It was also found that the cyclic creep strain response to the humidity cycle was dependent on the peak relative humidity attained during the test.

Using coated board samples and small humidity sensors that can fit between flutes, the effect of WVTR on the performance of corrugated board cyclic humidity bending creep was also studied.

Ring crush creep of linerboard in changing environmental conditions

Andrew Conn* and Ian Parker†

*Research Fellow, Australian Pulp and Paper Institute, Monash University, Australia
†Assoc. Prof., Australian Pulp and Paper Institute, Monash University, Australia

The Ring Crush Test (RCT) results in linerboard failure through both compressive and buckling forces. Although no intrinsic property of the linerboard is measured by the RCT it thought to replicate the failure mechanism of the linerboard in the box wall. It is used commercially to evaluate the contribution of the linerboard to box stacking strength. Recently the short term RCT has been extended to evaluate the long term viscoelastic creep effects under changing environmental conditions – Ring Crush Creep (RCC). It is hoped that RCC may be useful in understanding and evaluating box performance in similar changing environmental conditions.

RCC experiments have been conducted with a variety of environmental conditions. These conditions include both constant and cyclic humidity profiles. Further experiments were conducted using different humidity profiles inside and outside the test ring. Results from both commercial linerboard and several types of handsheets will be presented and discussed.

Abstract
Simulation of a corrugated board tube under accelerated creep compression

In this study the creep behaviour of a corrugated board box is studied using the finite element method. Paperboard is modelled as a three layered material. The outer layers have the properties of the liners and the center layer has properties equivalent to the corrugated core layer. The distinct paper layers are modelled as an orthotropic linear viscoelastic material with moisture content dependent parameters. The moisture content of the paper is described as a function of the relative humidity of the environment and absorbtion parameters of the paper. Hence, the moisture content and the viscoelastic parameters are not constant through paper thickness according to the accelerated creep theory of Coffin and Habeger. All parameter values of the model were taken from literature. Using this model stresses, strains and displacements of a corrugated board tube were studied for several scenarios with varying temperature and relative humidity. This study results in recommendations for storage of corrugated board containers.

C.L.M. van Weert
ATO
P.O. Box 17
6700 AA Wageningen, The Netherlands
tel +31 (317) 477521
fax +31 (317) 475347
c.l.m.vanweert@ato.wag-ur.nl

TITLE: Develop corrugated board performance specifications for boxes containing "flowable" products.

AUTHOR: Dr. Paul Singh, Professor, Michigan State University

ABSTRACT:

This study investigated the performance of boxes made from various grades of corrugated board that contain high weight density "flowable" products such as printed brochures, nuts and bolts, etc. that can cause the board to rupture and tear when subjected to vibration and drops. Concentrated stresses develop in the edges and corners of the box which weaken the material there and eventually cause failure. In recent years, most box suppliers have started to use ECT specified board which does not truly predict failure of the corrugated box for these types of products. ECT is a good predictor for top/bottom compression strength but does not predict containment of flowable products well. The study investigated various box/product combinations. Box styles were RSC's of three different sizes and single wall and double wall corrugated board. Material properties such as burst strength, ECT, FCT, and puncture strength were used to predict failure. Lab simulated drop tests were performed in accordance with International Safe Transit Association (ISTA) Project 3C for the small parcel environment. Flowable products that have shown failure in the parcel shipping environment were selected.

Mail all correspondence to:

Dr. Paul Singh
Professor
School of Packaging
Michigan State University
East Lansing, MI 48824-1223

Tel: 517 355 7614
Fax: 517 353 8999
e-mail: singh@msu.edu

I. Kajanto, P. Miettinen, Fast measurement of creep properties of paperboard and its use in predicting the creep response of paperboard boxes

KCL Science & Consulting
P.O. Box 70
FIN-02151 Espoo
Finland

Abstract

Tools were developed for estimating the creep response of a paperboard packages in various loading situations. The method is based on measuring the creep response of the paperboard and by calculating the behavior of the package using the finite element method. The power of the method was demonstrated in a simple vertical loading situation.

To measure the creep response of paperboard, it was constructed a long-span compression tester, with which the creep strain over time could be measured. The creep was measured with a high load (> 50% of compression strength), and a simple power-form creep-law is fitted to the data.

Creep was also characterized with the calculatory lifetime, which is the time needed for the material to break under a certain load. This allows a single number to be used instead of the three parameters of the creep law.

The apparatus was tested by measuring commercial folding boxboard samples. These showed systematic variation in the creep properties as a function of grammage. This was suspected to come from the different creep properties of chemical and mechanical pulp. The effects of paper machine factors, orientation and drying shrinkage, were negligible.

The creep laws thus obtained were used in calculating the creep response of packages with the finite element method. To verify the results, it was constructed a device to creep test the packages. The creep rate of lidless packages could be calculated with the FEM. With lidded packages, problems were caused by uncertainties in the measurements.

The Influence of Heterogeneity on Tensile Accelerated creep in Paper

Chuck Habeger, Douglas Coffin

The Institute of Paper Science and Technology

Abstract

The presentation begins with a brief review of our preferred explanation for accelerated creep. We previously argued that accelerated creep is a result of the load dependence of the creep constitutive equation (JPPS 26(4) pp. 145–157 (2000)). Materials suffer more creep when subjected to a cyclic load than when held a constant load of the same average magnitude. Moisture cycling results in localized load cycling and therefore in additional creep. There are two ways this can happen. We call one of them "moisture-gradient-driven accelerated creep:" during sorption, transient moisture gradients pass through the sample, and differential swelling leads to stress gradients. The other is "heterogeneity-driven accelerated creep" Moisture cycling combined with spatial variability in hygroexpansion can also produce localized stress cycling.

If the humidity is changed rapidly compared to the sample sorption time, if the humidity cycle time is not much less than or much greater than the sample sorption time, and if the moisture transport conditions are such that a significant portion of moisture gradient is across the sample, moisture-gradient-driven accelerated creep will be observed in hydrophilic materials. Heterogeneity-driven accelerated creep doesn't have the same stringent requirements on sorption conditions, but it can only occur in materials made of parts with disparate responses to moisture. We contend that, if properly cycled, all hydrophilic materials will exhibit extra creep. We attribute this general action to moisture-gradient-driven accelerated creep. Heterogeneity-driven accelerated creep is a rarer phenomenon that we suspect is also active in paper.

Because of the great difference between radial and axial hygroexpansion of wood fibers, paper has an unusual opportunity to display heterogeneity-driven accelerated creep. Fibers bonded together in the sheet will often have different orientations. Hygroexpansion results in dimensional incompatibilities, and cyclic humidity changes cause cyclic, fiber-level stress gradients. Compared to similar, but-homogeneous materials, paper suffers a great deal of accelerated creep. Cellophane has more hygroexpansion and greater creep enhancement through load cycling than does paper, yet it is less prone to accelerated creep. The reason for this may well be that paper is also subject to heterogeneity-driven accelerated creep.

To address the question of the role of heterogeneity in paper-accelerated creep, we tested papers made from a combination of furnishes. We selected bleached kraft softwood and thermo-mechanical pulps (TMP). When dried under full restraint, the pure TMP sheets had about 20% more hygroexpansion than the BKS ones. We compared sheets made from 50-50 blends of the two pulps with the single-furnish pulps and mixed-furnish multi-ply sheets with single-furnish multi-ply sheets. After deciding on a method to quantitatively rate accelerated creep, we concluded that heterogeneous layering did contribute to accelerated creep, whereas fiber blending did not. We surmise that the extra fiber-level heterogeneity contributed by fiber blending was small compared with that already present because of anisotropic fiber swelling. However, layering with plies of different hygroexpansion opened up a new scale for heterogeneity-driven accelerated creep.

5th International Symposium

Moisture and Creep Effects on Paper, Board and Containers

Marylands Country House, Marysville, Victoria, Australia

26 & 27 April, 2001

Information Booklet

Sponsored by AMCOR

APPI AUSTRALIAN PULP & PAPER INSTITUTE

Appita

General Information

Symposium Venue
Marylands Country House
22 Falls Road, Marysville Vic 3779
Australia
Phone: + 61 3 5963 3204
Fax: + 61 3 5963 3251
Email: info@marylands.com.au

Registration Desk
All delegates should register at the Symposium Registration Desk after checking in to Marylands Country House.

Hours of Operation

Wednesday 25 April, 2001	5.00pm – 6.30pm
Thursday 26 April, 2001	8.30am – 5.00pm
Friday 27 April, 2001	8.30am – 5.00pm

Message Board
A message board will be located near the Symposium Registration Desk and delegates are asked to check this board during the Symposium.

Delegate Registration includes:
3 nights accommodation, all meals during in the Symposium, coach transfers from/to Melbourne, program, name badge, satchel, proceedings (distributed after the Symposium).

Day Registration includes:
Morning/afternoon teas and lunch on day of registration, program, namebadge and satchel.

Partner's Registration includes:
Evening meals, breakfast, lunch Thursday and Friday, coach transfers from/to Melbourne and name badge.

Accommodation
Please note that any room service, mini bar etc. Will be at your own expense. Only meals included in the registration fee are provided. Incidental charges must be finalised with the Marylands Country House upon departure.

Name Badge
Each delegate/partner will be given a name badge when they register at the Symposium Registration Desk. Please ensure you wear this name badge at all times whilst attending Symposium sessions and functions.

Special Dietary Requirements
If you have indicated a special dietary requirement or disability assistance on your registration form, please make yourself known to the staff at the Symposium Registration Desk.

Non Smoking Policy
Marylands Country House is a smoke free venue.

Coach Transfers
On Saturday your coach will depart Marylands Country House at 9.00am for return to Spencer Street Railway Station, arriving at approximately 11.00am.

Post Symposium Tour : Healesville Sanctuary
On Saturday your coach will depart Marylands Country House at 9.00am for arrival at Healesville Sanctuary at 10.30am. On arrival you will be met and given a guided tour of the Sanctuary. At 12noon there will be a Bird of Prey Presentation.

A BBQ lunch will be served at 12.45pm.

Your coach will depart for De Bortolli Winery at 2.00pm for a tasting of some of Victoria's famous wines. You will arrive at Spencer Street Railway Station at approximately 5.00pm.

Please have your ticket ready for collection as you board the coach. Additional tickets can be purchased from the Symposium Registration Desk up until 3.00pm Friday. Cost: AUD65.00

Partner's Tours
It is suggested that Partners enquire at Marylands Country House for any relevant tours whilst in Marysville.

Disclaimer
The speakers, topics and times are correct at the time of printing. In the event of unforeseen circumstances, the Organising Committee reserves the right to delete or alter items in the Symposium Program.

Liability/Insurance
In the event of industrial disruptions or natural disasters, the Organising Committee and PR Conference Consultants cannot accept responsibility for any financial or other losses incurred by the delegates, nor can the Organising Committee and PR Conference Consultants take responsibility for injury or damage to persons or property occurring during the Symposium. Insurance is the responsibility of the individual delegate/partner.

Cancellation Policy
There is no refund for cancellations made during the Symposium.

Technical Program
Thursday 26th April

Opening– Chair: Ian Parker
09:00 Opening Comments: Chair
09:30 **Keynote Speaker:** ***Russell Rankin***
Food into Asia.

10:30 **Morning Tea**

Session 1 – Chair: Russell Allan
11:00 A more mechanistic model of the compression strain-load response of paper.
Thomas Urbanik
11:30 Influence of heterogeneity on tensile accelerated creep in paper.
Chuck Habeger & Douglas Coffin
12:00 Effect of relative humidity cycles on the mechano-sorptive creep stiffness.
Joel Panek & Christer Fellers

12:30 **Lunch**

Session 2 – Chair: Ian Chalmers
13:30 Paper temperature and moisture measurement.
Ross Chiodo
14:00 The difference between static and sonic moduli of paper and the effect of moisture content on this difference.
Douglas Coffin, Jan Lif & Christer Fellers
14:30 Performance of Xitec.
Peter McKinlay

15:00 **Afternoon Tea**

Session 2 – Chair: TBA Doug.
15:30 Simulation and measurement of fibre network deformation due to single fibre hygroexpansion.
Jens Schedin & Tomas Nordstrand – sick.
16:00 Factors influencing dimensional stability in paper and board.
Ahsan Qureshi & Ian Parker
16:30 Close

AMCOR

Technical Program
Friday 27th April

Session 4 – Chair: Christer Fellers

09:00 Analysis of physical paper behavior subjected to previous compression and tensile strains under different relative humidities
Isabelle Desloges-Vullierme & Jean-Marie Serra-Tosio

09:30 Cyclic humidity bending creep of corrugated board. Measurement, modelling and effect of WVTR.
Andrew McKenzie & Ian Chalmers

10:00 Ring crush creep of linerboard in a changing environment.
Andrew Conn & Ian Parker

10:30 **Morning Tea**

Session 5 – Chair: Thomas Urbanik

11:00 Relative humidity and cushioning of currugated fibreboard.
Michael Sek & Jim Kirkpatrick

11:30 Modelling Box Design.
Russell Allan

12:00 Simulation of a corrugated board tube under accelerated creep compression.
Kees van Weert

12:30 **Lunch**

Session 6 – Chair: Jean-Marie Serra-Tosio

13:30 Box design, creep and the distribution chain.
Russell Allan

14:00 Develop corrugated board performance specifications for boxes containing "flowable" products.
Paul Singh

14:30 Fast measurement of creep properties of paperboard and its use in predicting the creep response of paperboard boxes.
Isko Kajanto & Pasi Miettinen KCL

15:00 **Afternoon Tea**

Session 7 – Chair: Ian Parker

15:30 Imaging and modelling porous structures.
Mark Knackstedt

16:00 Closing Comments: Chair

16:30 Close

General Program

Wednesday 25th April

15:00 Coach leaves Melbourne for Marysville
18:00 Check-in at Marylands Country House
19:00 Dinner

Thursday 26th April

07:30 Breakfast
09:00 Technical Program Starts
16:30 Technical Program Finishes
19:00 Symposium Dinner

Friday 27th April

07:30 Breakfast
09:00 Technical Program Starts
16:30 Technical Program Finishes
19:00 Dinner

Saturday 28th April

07:00 Breakfast
09:00 Coach departs for Spencer Street Station, Melbourne
09:00 Coach departs for tour group to Healesville Sanctuary & winery
12:45 BBQ lunch
14:00 Coach departs for De Bortolli winery
17:00 Approximate arrival of tour group at Spencer Street Station, Melbourne

APPI
AUSTRALIAN PULP & PAPER INSTITUTE

Appita

The organisers of the

5th International Symposium

on the

Moisture and Creep Effects on Paper, Board and Containers

thank the principle sponsor

AMCOR

5th International Symposium

Moisture and Creep Effects on

Paper, Board and Containers

26 & 27 April, 2001

Marylands Country House
Australia

ATTENDEE'S LIST

CREEP 2001

5th International Symposium on the Moisture and Creep Effects on Paper, Board and Containers

People who are Confirmed Delegates

24-Apr-01

Name	Organisation	Full Address	E-Mail Address	Business Telephone Number	Business Fax Number
MR RUSSELL ALLAN	Amcor Research	Manager, Fibre Technology Amcor Research Private Bag 1 FAIRFIELD VIC 3078	russell.allan@amcor.com.au	03 9490 6151	03 9499 4295
DR WARREN BATCHELOR	Australian Pulp & Paper Institute	Lecturer Department of Chemical Engineering Australian Pulp & Paper Institute Monash University, Clayton Campus P.O. Box 36 MONASH UNIVERSITY VIC 3800	warren.batchelor@eng.monash.edu.au	03 9905 3452	03 9905 3413
MR JAMES BONHAM	Australian Paper	Product Development Manager Australian Paper 685 Burke Road CAMBERWELL VIC 3124	jim.bonham@paperlinx.com.au	03 9811 9889	03 9811 9205
MR IAN CHALMERS	Papro	Group Leader Papro Forest Research P.O. Bag 3020 ROTORUA NEW ZEALAND	Ian.Chalmers@forestresearch.co.nz	64 7 343 5899	64 7 343 5695
MR ROSS CHIODO	Visy Industries	Product Development Specialist Visy Industries 13 Rex Crescent CAMPBELLFIELD VIC 3061	ross.chiodo@visy.com.au	03 9247 9586	03 9247 4595
DR THOMAS CLARK	Carter Holt Harvey Pulp & Paper	Technical Development Manager Carter Holt Harvey Pulp & Paper 640 Great South Road Manuka City Private Bag 92-106 AUCKLAND NEW ZEALAND	thomas.clark@chh.co.nz	+64 9 262 6309	+64 9 262 6079
DR DOUGLAS COFFIN	IPST	Associate Professor/Unit Leader IPST 500 10th Street NW ATLANTA GA 30318 USA	doug.coffin@ipst.edu	+ 1 404 824 9722	+ 1 303 894 4778
DR ANDREW CONN	Australian Pulp & Paper Institute	Research Fellow Department of Chemical Engineering Australian Pulp & Paper Institute Monash University P.O. Box 36 MONASH UNIVERSITY VIC 3800	andrew.conn@eng.monash.edu.au	03 9905 5088	03 9905 3413
MS JENNIE DAVIDSON	Carter Holt Harvey Packaging	Laboratory Manager Carter Holt Harvey Packaging 862 Great South Road PENROSE AUCKLAND NEW ZEALAND	Jennie.Davidson@chh.co.nz	64 9 579 1373	64 9 579 2226
MS ISABELLE DESLOGES	E.F.P.G	Associate Professor E.F.P.G 461 rue de la papeterie, BP65 St Martin d'Heres 38402 FRANCE	Isabelle.Desloges@efpg.inpg.fr	+33 476 826 900	+33 476 826 933
DR ROLAND ETTL	Business Unit Paper Chemicals	Product Development Business Unit Paper Chemicals BASF Aktiengesellschaft 67056 GERMANY	roland.ettl@basf-ag.de		

Name	Organisation	Full Address	E-Mail Address	Business Telephone Number	Business Fax Number
PROF CHRISTER FELLERS	STFI	Research Group Leader STFI Box 5604 STOCKHOLM 114 86 SWEDEN	christer.fellers@stfi.se	+46 8 676 7000	+46 8 214 235
MR DAHLSON FORSYTH	Carter Holt Harvey Packaging	Manager - Product Development Carter Holt Harvey Packaging 862 Great South Road PENROSE AUCKLAND NEW ZEALAND	Dahlson.Forsyth@chh.co.nz	64 9 579 1268	64 9 579 2226
MR CARL GARLAND	CSIRO - FFP	Scientist CSIRO - FFP Bayview Road CLAYTON VIC 3169	carl.garland@ffp.csiro.au	03 9545 2315	03 9545 2448
DR CHUCK HABEGER	IPST	Prof of Physics IPST 500 10th Street NW ATLANTA GA 30318 USA	chuck.habeger@ipst.edu	+ 1 404 894 7534	+ 1 404 894 4778
DR RICHARD HELMER	CSIRO Forestry & Forest Products	Scientist CSIRO Forestry & Forest Products Bayview Road CLAYTON VIC 3169	richard.helmer@ffp.csiro.au	03 9545 2283	03 9545 2448
MR ISKO KAJANTO	KCL	Senior Consultant KCL PO Box 70 FIN - 02151 FINLAND	isko.kajanto@kcl.fi	+ 358 9 437 1491	+ 358 9 464305
MR JIM KIRKPATRICK	Amcor Research	Senior Consultant Amcor Research Private Bag 1 FAIRFIELD VIC 3078	jim.kirkpatrick@amcor.com.au	03 9490 6136	03 9499 4295
DR MARK KNACKSTEDT	Australian National University	Research Fellow Australian National University CANBERRA ACT 0200	mak110@rsphysse.anu.edu.au	02 6125 2495	02 6125 0732
DR GERD MATTHESIUS	Carter Holt Harvey	Manager - Cont. Development Carter Holt Harvey State Highway 1 TOKOROA NEW ZEALAND	gerd.matthesius@chh.co.nz	69 7 886 3520	
MR ANDREW MCKENZIE	Carter Holt Harvey	Product Development Engineer Carter Holt Harvey State Highway 1 TOKOROA NEW ZEALAND	andrew.mckenzie@chh.co.nz	64 7 886 3543	64 7 886 3614
MR PETER MCKINLAY	Amcor Research	Consultant Pattern Consulting Amcor Research Private Bag 1 FAIRFIELD VIC 3078	peter.mckinlay@amcor.com.au	03 9490 6100	03 9499 4295
MR PARIKSHITI MHAISPURKAR	Monash University	PG Student Monash University Building 59, Clayton Campus CLAYTON VIC 3800	parikshiti.mhaispurkar@eng.monash.edu.au	03 9905 5076	03 9905 3413
MR PASI MIETTINEN	KCL	Research Engineer KCL PO Box 70 FIN-02151 FINLAND	pais.miettinen@kcl.fi	+358 9 43711	
MR DEXTER MORGAN	PAPRO	Scientist PAPRO Sala Street ROTORUA NEW ZEALAND	mrgand@xtra.co.nz	+ 64 7 343 5789	+ 64 7 343 5695
MR TOMAS NORDSTRAND	SCA Packaging Research	Section Manager SCA Packaging Research Box 716 85121 SWEDEN	tomas.nordstrand@research.sca.se	+ 4660 193 076	+ 4660 193 804
ASSOC PROF IAN PARKER	Monash University	APPI Monash University PO Box 36 MONASH UNIVERSITY VIC 3800	ian.parker@eng.monash.edu.au	03 9905 5078	03 9905 3413
MR AHSAN QURESHI	Monash University	Student Department of Chemical Engineering Monash University P.O. Box 36 MONASH UNIVERSITY VIC 3800		03 9905 3456	03 9905 3413

Name	Organisation	Full Address	E-Mail Address	Business Telephone Number	Business Fax Number
MR RUSSELL RANKIN	Food into Asia Program	Food into Asia Program			
ASSOC PROF MICHAEL SEK	Victoria University	Victoria University P.O. Box 14428 MCMC MELBOURNE VIC 8001	Michael.Sek@vu.edu.au	03 9688 4227	03 9688 4139
MR JIM SELWAY	Amcor Fibre Packaging	Amcor Fibre Packaging 971 Burke Road CAMBERWELL VIC 3124	jim.selway@amcor.com.au	03 9811 7138	
ASSOC PROF. JEAN-MARIE SERRA-TOSIO	E.F.P.G	Head of Research Paper Physics E.F.P.G Domaine Universitaire 461, rue de la papeterie 38402 FRANCE	Jean-Marie.SERRA-TOSIO@efpg.inpg.fr		+33 0476 826933
MR ERN SHAW	Amcor Research	Principle Research Engineer Amcor Research Private Bag 1 FAIRFIELD VIC 3078	ern.shaw@amcor.com.au	03 9490 6100	03 9499 4295
DR PAUL SINGH	Michigan State University	Professor School of Packaging Michigan State University EAST LANSING 48824 USA	singh@msu.edu	+517 355 7614	+517 353 8999
MR FREDRIK SOLHAGE	EKA Chemicals AB	R & D Development Engineer/Project Leader EKA Chemicals AB S-44580 SWEDEN	JFS@RBO.EKACHEMICALS.COM	+46 31 587 493	+46 31 587 747
MR JAMES SOUTHWELL	PCA	Senior Manager - Technical Development PCA 250. S. Shaddle MANDELEIN IL 60060 USA	jsouthwell@packagingcorp.com	847 482 2091	847 482 2100
DR ATSUSHI TANAKA	Oy Keskuslaboratorio	Research Scientist Oy Keskuslaboratorio Tekniikantie 2 PO Box 70 ESPOO FIN-02151 FINLAND	atsushi.tanaka@kcl.fi	+ 358 9 437 1460	+ 358 9 464 305
MR THOMAS URBANIK	U.S. Forest Products Laboratory	Research Engineer U.S. Forest Products Laboratory 1 Gifford Pinchot Drive MADISON, WI 53705-2398 USA	turbanik@fs.fed.us	+608 231 9428	+608 231 9538
MR CORNELIS van WEERT	ATO	ATO Bornsesteeq 59 WAGENINGEN 6700AA NETHERLANDS	C.L.M.vanWeert@ato.dlo.nl	0317 477 521	0317 475 347
DR KEE WOO	Carter Holt Harvey Pulp & Paper	Manager, Paper Chemistry Carter Holt Harvey Pulp & Paper Private Bag 92-808 PENROSE AUCKLAND NEW ZEALAND	kee.woo@chh.co.nz	64 9 525 4536	64 9 525 4548

40 People Listed

Top row from left: Doug Coffin, Jean-Marie Serra-Tosio, Ian Chalmers. Bottom row from left: Tom Urbanik, Ian Parker, Christer Fellers